UNIVERSITÀ
DEGLI STUDI
DI PADOVA

Sede Amministrativa: Università degli Studi di Padova

Dipartimento di Biologia

SCUOLA DI DOTTORATO DI RICERCA IN: BIOSCIENZE E BIOTECNOLOGIE
INDIRIZZO: BIOTECNOLGIE
CICLO XXVI

Anticancer activity of liposomal cisplatin in preclinical models of cervical and ovarian cancer

Direttore della Scuola: Prof. Giuseppe Zanotti
Coordinatore d'indirizzo: Prof.ssa Fiorella Lo Schiavo
Supervisore: Prof. Giuseppe Zanotti
Co-supervisori: Prof. Alfonso Colombatti
Dott.ssa Aldinucci Donatella

Dottoranda: Naike Casagrande

To my grandparents

TABLE OF CONTENTS

1. ABSTRACT

Cisplatin-based chemotherapy improves survival in cervical and ovarian cancer; however, treatment is associated with tumor resistance and significant toxicity.
Lipoplatin (Regulon Inc., Mountain View, California) is a liposomal encapsulated form of cisplatin, developed in an effort to reduce cisplatin's systemic toxicity, while simultaneously improving the targeting of drugs to primary tumor and metastasis. Lipoplatin has been successfully administered in several randomized Phase II and III clinical trials, but not in cervical and ovarian cancer.
The aim of this project was to analyze the antitumoral activity of lipoplatin in cisplatin-sensitive and cisplatin-resistant cervical and ovarian cancer cells.
I evaluated the antiproliferative activity of lipoplatin, with cisplatin as reference drug, in the ME-180 cervical cancer cell line and its cisplatin-resistant clone R-ME-180, and in a panel of ovarian cancer cell lines: A2780, its cisplatin-resistant clone A2780cis, MDAH, OVACR3, OVCAR5, SKOV3, and TOV21G. Results demonstrated that lipoplatin exhibited a potent antitumoral activity in all the tested cell lines, including cisplatin-resistant cells, indicating that there is no cross-resistance between the two drugs.
Lipoplatin induced apoptosis, as evaluated by Annexin-V staining and DNA fragmentation. In particular, it induced the mitochondrial apoptotic pathway causing mitochondrial membrane permeabilization, cytochrome-c release, Bcl-2 down-regulation, but Bax up-regulation, and caspases 9 and 3 activation. At the same experimental conditions cisplatin induced apoptosis only in cisplatin-sensitive cells. Moreover, lipoplatin, but not cisplatin, increased reactive oxygen species (ROS) accumulation and inhibited the enzymatic activity of thioredoxin reductase (TrxR), an enzyme involved in ROS detoxification and over-expressed in many tumor cells contributing to drug resistance. Furthermore, lipoplatin reduced EGFR expression and inhibited both migration and invasion.
Multiple drug treatment is widely used in chemotherapy to obtain an additive or a synergistic effect (more than additive). I combined lipoplatin with the chemotherapeutic agents mostly used in ovarian cancer treatment. The results showed that the combination of lipoplatin with doxorubicin or abraxane demonstrated a synergistic effect, whereas the combination of lipoplatin with docetaxel or paclitaxel was less effective or at best additive.
In the ascites of ovarian cancer patients there are multicellular aggregates or spheroids that are involved in tumor progression. Thus, spheroid-based assays are more predictive of *in vivo* therapeutic efficacy because they more closely resemble tumor microenvironment. Furthermore, cancer stem cells (CSC), rare tumor cells involved in initiating cancer growth, drug resistance, and disease recurrence, are also present in spheroids. The treatment with lipoplatin reduced stem cell markers in a dose-dependent manner and inhibited spheroid formation in both cervical and ovarian cancer models. Furthermore, it decreased ovarian cancer spheroid growth, vitality, and migration.

Finally, lipoplatin treatment of nude mice with cervical and ovarian tumors significantly inhibited tumor growth *in vivo*, with low toxicities. Moreover, even after treatment interruption the tumors did not show any regrowth.

In conclusion, in this project lipoplatin demonstrated an antitumoral activity in monolayer cultures, three-dimensional spheroids, and *in vivo* studies using cisplatin-resistant cervical and ovarian cancer cells. These promising results suggest lipoplatin as a novel chemotherapeutic agent for the treatment of cervical and ovarian cancer.

2. SOMMARIO

Il cisplatino è uno dei farmaci più utilizzati per il trattamento del carcinoma della cervice e dell'ovaio. Purtroppo il suo utilizzo in chemioterapia presenta importanti limitazioni, quali l'elevata tossicità e l'insorgenza di resistenza intrinseca o acquisita.
Il lipoplatino è una formulazione liposomiale del cisplatino (Regulon, Inc., Mt. View, U.S.A), sintetizzata allo scopo di ridurre la tossicità sistemica del cisplatino e contemporaneamente di incrementarne l'accumulo nel tumore primario e nelle metastasi. Studi clinici di Fase II e III sono stati effettuati in diversi tumori ma non nel carcinoma della cervice uterina e dell'ovaio.
In questo lavoro è stata analizzata l'attività antitumorale del lipoplatino in modelli preclinici di carcinoma della cervice uterina e carcinoma ovarico sensibili e resistenti al cisplatino.
L'attività antiproliferativa del lipoplatino è stata studiata nella linea cellulare derivata da carcinoma della cervice uterina ME-180 e nel suo clone resistente al cisplatino R-ME-180, come pure in un pannello di linee cellulari derivanti da carcinoma ovarico: A2780, il suo clone cisplatino-resistente A2780cis, MDAH, OVACR3, OVCAR5, SKOV3, e TOV21G. Il cisplatino è stato introdotto nello studio come farmaco di riferimento. I risultati hanno dimostrato che il lipoplatino esibisce una potente attività antitumorale in tutte le linee cellulari analizzate, incluse le cisplatino-resistenti, dimostrando assenza di cross-resistenza con il farmaco cisplatino.
Il lipoplatino induce apoptosi, valutata tramite l'esternalizzazione della fosfatidilserina (marcatore precoce di apoptosi) e la frammentazione del DNA. In particolare, il lipoplatino attiva la via mitocondriale dell'apoptosi, come dimostrato dalla depolarizzazione della membrana mitocondriale, il rilascio del citocromo-c , la diminuzione dell'espressione della proteina anti-apoptotica Bcl-2, l'incremento dell'espressione della molecola pro-apoptotica Bax e l'attivazione delle caspasi 9 e 3. Nelle stesse condizioni sperimentali il cisplatino attiva l'apoptosi soltanto in cellule sensibili al cisplatino.
L'enzima tioredoxina reduttasi (TrxR) svolge una funzione ossidoriduttiva proteggendo la cellula da stress ossidativo. Un elevato livello dell'enzima si osserva in diversi tipi di tumore e sembra essere associato alla resistenza al cisplatino. I miei studi hanno dimostrato che il lipoplatino, ma non il cisplatino, inibisce l'attività enzimatica della TrxR incrementando la produzione di radicali liberi dell'ossigeno (ROS). Inoltre il lipoplatino riduce l'espressione del recettore del fattore di crescita dell'epidermide (EGFR), un recettore di membrana *over*-espresso nei tumori, coinvolto nella proliferazione e nella migrazione delle cellule tumorali. Anche la migrazione e l'invasione cellulare vengono ridotte dal trattamento con lipoplatino.
Molto spesso in chemioterapia si somministra una combinazione di più farmaci (polichemioterapia) per ottenere un effetto additivo e/o sinergico. Si è quindi combinato il lipoplatino con i chemioterapici più utilizzati nel trattamento del

carcinoma ovarico. La combinazione del lipoplatino con i farmaci doxorubicina e abraxane dimostra effetti sinergici, mentre la combinazione con docetaxel e paclitaxel è meno efficace con effetti quasi additivi.
Nell'ascite di pazienti affette da carcinoma ovarico si possono ritrovare aggregati multicellulari, o sferoidi, che sembrano essere coinvolti nella progressione tumorale. Gli sferoidi rappresentano un valido modello sperimentale con caratteristiche biologiche e molecolari simili ai tumori solidi, tra queste la presenza di cellule staminali cancerose, ossia cellule con grandi capacità rigenerative e di resistenza alle terapie in grado di alimentare la crescita del tumore. Il trattamento con lipoplatino diminuisce in maniera dose-dipendente i marcatori di staminalità e inibisce la formazione di sferoidi in entrambi i modelli sperimentali. Inoltre riduce la dimensione, la vitalità e la disseminazione di sferoidi di carcinoma ovarico.
Infine il lipoplatino diminuisce la crescita di tumori xenografi derivanti da cellule di carcinoma della cervice uterina e dell'ovaio con ridotta tossicità. Anche in seguito all'interruzione del trattamento i tumori non riprendono la crescita.

Concludendo il lipoplatino dimostra un'attività antitumorale in colture cellulari tradizionali, in colture tridimensionali o sferoidi ed *in vivo*, sia di cellule derivanti da carcinoma della cervice uterina cisplatino-resistenti che da carcinoma ovarico. Questi risultati molto promettenti suggeriscono un potenziale utilizzo di questa formulazione liposomiale di cisplatino per il trattamento di pazienti affette dalle suddette patologie.

3. INTRODUCTION

3.1 Chemotherapeutic agents

Cancer is a term used for diseases in which abnormal cells divide without control and are able to invade other tissues. According to the world health organization (WHO) more than 14.0 million people are diagnosed with cancer every year. It is the leading cause of death worldwide and accounted for 8.2 million deaths (13% of all deaths) in 2012.

One of the most common treatments for cancer is chemotherapy, that is the use of anticancer drugs to treat cancerous cells. Chemotherapy may be used alone for some types of cancer or in combination with other treatments such as radiation or surgery. Often, a combination of chemotherapy drugs is used to fight a specific cancer (Gleeson et al., 2008).

The majority of current anticancer drugs exert their effects by targeting and reducing enhanced cellular proliferation and division of cancer cells. The rationale being that cancer cells are more likely to be replicating than normal cells. Unfortunately as their action is not specific, they are associated with significant toxicity. Therefore effective use of cancer chemotherapy requires an understanding of the principles of tumor biology, cellular kinetics, pharmacology, and drug resistance (Gleeson et al., 2008).

Classifying cytotoxic drugs according to their mechanism of action is the preferred system in use between clinicians (Figure 3.1).

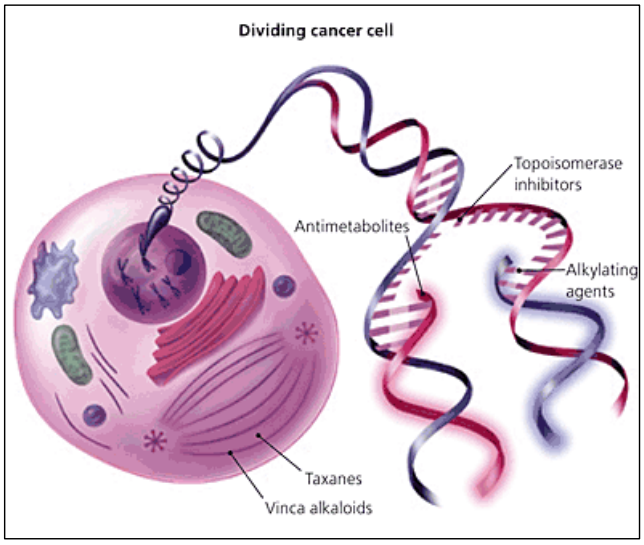

Figure 3.1 Mechanisms of traditional chemotherapy.

ALKYLATING AGENTS

These highly reactive compounds produce their effects by covalently linking an alkyl group (R-CH2) to a chemical species in nucleic acids or proteins. The site at which the cross-links are formed and the number of cross-links formed is drug

specific. Most alkylating agents are bipolar, i.e. they contain two groups capable of reacting with DNA. They can thus form bridges between a single strand or two separate strands of DNA, interfering with the action of the enzymes involved in DNA replication. The cell then either dies or is physically unable to divide or triggers apoptosis. The damage is most serious during the S-phase, as the cell has less time to remove the damaged fragments. Examples include: nitrogen mustards (e.g. melphalan and chlorambucil); oxazaphosphorenes (e.g. cyclophosphamide, ifosfamide); alkyl alkane sulphonates (busulphan); nitrosureas (e.g. carmustine (BCNU), lomustine (CCNU)); tetrazines (e.g. dacarbazine, mitozolomide and temozolomide); aziridines (thiopeta, mitomycin C); procarbazine (WARWICK, 1963).

ANTIMETABOLITES

Antimetabolites are compounds that bear a structural similarity to naturally occurring substances such as vitamins, nucleosides or amino acids. They compete with the natural substrate for the active site on an essential enzyme or receptor. Some are incorporated directly into DNA or RNA. Most are phase-specific, acting during the S-phase of the cell cycle. There are three main classes: folic acid antagonists (e.g. methotrexate); pyrimidine analogues (e.g. 5-fluorouracil, cytarabibe); purine analogues (6-Mercaptopurine (6MP) and thioguanine are derivatives of adenine and guanine, respectively) (Pizzorno et al., 2000).

ANTIMICROTUBLE AGENTS

Vinca alkaloids

The two prominent agents in this group are vincristine and vinblastine that are extracted from the periwinkle plant. Upon entering the cell, they bind rapidly to the tubulin. The binding occurs in the S phase. Polymerization of microtubules is blocked, resulting in impaired mitotic spindle formation in the M phase. Other newer examples include vindesine and vinorelbine (Malhotra and Perry, 2003).

Taxanes

Paclitaxel and docetaxel (Taxotere) are semisynthetic derivatives of extracted precursors from the needles of yew plants. These drugs have a novel 14-member ring, the taxane. Unlike the vinca alkaloids, which cause microtubular disassembly, the taxanes promote microtubular assembly and stability, therefore blocking the cell cycle in mitosis (Malhotra and Perry, 2003).

CYTOTOXIC ANTIBIOTICS

Most antitumor antibiotics have been produced from bacterial and fungal cultures (often Streptomyces species). They affect the function and synthesis of nucleic acids in different ways. Anthracyclines (e.g. doxorubicin, daunorubicin, epirubicin) intercalate with DNA and affect the topoiosmerase II enzyme. Actinomycin D intercalates between guanine and cytosine base pairs. This interferes with the transcription of DNA at high doses. At low doses DNA-directed RNA synthesis is blocked. Bleomycin consists of a mixture of glycopeptides that cause DNA fragmentation. Mitomycin C inhibits DNA synthesis by cross-linking DNA, acting like an alkylating agent.

PLATINUM AGENTS

Platinum-based are coordination complexes of platinum and are the most widely used classes of cancer therapeutics. Today, there are three platinum chemotherapeutics approved by the U.S. Food and Drug Administration, cisplatin, carboplatin, and oxaliplatin (Kelland, 2007).

Platinum-based antineoplastic agents cause crosslinking of DNA as monoadduct, interstrand crosslinks, intrastrand crosslinks or DNA protein crosslinks. The resultant crosslinking inhibit DNA repair and/or DNA synthesis in cancer cells. Platinum-based antineoplastic agents are sometimes described as "alkylating-like" due to similar effects as alkylating antineoplastic agents, although they do not have an alkyl group (Kostova, 2006).

TOPOISOMERASE INHIBITORS

Topoisomerases are responsible for altering the 3D structure of DNA by a cleaving/unwinding/rejoining reaction. They are involved in DNA replication, chromatid segregation and transcription. The efficacy of topoisomerase inhibitors in the treatment of cancer is based solely on their ability to inhibit DNA replication (Guichard and Danks, 1999). The drugs are phase-specific and prevent cells from entering mitosis from G2. There are two broad classes:

Topoisomerase I inhibitors

Camptothecin, derived from Camptotheca acuminate (a Chinese tree), binds to the enzyme-DNA complex, stabilizing it and preventing DNA replication. Irinotecan and topetecan have been derived from this prototype.

Topoisomerase II inhibitors

Epipodophyllotoxin derivatives (e.g. etoposide, vespid) are semisynthetic derivatives of Podophyllum peltatum, the American mandrake. They stabilize the complex between topoisomerase II and DNA that causes strand breaks and ultimately inhibits DNA replication (Pommier, 2006).

OTHERS

Includes drugs that do not fall into any of these categories (Monoclonal antibodies, signaling inhibitors) (Boulikas, 2007).

3.2 Cisplatin

3.2.1 Discovery

Cisplatin is characterized by a square planar configuration with a central atom of platinum linked to two chloride and two NH_3 groups. Although the synthesis and characterization of cisplatin was first reported by Michel Peyrone in 1844 (Peyrone, 1844), its anticancer properties remained unnoticed for about 125 years, until the mid-1960s, when Rosenberg and co-workers serendipitously studied the effects of electric fields on *Escherichia coli* growth (Rosenberg et al., 1965). The platinum electrodes released by redox reactions some platinum complexes which provoked complete stop of cell division in the bacterial rods. Amongst the platinum complexes formed, the *cis* form of the platinum(II) complex,

$[PtCl_2(NH_3)_2]$ or cis-diamminedichloroplatinum(II) (CDDP), was identified as the main antiproliferative agent; the *trans* complex was found to be ineffective (Rosenberg et al., 1967, 1969) (Figure 3.2).

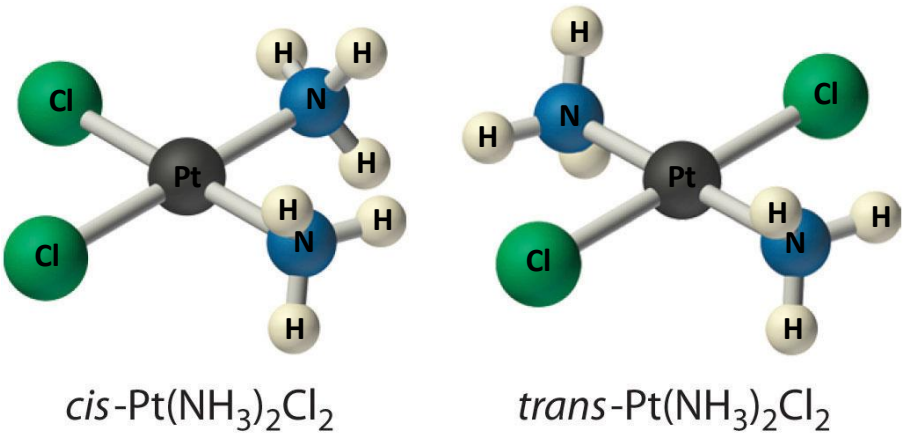

Figure 3.2 Schematic representation of the two stereoisomers cisplatin (left) and transplatin (right).

Given these results, it was reasoned that the complex may be interesting to be assessed for its anticancer activity. To this end cisplatin was tested against Sarcoma 180 tumors in Swiss white mice. The complex demonstrated "potent" activity, shrinking large solid tumors, and the mice survived and were healthy. In fact, after 6 months the cured mice did not show any signs of cancer (Rosenberg and VanCamp, 1970). Based on these results cisplatin entered clinical trials. In December 1978 *cis*-$[PtCl_2(NH_3)_2]$ received U.S. Food and Drug Authority approval as an anti-cancer drug for testicular and ovarian cancers. The formulated drug containing sodium chloride and mannitol is marketed under the name of Platinol^{TM}. The bulk *cis*-$[PtCl_2(NH_3)_2]$ is referred to as cisplatin. In the U.K. the drug is known as Neoplatin^{TM}, and this received approval in March 1979 (Wiltshaw, 1979).
In the next years cisplatin developed into one of the most successful and widely used drugs in cancer chemotherapy and it still continues to be a cornerstone in modern chemotherapy, playing an important role among cytotoxic agents in the treatment of epithelial malignancies (Rosenberg, 1977).

3.2.2 Pharmacology and mechanism of action

Cisplatin is administered to cancer patients by intravenous injection as sterile saline solution, that is, containing salt, specifically sodium chloride. Following administration in the bloodstream of a patient, cisplatin encounters a relatively high chloride concentration in the blood plasma (approximately 100 mM) that limits replacement of its chloride ligands by water molecules (process of aquation). However, cisplatin is vulnerable to attack by proteins found in blood

plasma, particularly those that contain thiol groups, such as human serum albumin (66-kDa protein) and the amino acid cysteine. In fact, studies have shown that one day after cisplatin administration, 65–98% of the platinum in blood plasma is protein bound (DeConti et al., 1973; Ivanov et al., 1998). Although many of its severe side effects have been attributed to protein binding, the exact role of Pt-protein complexes in the mechanism of action of the metallodrug is still not well understood. It is possible that major serum proteins, albumin and transferrin, might take over a transport and delivery function for cisplatin, and other antitumor metal complexes, and thereby influence their overall distribution and efficacy. Albumin, for instance, is taken up by tumor cells at increased levels in comparison to normal cells and has been exploited as a carrier protein for organic anticancer drugs (Will et al., 2008).

The biochemical mechanism by which cisplatin crosses the cell membrane still remains unclear. Early studies reported that cisplatin uptake was not inhibited by its structural analogues and this entry into the cell did not seem to be dependent on an optimum pH (Mann et al., 1991). In addition, cisplatin accumulation in the cell proceeded linearly with time over 60 minutes and did not reach a plateau up to a drug concentration of 1 mM. So, it was suggested that passive diffusion was the main mechanism by which cisplatin enters the cell. However, it was found later that a certain degree of cisplatin uptake seemed to be energy dependent and could be modulated by pharmacological agents such as the Na+/K+-ATPase inhibitor ouabain and the membrane-interactive agents amphotericin B and digitonin (Gately and Howell, 1993). Recently, carrier import proteins, like the organic cation transporter OCT/SLC22A, or the high-affinity copper transporter 1 (CTR1), were identified as cellular uptake mechanisms for cisplatin (Ciarimboli et al., 2010). Indeed, observations point towards a direct connection between the cellular concentrations of copper and platinum, which leads to propose an active transport for cisplatin in addition to passive diffusion.

The intracellular chloride concentration is relatively low (approximately 4-20 mM) and hence one, or both, of the chloro ligands of the intact cisplatin are replaced by water, forming a reactive, positively charged species that cannot readily leave the cell. These mono and diaquo species of cisplatin are very reactive towards nucleophile centres of biomolecules because H_2O is a much better leaving group than Cl^- (Figure 3.3).

In the cytoplasm there are many cellular components that have soft nucleophilic sites such as membrane phospholipids, cytoskeletal microfilaments, thiol-containing peptides and proteins, RNA, that may react with cisplatin (Jordan and Carmo-Fonseca, 2000). Hence, of interest is the observation that only 5-10% of covalently bound cell-associated cisplatin is found in the genomic DNA fraction, whereas 75-85% of the drug binds to proteins and other cellular constituents (Akaboshi et al., 1992). The most important non-DNA target of cisplatin is probably the tripeptide glutathione (GSH), which is present in cells at high concentrations (0.5-10 mM) (Figure 3.3).

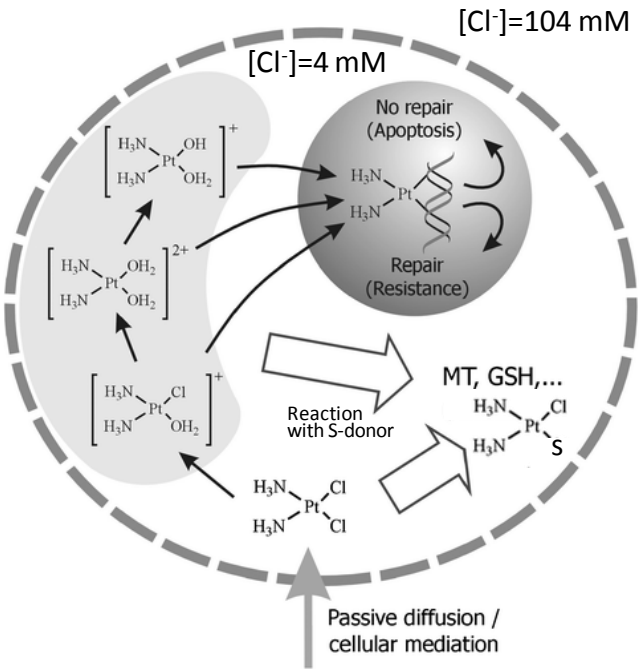

Figure 3.3 The cellular uptake of cisplatin and its targets.

GSH and other thiol-containing biomolecules such as metalothioneins (MT) bind quickly to platinum (Fuertes et al., 2003). Cisplatin binding to GSH and MT has primarily been associated with negative pharmacological properties, including the development of resistance and toxicity. On the other hand, cisplatin may alter the activity of enzymes, receptors, and other proteins through coordination to sulfur atoms of cysteine and/or methionine residues and to nitrogen atoms of histidine residues. In fact, binding of cisplatin to methionine 1 (met1) and/or histidine 68 (his68) of ubiquitin may inhibit the ubiquitin-proteasome pathway of selective degradation of cellular proteins, which ends up in cytotoxic events (Peleg-Shulman and Gibson, 2001). In addition, it has been found that cisplatin, besides inhibiting *in vitro* the activity of heat shock protein 90 (Hsp90), and ATP-binding chaperone, efficiently and specifically blocks its C-terminal ATP binding site. The C-terminal of Hsp90 *via* its ATP hydrolytic function is involved in the correct folding of proteins which play a role in signal transduction and cell cycle regulation (Söti et al., 2002).

The effects of cisplatin on RNA and DNA have been studied extensively. Although cisplatin can coordinate to RNA, this interaction is not believed to play an important role in cisplatin's physiological mechanism of action because a single damaged RNA molecule can be replaced by newly synthesized material, and studies have revealed that cisplatin does not affect RNA synthesis. Moreover, when cisplatin was administrated *in vitro* at its lethal dose to a strain of cancer cells, only a small fraction (1 to 10%) of RNA molecules were damaged. On the contrary, there is strong evidence that cellular DNA is the main target of the drug (Rabik and Dolan, 2007).

The nitrogen atoms position 7 (N7) on the purine ring of guanine, and in less extend adenine, located in the major groove of the double helix are the most accessible and reactive nucleophilic sites for platinum coordination to DNA. These N7 atoms are free to coordinate to cisplatin because they do not form hydrogen bonds with any other DNA bases. Binding of cisplatin to DNA is irreversible and structurally different adducts are formed (Figure 3.4). Three different types of lesions can form on purine bases of DNA: monoadducts, intrastrand crosslinks, and interstrand crosslinks. Monoadducts are first formed as one molecule of water is lost from aquated platinating agents; however, greater than 90% of monoadducts then react to form crosslinks. Cisplatin forms about 65% 1,2-d(GpG) intrastrand crosslinks, 25% 1,2-d(ApG) intrastrand crosslinks, 13% interstrand or intrastrand crosslinks on d(GpXpG) sequences, and less than 1% remains monofunctional adduct (Egger et al., 2008). Protein-DNA crosslinks are also formed by cisplatin (Figure 3.4).

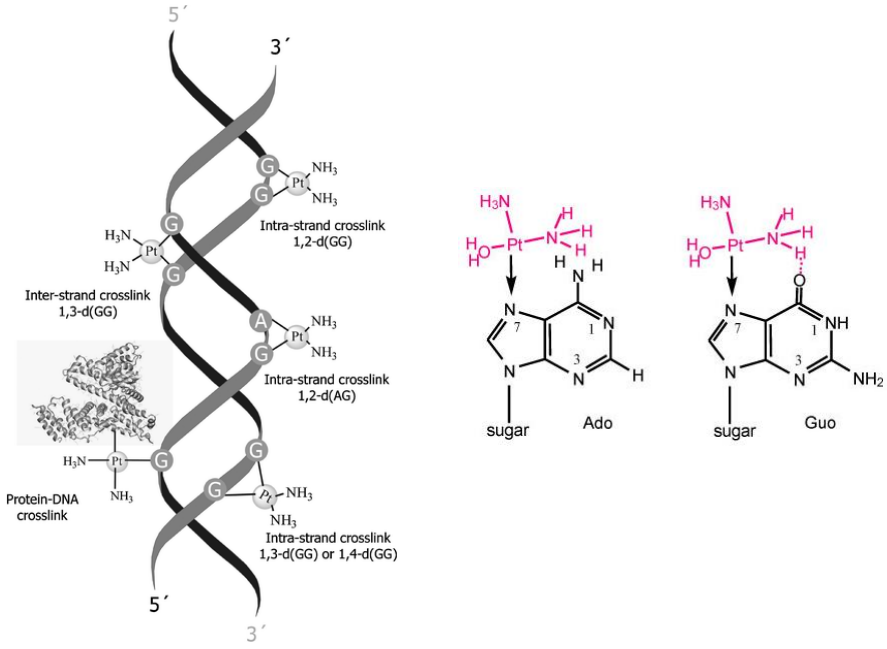

Figure 3.4 Main adducts formed in the interaction of cisplatin with DNA (left). Cisplatin coordination to the N7 atoms of the purine (guanine and adenine) bases (right).

Also *trans*-platin or transplatin binds to DNA almost exclusively by coordination to the N7 atom of purine bases. Therefore, from a biochemical point of view the lack of pharmacological activity of transplatin must be related to the different type of DNA adducts formed by this *trans* isomer relative to cisplatin. Due to steric reasons, transplatin mainly forms 1,3-intrastrand and interstrand cross-links. Therefore, it is generally assumed that the 1,2-intrastrand DNA adduct is responsible for cisplatin cytotoxicity, although this is not a proven fact (Cepeda et al., 2007).

When cisplatin binds to DNA forming adducts, it promotes superhelical unwinding and shortens the double helix. Cisplatin intrastrand crosslinks bend the

double helix by 32-35° toward the major groove. Both 1,2-d(GpG) and 1,2-d(ApG) intrastrand crosslinks unwind DNA by 13°, while the 1,3-d(GpXpG) intrastrand lesion unwinds DNA by 34°. Interstrand lesions induce even more steric changes in DNA (Rabik and Dolan, 2007).

When DNA is damaged, the cell cycle is arrested to provide time for repair. Cell-cycle checkpoints monitor the proper order of events in the cell because failures in replication lead to the acquisition and accumulation of genetic alterations, which can ultimately cause tumorigenesis. The G1/S checkpoint ensures that damaged DNA is not replicated. Cisplatin does not cause G1 arrest in all cases. The G2/M checkpoint allows for the repair of DNA that was damaged late in the S or G2 phase of the cell cycle before mitosis, to prevent damaged DNA from being segregated into daughter cells. It has been proposed that such G2 arrest is essential to the process of engaging cell death following cisplatin treatment. When DNA damage occurs, ataxia telangiectasia mutated (ATM) and its related ataxia-telangiectasia and Rad3-related (ATR) kinase activate checkpoint kinases CHK1 and CHK2 through phosphorylation, which in turn phosphorylate cell division cycle 25C (CDC25C). The phosphorylated CDC25C promotes its binding to 14-3-3 adaptor proteins and is thereby separated from CDC2 by translocation of CDC25C to the cytoplasm. As a result, CDC2 phosphorylation is elevated and causes cells to arrest in G2 (Liu et al., 2000; Matsuoka et al., 2000).

Cisplatin damaged DNA can be repaired by nucleotide excision repair proteins (NER), mismatch repair (MMR) proteins, and DNA-dependent protein kinase protein (DNA-PK) (Ahmad, 2010).

Nucleotide excision repair proteins are ATP-dependent multiprotein complexes that recognize the bending induced on DNA by 1,2-intrastrand cross-links, and subsequently excise the part of the DNA that includes the kink as 27- to 29-base-pair oligonucleotides. The gap that remains is then filled by DNA polymerase. There are 9 major proteins involved in NER in mammalian cells. Deficiencies in certain proteins leads to disease; protein names are associated with the disease. XPA, XPB, XPC, XPD, XPE, XPF, and XPG all derive from *xeroderma pigmentosum* and CSA and CSB represent proteins linked to Cockayne syndrome. Additionally, the proteins ERCC1, RPA, RAD23A, RAD23B, and others also participate in nucleotide excision repair. NER can be divided into two subpathways: global genomic NER (GG-NER) and transcription coupled NER (TC-NER). The two subpathways differ in how they recognize DNA damage but they share the same process for lesion incision, repair, and ligation (Zhang et al., 2009). It has been reported that at least 16 genes are essential for the DNA damage recognition and excision function of the intrastrand adducts formed by cisplatin between two adjacent guanines (Bruhn et al., 1992). NER appears also to be a major mechanism of cisplatin resistance.

Mismatch repair is a post-replication repair system that corrects unpaired or mispared nucleotides in DNA caused by DNA-platinum adducts. The mismatch repair system involves at least five proteins (MLH1, MSH2, MSH3, MSH6 and PMS2) and functions as a repair mechanism that needs ATP. MMR is a

comparative small contributor to the cisplatin resistance phenotype in comparison with NER. In fact in ovarian and colon cancers an intact MMR system appears to be essential for the linkage of DNA damage/repair with the initiation of apoptosis (Reed, 1999).

The DNA-PK protein mainly repairs DNA double-strand breaks (DSB) induced by cell exposure to ionizing radiation. However, it has been described that the DNA-PK protein can also interact with cisplatin-DNA lesions (Turchi and Henkels, 1996). DNA binding of the Ku subunits of DNA-PK *in vitro* is essential to activate the kinase activity of DNA-PK to phosphorylate itself or transcription factors. Interestingly, it has been reported that in ovarian cancer cells the presence of cisplatin-DNA adducts serves to inhibit the ability of the Ku subunits of DNA-PK to translocate on a duplex DNA substrate resulting in inhibition of the kinase activity (Henkels and Turchi, 1997).

DNA damage recognition proteins include over 20 individual candidate (Vaisman et al., 1998). Special attention is focused on recognition of cisplatin modified DNA by high-mobility group (HMG) proteins. The HMG domain proteins are the largest extensively characterized group of non-histone chromosomal proteins. They can bind to specific structures in DNA or in chromatin with little or no specificity for target DNA sequence. Two families of HMG have been reported. The first consists of proteins containing two or more HMG domains; it includes HMG1 and HMG2 proteins, the nucleosomal RNA polymerase I transcription factor upstream binding factor (UBF) and the mitochondrial transcription factor (mtTF). In the second family there are proteins containing a single HMG domain, such as tissue-specific transcription factors (Cepeda et al., 2007).

Several HMG domain proteins recognize and bind to cisplatin-modified DNA. The greatest attention has been concentrated on the studies of recognition of platinated DNA by HMGB1 and HMGB2. In particular, HGMB1 recognizes the major 1,2- d(GpG) intrastrand cisplatin-DNA adduct and may avoid that NER can repair this DNA lesion. In addition, HMGB1 has been linked to other DNA-dependent pathways. Hence, HMGB1 (i) may activate cleavage of recombination activation genes 1 and 2 (RAG1 and RAG2), (ii) may stimulate the binding of sequence-specific transcription factors, (iii) may interact with the MMR protein MutSa then having a possible role in mismatch repair, (iv) binds to the tumor suppressor protein p53 *in vitro* therefore increasing p53 DNA-binding activity, and (v) HMGB1 affinity for platinated DNA is significantly improved in the presence of p53 (Wang and Lippard, 2005). However, it should be pointed out that all these biochemical functions attributed to HMGB1 in response to cisplatin damage to DNA are dependent on the cell type.

3.2.3 Signals Transduction from Cisplatin-DNA Damage

The likely role of DNA damage recognition proteins is to transduce DNA damage signals to downstream effectors. As a consequence of exposure to cisplatin,

different signaling pathways are affected. There is no general concept applicable to all types of tumor. It is evident that response to cisplatin is defined by cell specificity. Nevertheless numerous data revealed changes in activity of most important signaling pathways involved in cell proliferation, differentiation and cell death such as phosphatidylinositol 3-kinase (PI3K)/Akt, Mitogen-Activated Protein Kinase (MAPK), as well as signaling pathways involved in realization of death signals dependent or independent of death receptors (Wang and Lippard, 2005). It is very important to note that alteration in signal transduction upon cisplatin treatment could be the consequence of both, DNA damage or interaction with proteins that are relevant for appropriate molecular response or in triggering programmed cell death pathways. Indeed, as mentioned before, most cisplatin molecules bind to proteins rather than DNA.

The PI3K/Akt pathway is frequently activated in cancer cells. AKT molecule, as most important Ser/Thr protein kinase in cell survival, protects cells from damage induced by different stimuli, as well as cisplatin (Datta et al., 1999). Cisplatin downregulated XIAP protein level and promoted AKT cleavage resulting in apoptosis in chemosensitive but not in resistant ovarian cancer cells. Furthermore, PTEN is a tumor suppressor gene product believed to promote apoptosis primarily *via* inactivation of the PI3K/Akt cell survival pathway (Dan et al., 2004).

A protein marked as the most important in the signaling of DNA damage is c-Abl which belongs to Src family of non receptor tyrosine kinases (Cepeda et al., 2007). This molecule acts as transmitter of DNA damage triggered by cisplatin from nucleus to cytoplasm. Moreover, sensitivity to cisplatin induced apoptosis is directly related with c-Abl content and could be blocked by c-Abl overexpression (Wang and Lippard, 2005).

Cisplatin induces oxidative stress and is an activator of stress-signaling pathways especially of the MAPK cascades. These enzymes are highly important in definition of cellular response to applied treatment because they are the major regulators of cell proliferation, differentiation, and cell death. Extracellular signal-related kinase (ERK) preferentially responds to growth factor and cytokines, but also determines cell reaction to different stress conditions, particularly, oxidative. Cisplatin treatment mainly activated ERK in a dose- and time-dependent manner (Wang et al., 2000). Acquisition of cisplatin resistance by ovarian carcinoma cells was associated with the loss of ERK activation in response to cisplatin (Boulikas, 2007). Regardless of numerous evidences about its critical role in cisplatin-mediated cell death, ERK is not the only molecule from MAP family which responded to cisplatin. Several studies revealed c-Jun N-terminal kinase (JNK) activation upon the cisplatin addition (Mansouri et al., 2003). However, similarly to other molecules previously mentioned, this signal is not the unidirectional and could be responsible for realization but also protection from death triggered by cisplatin. Finally, there are numerous evidences about highly important role of a third member of MAP kinases, p38, in response to cisplatin. Lack of p38 MAPK leads to appearance of resistant phenotype in human cells (Hernández Losa et al., 2003). Early and short p38 activation is principally described in cells

unresponsive to cisplatin, while long-term activation was found in sensitive clones. Moreover, in the light of the fact that this kinase has a role in modifying the chromatin environment of target genes, its involvement in cisplatin induced phosphorilation of histon 3 was determined (Wang and Lippard, 2004).

TRAIL (tumor necrosis factor alpha(α)-related apoptosis inducing ligand) is a potent inducer of apoptosis through caspase-3 activation and PARP cleavage. The presence of cysteine rich domain in the structure of TRAIL specific death receptors, DR4 and DR5, indicated possibility that cisplatin directly interact with them (Gómez-Ruiz et al., 2012). Cisplatin may also induce apoptosis through the Fas/Fas ligand signaling complex (with activation of caspase 8, then caspase 3), although clearly cisplatin-induced apoptosis involves different pathways (Siddik, 2003). Recent evidence about the biochemical mechanisms that mediate cisplatin cytotoxicity support the ability of cisplatin to induce oxidative damage, to interfere with cell metabolism and how this is the basis of its antineoplastic activity as well as of its main side effects. The increase of various reactive oxygen species (ROS) has been observed during cisplatin treatment. Several mechanisms have been proposed to account for the ROS generation under this condition. First, the depletion or inactivation of GSH and related antioxidants by cisplatin is expected to shift the cellular redox status, leading to the accumulation of endogenous ROS and oxidative stress within the cell. Second, cisplatin might induce mitochondrial dysfunction and increase ROS production by disrupting the mitochondrial respiratory chain. Moreover, cisplatin shifts cancer cell metabolism from glycolysis to oxidative phosphorylation (OXPHOS). OXPHOS is the source of ATP and ROS, which are essential for the p53-mediated apoptosis (Macciò and Madeddu, 2013).

Evaluation of a 60 human tumor cell line panel conducted by the National Cancer Institute (NCI) revealed that functional p53 protein is very important for successful response to cisplatin treatment (Wang and Lippard, 2005). This tumor suppressor gene, a transcription factor that is considered a “guardian of the genome”, is crucial for many cellular processes and determines the balance between cell cycle arrest as a chance for repair and induction of apoptotic cell death. However, despite extensive NCI studies, there are controversial data about correlation between cisplatin sensitivity and p53. In addition, protein involved or influenced by p53 pathway, such as Aurora kinase A, cyclin G, BRCA1 as well as pro-apoptotic or anti-apoptotic mediators are also able to control cisplatin toxicity (Wang and Lippard, 2005) (Figure 3.5).

Finally, the end result of cisplatin treatment is the activation of caspases leading to apoptosis, to cell cycle arrest, mitochondrial apoptotic pathway, to DNA damage-induced apoptosis, as well as to upregulation in the expression levels of transcription factors that are tightly linked to apoptosis. Moreover, necrosis or accidental cell death due to general cell machinery failure was also reported as a cell-killing mechanism for cisplatin (Gonzalez et al., 2001; Lau, 1999).

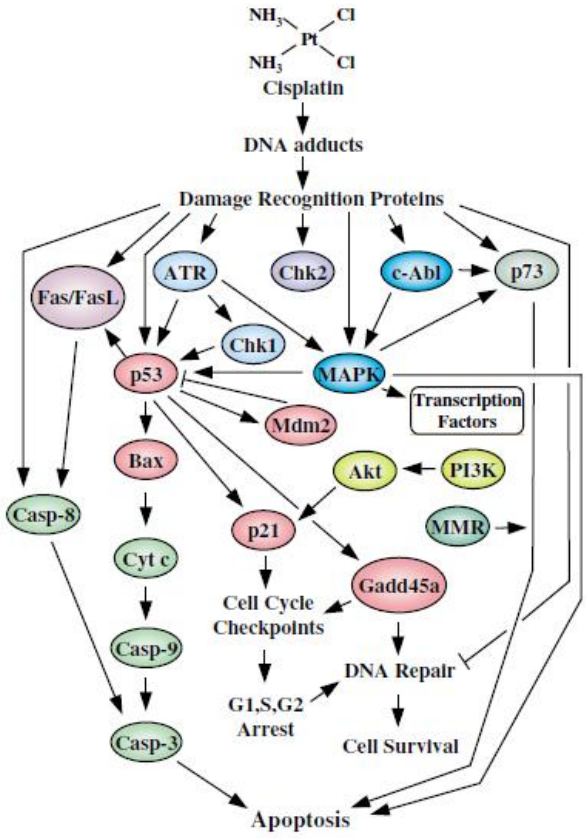

Figure 3.5 Overview of pathways involved in mediating cisplatin-induced cellular effects. Cell death or cell survival will depend on the relative intensity of the signals generated and the crosstalk between the pathways involved.

Even though cisplatin continues to be one of the most widely used drugs in modern chemotherapy its clinical applications is hundred by two major limitations: the development of cisplatin resistance by tumors and the related severe toxic side effects.

3.2.4 Cisplatin resistance

The use of cisplatin in cancer chemotherapy is limited by the insurgence of acquired or intrinsic resistance after drug exposure.

Acquired resistance. This type of resistance develops both in patients undergoing chemotherapy and in cell lines exposed to increasing concentrations of cisplatin until they have reached a high tolerance for the drug.

Intrinsic resistance. This type of resistance is a phenomenon encountered in patient tumors that are naturally unaffected by platinum treatment. Some cell lines cultured from these patients were more proficient at removing cisplatin-DNA adducts than cell lines with normal cisplatin sensitivity (Zwielly et al., 2011).

In nature, intrinsic and acquired drug resistance occurs in all living organisms, from bacteria to human cancer cells. Resistance is a natural cellular self-defense

mechanism developed by evolution to protect cells from toxic natural products and other environmental stressors. During the development of cisplatin resistance in human cancer cells *in vivo* and *in vitro*, numerous epigenetic and/or genetic changes can occur, probably reflecting activation of many different pathways that protect cells against environmental toxins (Shen et al., 2012).
Because cisplatin has many different routes of cell entry and multiple cellular targets, resistance to this platinum compound is very complex, requiring multiple pathways, with profound changes at both the molecular and cellular levels (Shen et al., 2012). Therefore, although the large number of biochemical studies carried out on cisplatin activity have not clearly established yet the molecular bases of tumor resistance to this drug in any type of cell, at least they have identified several mechanisms that can contribute to this process (Figure 3.6).

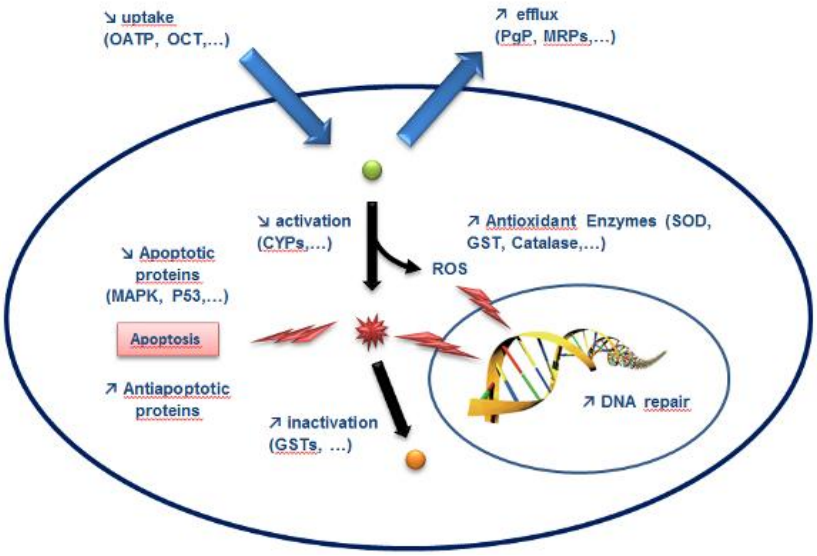

Figure 3.6 Representation of different mechanisms involved in cisplatin resistance. ↗: increase; ↘: decrease.

Resistance to cisplatin is generally considered a multifactorial phenomenon, which can develop as a result of decreased intracellular drug concentration due to decreased uptake, increased efflux, or due to increased inactivation by sulfhydryl molecules, such as glutathione. Increased excision of the adducts from DNA by repair pathways or increased lesion bypass can result in resistance. Finally, altered expression of regulatory proteins involved in signal transduction pathways that control apoptosis can also affect sensitivity to the drug (Kartalou and Essigmann, 2001). While it is possible that only one of these mechanisms may lead to resistance to cisplatin, it is more likely that a combination of these mechanisms results in a cisplatin-resistant tumor (Rabik and Dolan, 2007) (Figure 3.6).

3.2.4.1 Reduced drug accumulation

A major mechanism of resistance to cisplatin is a decreased effective concentration of drug in the cell. Reduction in cisplatin concentration of 20–70% has been observed in cell lines resistant to cisplatin. This can be due either to decreased influx or increased efflux. It has long been presumed that cisplatin is taken up passively by the cell, as uptake is not saturable, nor is it inhibited by structural analogs. Accordingly, increased accumulation and therefore, increased toxicity can be attained *in vivo* by increasing the fluidity of the membrane by hyperthermia (Toffoli et al., 1989). However, as mentioned before, a role for transporters or gated channels has also been postulated in addition to passive diffusion. In this regard the copper transporter 1 (CTR1), has been shown to have a substantial role in cisplatin influx. Indeed, experiments with the yeast protein CTR1 and cisplatin, revealed that mutation or deletion of the CTR1 gene leads to stronger cisplatin resistance and to intracellular reduction of platinum levels in yeast and in mouse cells (Ishida et al., 2002). Interestingly, cisplatin accumulation in cells became increased when human CTR1 gene was overexpressed, although the ability of the drug to access its cytotoxic targets was unaltered (Holzer et al., 2004). On the other hand, it has been found that copper-transporting P type adenosine triphosphate (ATP7B), which regulates copper homeostasis in the cell, has a role in cisplatin efflux and is associated with cisplatin resistance *in vitro* (Komatsu et al., 2000), and in various cancers (Nakayama et al., 2004). Hence, expression of *ATP7B* in human carcinoma cells modulates sensitivity to cisplatin and copper through a more efficient efflux of the two agents (Holzer et al., 2004). Altogether these data indicate that there is a connected transport for copper and cisplatin because both copper and cisplatin (i) can reduce the uptake of each other, (ii) trigger the degradation and delocalization of CTR1, and (iii) also show bidirectional cross-resistance (Cepeda et al., 2007; Katano et al., 2002).

The multidrug resistance-associated protein MRP1 (ABCC1) and other MRPs are now known to play important roles in detoxification and chemoprotection by transporting a wide range of compounds, especially secondary metabolite conjugates of lipophilic substances with glutathione, glucuronate, and sulfate. Although they modulate the pharmacokinetics of many drugs, no direct correlation with cisplatin resistance has been found *in vitro* or in patients.

Whereas, another exporter protein implicated in cisplatin resistance through drug efflux is the ATP-binding cassette, sub-family C 2 (ABCC2 also known as MRP2 or cMOAT) (Kool et al., 1997).

One important consequence of selection of human cervical epidermal carcinoma cells KB in cisplatin is the reduced expression and internalization of Glut1 (glucose transporter 1), normally located on the cell surface. This reduces glucose uptake, resulting in induction of Sirt1 in cisplatin-resistant cells, causing cisplatin resistance (Liang et al., 2008). The mitochondrial phenotype associated with up-regulation of Sirt1 by glucose starvation, or Sirt1 transfection, decreases apoptosis and makes cells more resistant to cisplatin. Therefore, although Glut1 is not

proposed to directly transport cisplatin, the mislocalization of the transporter exacerbates the cisplatin resistance phenotype.
Reduced endocytosis is another way for cells to decrease uptake of cisplatin normally achieved *via* cellular fluid-phase endocytosis. Liang and coworkers (Liang et al., 2006) further tracked lipids in the endocytic recycling compartment (ERC) and found that the distribution of the ERC is altered in early-stage cisplatin-resistant human epidermoid carcinoma KB-CP.5 cells, compared with parental KB-3-1 cells. In addition, cells with a dispersed ERC under non permissive conditions were more resistant to cisplatin, indicating that this resistance might be due, in part, to reduced uptake of cisplatin resulting from an endocytic defect. Therefore, a defective endocytic pathway may constitute a cellular defense mechanism that protects the cell against toxic compounds from the exogenous environment by reducing influx of the compounds.

3.2.4.2 Inactivation of cisplatin by sulfur-containing molecules

Resistance to cisplatin because of enhanced inactivation by intracellular proteins, including the abundant nucleophilic glutathione (glutamylcysteinylglycine, GSH) and the cysteine-rich metallothionein, has also been reported (Godwin et al., 1992).
In particular, increased GSH may cause resistance by binding/inactivating cisplatin, enhancing DNA repair, or reducing cisplatin-induced oxidative stress (Siddik, 2003).
The metabolic synthesis of glutathione involves peptide bond formation between cysteine and glutamic acid (rate limiting step catalyzed by γ-glutamylcysteine synthetase, γ-GCS), followed by peptide bond formation with glycine. Cisplatin can be covalently linked to GSH after nucleophilic attack of the glutathione thiolate anion, and this complex can be transported out of the cell by the ATP-dependent glutathione S-conjugate export pump (Ishikawa and Ali-Osman, 1993). Conjugation with GSH inhibits the conversion of monoadducts to crosslinks, thereby reducing the cytotoxic potential of the adducts. In addition, GSH might protect cells by maintaining the dNTP pool size needed for DNA repair, by maintaining functional repair enzymes such as polymerase α, and by buffering endogenous drug-induced oxidative stress. This is consistent with reports that cells overproducing the Bcl-2 protein have correspondingly higher intracellular GSH levels, which may contribute to the anti-apoptotic functions of Bcl-2 (Hockenbery et al., 1993).
Increases in GSH have been demonstrated in a number of cisplatin-resistant tumor models, and confirmed in clinical studies (Wolf et al., 1987). Furthermore, in a panel of resistant ovarian tumor models, prominent elevations in GSH levels have been correlated directly with resistance. Such elevations may occur as a result of increased expression of the γ-GCS gene (Godwin et al., 1992; Lai et al., 1989). Overexpression of g-glutamyltransferase (γ-GT) in cisplatin resistance is also

observed, and this may further exacerbate inactivation of cisplatin (Daubeuf et al., 2002).

γ-GT is another key player in GSH homeostasis, and generates cysteinylglycine during GSH catabolism. Since cysteinylglycine is 10-fold more reactive toward cisplatin than is GSH, the overproduction of the more reactive thiol by γ-GT is potentially a major contributor to GSH-mediated resistance.

Metallothioneins are a family of cysteine rich proteins involved in Zn2+ homeostasis and in the detoxification of heavy metals such as cadmium. Metallothioneins bind to cisplatin in a protein:drug ratio of 1:10 and may affect sensitivity to the drug (Pattanaik et al., 1992).

The increase in metallothionein, up to five-fold over basal levels, have been observed in cisplatin-resistant murine and human tumor models (Kasahara et al., 1991). It is noteworthy that in some studies, changes in metallothionein levels in resistant cell lines, or in human ovarian tumor biopsies taken before and after cisplatin based therapy, have not been observed (Murphy et al., 1991). These variations in the reported data again emphasize the multifactorial nature of resistance and also that the increase in metallothionein is not necessarily an absolute requirement for cells to attain the resistance phenotype (Siddik, 2003).

3.2.4.3 Increased repair of platinum-DNA adducts

Cell lines selected for resistance to cisplatin after prolonged culture in the presence of cisplatin have significantly higher levels of repair than the corresponding parental cell lines, indicating that DNA repair is an important determinant of cisplatin resistance. Moreover, differential capacity to repair cisplatin adducts is postulated to be responsible for part of the variability in clinical response to cisplatin-based chemotherapy (Jones et al., 1994). A cell line established from the tumor of an ovarian cancer patient that was not responding to chemotherapy had a three-fold higher repair synthesis activity than the cell line established from the tumor of the patient prior to the onset of resistance (Lai et al., 1988).

Nucleotide excision repair is believed to be the main process by which platinum adducts are removed from DNA. Mammalian cells deficient in nucleotide excision repair are more sensitive to cisplatin than the corresponding wild type cells. Excision repair assays using both human cell extracts or a reconstituted excinuclease confirmed that the 1,3-d(GpTpG) adduct is more efficiently repaired than the 1,2-d(GpG) or 1,2-d(ApG) adducts. No repair is detected for a cisplatin interstrand crosslink (Zamble et al., 1996). Interestingly, enhanced expression of XPA mRNA is observed in tumor tissues from ovarian cancer patients that are resistant to platinum-based chemotherapy compared to levels in tissues of patients that respond favorably to chemotherapy. Furthermore ERCC1 mRNA levels correlate with response to platinum-based chemotherapy with the higher mRNA levels observed in tumors refractory to chemotherapy (Dabholkar et al., 1994). Of

great importance is the recent observation that testicular tumor cells have low levels of the XPA protein and the ERCC1–XPF endonuclease complex. These proteins are necessary for nucleotide excision repair, indicating that the unique sensitivity of testicular cells to cisplatin may be attributed to the inability of these cells to repair cisplatin damage (Köberle et al., 1999).

Cisplatin-resistant cell lines isolated after exposure to the drug *in vitro* frequently acquire the mutator phenotype associated with mismatch repair defects and are usually mutated in the hMLH1 genes (Aebi et al., 1996). Complementary studies with mismatch repair deficient cells have shown that inactivation of mismatch repair genes confers resistance to cisplatin. In particular, in colorectal and endometrial cancer cell lines. The importance of mismatch repair in clinical response was evaluated in a study that measured hMSH2 and hMLH1 expression in paired tumors of ovarian cancer patients obtained before and after platinum-based chemotherapy. The hMSH2 and hMLH1 expression decreased significantly after treatment, consistent with the ability of cisplatin treatment to select for mismatch repair deficient cells in an animal model. However, no association between the expression of either protein and overall survival was apparent, suggesting that hMSH2 and hMLH1 levels are not predictive of clinical response (Samimi et al., 2000).

HMG proteins are also implicated in cisplatin-mediated resistance. Several mechanisms have been proposed for how HMG domain proteins might modulate the sensitivity of cells to cisplatin but two of them seem to be the most feasible ones. The “repair shielding model” postulates that HMG proteins could protect cisplatin-DNA adducts from recognition by DNA repair enzymes (Ahmad, 2010). The second one, the so-called “hijacking model” establishes that HMG proteins could modulate cell cycle events subsequent to DNA damage and trigger cell death. Thus, this latter model postulates that the recognition by HMG cellular factors of cisplatin-DNA lesions would deviate them from their natural binding sites resulting in inhibition of vital cellular functions (Cepeda et al., 2007).

3.2.4.4 Increase of cisplatin adducts tolerance and failure of cell death pathways

A study of a panel of human ovarian cancer cell lines derived from patients who were or were not treated with cisplatin-based chemotherapy reveals that adduct level tolerance inversely correlates with sensitivity to cisplatin. Moreover, several reports have demonstrated that cisplatin-resistant cells have a higher capacity for adduct tolerance than the corresponding cisplatin sensitive parental cell lines (Johnson et al., 1997). The enhanced tolerance of cisplatin adducts has been correlated with the increased ability to replicate past cisplatin adducts. In order for platinated DNA to be replicated and tolerance to form, DNA polymerase must skip the platinum adduct, which is most commonly an intrastrand lesion. The classic DNA replication polymerases α, δ, and ε cannot bypass the lesion;

however, several polymerases have been shown to bypass intrastrand crosslinks by translesion synthesis namely, β, η, ζ, and ι (Havener et al., 2003). Overexpression of DNA polymerase β has been shown to lead to cisplatin resistance, while downregulation using anti-sense RNA leads to sensitivity (Albertella et al., 2005). The mutagenic consequence of replication bypass of a 1,2-d(GpG) adduct by DNA polymerase β was determined *in vitro* and revealed a 42% mutation frequency. The most frequent modifications are -1 deletions of the cytosine located immediately 5' of the adduct. In contrast, the overall mutation frequency *in vivo* is 21% and the most frequent modification are base substitutions, most of which occur at one of the platinated guanines (Hoffmann et al., 1996).

In addition to replication bypass, adduct tolerance could also be attained by inhibition of apoptosis. Alterations in the expression of regulators of apoptosis can alter the sensitivity of the cells to apoptosis following cisplatin treatment. For example, cells that express high levels of an apoptosis inhibitor or low levels of an apoptosis promoter would require higher levels of damage before they initiate apoptosis. Accordingly, reduced expression of Bax, which promotes apoptosis, is seen in cisplatin-resistant ovarian cancer cells (Sakakura et al., 1997) and, conversely, human head and neck squamous cell carcinoma cells expressing Bax are more sensitive to cisplatin, both in culture and in animals (Sugimoto et al., 1999). Furthermore, transfection of cells with Bcl-2 or Bcl-XL, which inhibit apoptosis, confers cisplatin resistance and downregulation of Bc-XL sensitizes cells to cisplatin (Taylor et al., 1999).

Caspases 3, 8, and 9 are important in cisplatin-induced apoptosis (Siddik, 2003). Loss of caspase 8 pathway was associated with cisplatin resistance in a squamous cell carcinoma of the head and neck (SCCHN) cell line. Decreased Fas expression or pathway activation after cisplatin may lead to inhibition of activation of caspases 3 and 8 (Siddik, 2003), and was associated with cisplatin resistance in germ cell tumors and ovarian cancer cells. Decreased cisplatin caspase 9 activation was noted in cells with normal mitochondrial cytochrome-c release and normal Bcl-2 and Bcl-XL expression (Stewart, 2007). Cisplatin-resistant cells have also been reported with abnormal mitochondrial membrane potential, intracellular distribution, or structure, and with up-regulation of cytochrome-c in the mitochondria, rather than release into the cytoplasm, in response to cisplatin (Isonishi et al., 2001).

Overall, there is preclinical evidence of an association of platinum resistance with abnormalities of a variety of apoptotic factors. The effect of altered expression of regulatory proteins appears to be cell type specific and is not predictive of clinical response to cisplatin-based chemotherapy. It is noteworthy however, that genes that are induced in response to cisplatin damage, are upregulated in some cell lines selected for resistance to cisplatin. Furthermore, studies with cells in culture might not always mirror the situation in tumors and therefore, cannot identify mechanisms of resistance operative *in vivo*. Studies with cell lines can serve as an initial screen for agents that might modulate cisplatin resistance. Some

mechanisms of resistance might only operate at the organism level and not at the cellular level (Kartalou and Essigmann, 2001).

3.2.5 Cisplatin toxicity

Despite the positive effects of platinum compounds patients receiving these agents experience severe side effects that limit the dose which can be administered. The ability to manage this induced toxicity is crucial for the success of cancer chemotherapy (Florea et al., 2011).
Toxicities associated with cisplatin range from mild to severe. The most common side effects are gastrointestinal toxicity, hearing loss (ototoxicity), decreased blood cell and platelet production in bone marrow (myelosuppression), damage of neurons (peripheral neuropathy), and damage to the kidney (nephrotoxicity), with the last two being the most serious (Rabik and Dolan, 2007) (Figure 3.7).

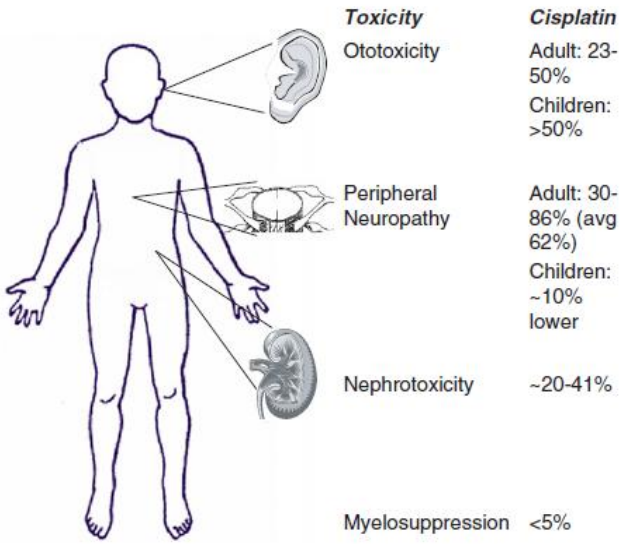

Figure 3.7 Toxicities associated with cisplatin treatment.

Gastrointestinal toxicity in the form of nausea and vomiting has been reported in most studies using fixed dosage regimen of cisplatin. The incidence of nausea ranges from 50 to 100%, and the incidence of vomiting ranges from 17 to 100%. Nausea and vomiting usually begins 1-6 hours after cisplatin administration. They usually do not last more than 24 hours, but anorexia and nausea may persist for up to a week (Wiltshaw and Kroner, 1976). Some investigators believe gastrointestinal toxicity is somewhat dose-dependent, whereas others believe severe nausea and vomiting can be seen at any dose level. Intravenous hydration before and after cisplatin seems to lessen the severity of drug-induced nausea and vomiting. A number of antiemetics have been used to prevent or treat nausea and vomiting. For the most part, none have been consistently helpful. Nabilone, has

been reported to have salutary effects against cisplatin induced gastrointestinal upset. Beneficial effects have also been reported with metoclopramide. Clearly, cisplatin-induced nausea and vomiting is a major problem, and more effective means to combat these bothersome side effects are needed (Von Hoff et al., 1979). Diarrhea has occasionally been encountered. No stomatitis has been reported with cisplatin administration (Von Hoff et al., 1979).

Ototoxicity occurs in approximately 23-54% of patients receiving cisplatin treatment, and in greater than half of pediatric patients receiving cisplatin. Platinum-based chemotherapeutic agents damage the outer hair cells of the cochlea (inner ear), resulting in functional deficits. The mechanisms underlying these troublesome side effects most likely involve the production of reactive oxygen species (ROS) in the cochlea, which can trigger cell-death pathways. One strategy to protect the inner ear from ototoxicity is pre-treatment with thiol-containing drugs that act as antioxidants, including sodium thiosulfate (STS), methionine, glutathione ester, and amifostine (Rybak and Whitworth, 2005).

Due to the renal excretion of cisplatin, the kidney accumulates a higher effective concentration of cisplatin than any other organ. This accumulation preferentially affects the terminal proximal tubule and the distal nephron and can cause either apoptosis or necrosis, depending on exposure time and concentration. Low, prolonged doses of cisplatin typically induce apoptosis, whereas necrosis is caused by short exposures to higher concentrations of cisplatin (Ikari et al., 2005). Similar to cisplatin-induced ototoxicity, nephrotoxicity related to cisplatin treatment is due to the production of ROS. ROS damage is thought to be mitigated by hypoxia-inducible factor 1a (HIF1a). Future studies hope to use activation of HIF-1 as a target for further protecting patients from nephrotoxicity, possibly with siRNA or gene therapy (Tanaka et al., 2005). The human organic cation transpoter (hOCT) has been proposed to be involved in potentiating cisplatin-induced nephrotoxicity in the proximal tubule. This transporter is expressed primarily in the kidney. After treatment with a concentration of cisplatin known to induce apoptosis, the hOCT2 substrate cimetidine was able to suppress cisplatin-induced apoptosis. Cotreatment of cisplatin with a hOCT2 inhibitor could lead to reduction in nephrotoxicity (Ciarimboli et al., 2005). Nephrotoxicity has largely been controlled by diuretics and pre-hydration of patients. Many anti-oxidant treatments, including tiopronin, N-acetylcysteine pre-treatment and sodium thiosulfate post-treatment, have been employed in protecting against nephrotoxicity (Dickey et al., 2005).

The dorsal root ganglia of the spinal cord are the primary location of cisplatin damage in the central nervous system. This explains the primary sensory neuropathy commonly observed in patients treated with cisplatin (Meijer et al., 1999). Cisplatin-induced neuropathy is characterized by decreased sensory nerve conduction velocity, possibly by acting as a calcium channel blocker. Co-treatment of rats with acetyl- L-carnitine was able to protect animals from neurotoxicity while having no effect on the anti-neoplastic activity of cisplatin (Pisano et al., 2003). Vitamin E has been shown to be decreased in patients treated

with cisplatin, and vitamin E deficiency causes a sensory neuropathy very similar to that observed with cisplatin treatment. Therefore, vitamin E was tested as a means to protect against cisplatin-induced neuropathy in a controlled clinical trial. Neurotoxicity, as measured by a peripheral neuropathy score, was significantly decreased in patients treated with cisplatin plus vitamin E, as compared with those treated with cisplatin alone (Bove et al., 2001). Erythropoietin has also been associated with neuroprotection *in vivo*. Carbamylated erythropoietin is currently undergoing further experimentation for long-term side effects, with future clinical trials planned (Bianchi et al., 2006).

Even though cisplatin has generally been regarded as nonmyelosuppressive, several investigators indicate hematologic toxicity may be dose-limiting. The drug affects all three blood elements. The incidence of leucopenia ranges from 0 to 50%; white blood cells counts of < 1500/mm^3 were seen in 3% of patients.. The degree of leucopenia seems to be dose-related and may be more common with the weekly schedule of drug administration. Leukopenia may be cumulative but is usually reversible. It is generally more severe in patients who have been extensively pretreated with many other cytotoxic drugs, particularly alkylating agents, and in patients who have had extensive prior radiotherapy (Talley et al., 1973). Thrombocytopenia has also been reported as a dose-limiting toxic effect of cisplatin. The incidence of thrombocytopenia (platelet count < 100,000/mm^3) ranges from 2 to 50%. Thrombocytopenia is dose-related and may be cumulative, but is usually reversibile; again, it is generally more severe in patients with a history of prior drug or radiation therapy. The incidence of cisplatin-induced anemia (hemoglobin drop of > 2.0 g/100 ml) ranges from 9 to 40%. There is no clear relationship between the dose or schedule of cisplatin administration and the severity of anemia. In summary, cisplatin can cause suppression of all three blood elements. Although it is still unclear which schedule or mode of administration causes the most myelotoxicity, it is clear that blood component support may be required when treating patients with cisplatin (Von Hoff et al., 1979).

3.3 Liposomal formulations

Despite being one of the most effective classes of chemotherapeutics, platinum drugs do have several significant shortcomings. Therefore, one of the key research areas in oncology has been to develop novel platinum analog drugs and engineer new platinum drug formulations to reduce side effects, to enhance the therapeutic index and the effectiveness against cisplatin-resistant tumors with a potential application in patients who relapse after first-line platinum-based treatment. However, in spite of over 30 years of intensive research, no more than 30 new platinum compounds, over 3,000, have exhibited adequate pharmacological advantages relative to cisplatin, in order to be tested in clinical trials (Fuertes et al., 2002). Only four were registered for clinical use (Boulikas et al., 2007), proving that the search for novel platinum compounds remains a difficult task.

The vast majority of platinum compounds synthesized have been abandoned because of low efficacy, high toxicity, low water insolubility and other reasons.
Another strategy to improve platinum drugs has been to improve the delivery of platinum therapeutics to tumors by use of nanoparticle drug delivery technology (Liu et al., 2013).
A key challenge in cancer therapy is to deliver anticancer drugs and other chemotherapeutics selectively to tumors while minimizing accumulation in normal tissues. Such targeted delivery can improve therapeutic efficacy while reducing toxicity. Although such differential drug delivery is generally not possible with small molecular drugs, nanocarrier-based delivery can overcome this challenge via the enhanced permeability and retention effect (EPR) that allows the extravasation of nanoparticles in the tumor area (Jain and Stylianopoulos, 2010). Indeed, a distinct feature of tumor tissue compared with normal tissue is its rapid formation of vasculature triggered by vascular endothelial growth factor and other growth factors overexpressed in various cancerous cells. These newly formed vessels do not have a smooth muscle layer so are defective and have a wider lumen, leading to irregular and leaky boundaries. The other key feature of tumor tissue is dysfunctional lymphatic drainage, resulting in ineffective clearance of extravascular proteins, particles, and white blood cells (Mattheolabakis et al., 2012).
Due to their large size, nanocarriers are not able to penetrate through the normal vasculature, but can penetrate through the leaky vasculature around tumor regions. Together with ineffective lymphatic drainage of tumor tissues, differential delivery/accumulation could be realized (Maeda and Matsumura, 2011). This effect, known as EPR effect, is considered to be passive targeting and is present in a wide variety of solid tumors. On the other hand, the passive accumulation of liposomes also occurs in tissues with discontinuous endothelium or fenestrated structure, such as the spleen, bone marrow and liver, while for tissues or organs with continuous non-fenestrated structure, where the tight endothelial junctions are ~5 nm, the extravasation of small liposomal carriers is prevented. The EPR effect is considered a heterogeneous process because it presents a high variability between different types of tumors, from patient to patient, and even within the tumor itself, where there are huge differences in vascular permeability. In addition, another important drawback associated with EPR effect is the penetration of nanoparticles in the tumor, which are able to cross not more than one or two cell layers (Zalba and Garrido, 2013). However, the pharmacokinetic profile of the encapsulated drug is basically modified in comparison with the free drug, with a view to obtain a pharmacodynamic advantage.
Liposomes were engenireed in 1965, when Alec Bangham and colleagues published the first description of swollen phospholipid systems that established the basis for model membrane systems. Within a few years, a variety of enclosed phospholipid bilayer structures consisting of single bilayers, initially termed ‘bangosomes’ and then ‘liposomes’, were described, and the early pioneers such as Gregory Gregoriadis, established the concept that liposomes could entrap drugs

and be used as drug delivery systems (Allen and Cullis, 2013; Gregoriadis et al., 1974).

Liposomes, small artificial vesicles of spherical shape defined as drug carrier nanoparticles, consist of an aqueous core entrapped by one or more phospholipid bilayers, where the polar head groups are oriented in the pathway of the interior and exterior aqueous phase. Liposomes membrane is composed of natural and/or synthetic lipids which are relatively biocompatible, biodegradable and non-immunogenic material (Akbarzadeh et al., 2013).

Liposomes are formed when a thin lipid film is hydrated with aqueous buffer solution (Bangham method), and are typically sonicated or repeatedly extruded through a 100 nm polycarbonate membrane to reduce their size and narrow their size distribution to afford small or large unilamellar liposomes, respectively (Akbarzadeh et al., 2013). In addition to the Bangham method, several other techniques, such as detergent-depletion, ether/ethanol injection, reverse phase evaporation, and emulsion methods, have been reported for preparing liposomes with high-entrapment efficiency, narrow size distribution, and long term-stability. Recently, some alternative methods including dense gas and supercritical fluid techniques have been introduced. Due to the differences in preparation methods and lipid compositions, liposomes can be classified according to their lamellarity (uni- and multilamellar vesicles), size (small [≤100 nm], intermediate [100-250 nm], or large [≥250 nm]), and surface charge (anionic, cationic, or neutral) (Chang and Yeh, 2012).

Liposomes allow the encapsulation of amphiphilic drugs, incorporating the hydrophilic drugs in the aqueous compartment and entrapping the lipophilic drugs in the bilayers. Encapsulation of hydrophobic drugs inside liposomes significantly increases their solubility in aqueous solution. The size, charge, and surface properties of liposomes, that influence the pharmacokinetic profile of the encapsulated drug, can be easily manipulated (increased drug stability via encapsulation) (Torchilin, 2005). It is thus possible to prolong the half-life of a cytotoxic drug in the systemic circulation (increased drug exposure time) and alter its biodistribution pattern, leading to elevated accumulation in tumor tissue (selective passive targeting) and a decreased dose to normal tissues. Formulation of therapeutics with liposomes can significantly reduce their side effect profile by avoiding non-targeted systemic drug exposure in the body. Upon accumulation at tumor sites, liposomes can also provide a unique opportunity to facilitate drug uptake into targeted cells or even localize the drugs to specific cellular compartments (Liu et al., 2013).

The use of liposomes as drug carriers presents some critical steps: the drug loading, the drug release, and the rapid cleareance of liposomes. However, due to extensive studies the efficacy of liposomal drug formulations has been enhanced by number of innovative strategies, such as remote drug loading (Haran et al., 1993), extrusion for homogeneous size (Olson et al., 1979), long-circulating (PEGylated) liposomes (Klibanov et al., 1990), triggered-release liposomes (Bibi et al., 2012), and ligand-targeted liposomes (Sapra and Allen, 2002).

A very early observation was the difficulty in retaining some types of molecules entrapped in the liposome (Gregoriadis, 1973). Changing the content of the liposome bilayer, in particular by incorporating of of cholesterol (Allen and Cleland, 1980) was shown to 'tighten' fluid bilayers and reduce the leakage of contents from liposomes. Switching from a fluid phase phospholipid bilayer to a solid phase bilayer also reduced leakage, as did incorporation of sphingomyelin into liposomes (Cullis and Hope, 1980).

Similar to biological membranes, liposomes have low permeability to hydrophilic drugs and high permeability to hydrophobic drugs. Indeed, to this day, retention of highly hydrophobic drugs such as paclitaxel in liposomes is problematic (Cabanes et al., 1998). A major advance in this area was the development of drug loading in response to transmembrane pH gradients. The term "remote loading" is often used to describe this procedure, because the drug is loaded after the vesicles are formed. The advantage of this is that the loading of the drug can be performed independent of the time and site of liposome manufacture. (Madden et al., 1990).

The retention properties of drugs in liposomes are drug dependent; drugs such as doxorubicin precipitate readily inside liposomes following accumulation and have excellent retention properties, whereas other drugs, such as ciprofloxacin, which do not readily precipitate, are more difficult to retatin (Maurer et al., 1998).

It is important to keep in mind that drug entrapped in liposomes is not bioavailable; it only becomes bioavailable when it is released. (Johnston et al., 2006). The drug must be delivered to the disease site and become bioavailable at a level within its therapeutic window, and at a sufficient rate, for a sufficient period, to have optimal therapeutic activity. Therefore, being able to trigger the release of liposomal contents once they reached the target site would lead to improvements in therapeutic outcomes (Allen and Cullis, 2013).

Two main types of triggers have been explored, remote triggers such as heat, ultrasound and light, and local triggers that are intrinsic to the disease site or cellular organelles such as enzymes and pH changes (Allen and Cullis, 2013).

The first trigger for drug release was hyperthermia (remote trigger); delivery of liposomal methotrexate was demonstrated to be four-fold higher in heated tumors versus non-heated control tumors (Weinstein et al., 1979). Other recent advances in remote-triggered release systems include the use of ultrasound to trigger drug release from echogenic ("bubble") liposomes; the use of light as a trigger in photosensitive liposomes; and magnetically responsive liposomes (Allen and Cullis, 2013). Liposomes can be designed to release their contents in the enzyme rich, low pH environment of endosome and lysosomes through the use of pH-triggered approaches. Liposomes can also be designed to release their contents through the use of lipids of peptides that facilitate fusion with the target cell membrane (Guo and Szoka, 2001). Enzyme-triggered release of liposome contents has also been studied for a variety of different enzymes including: phospholipase C, phospholipase A2, alkaline phosphatase, and matrix metalloproteinases (Allen and Cullis, 2013). However, in general, triggered

release approaches, although promising in concept, have been disappointing in practice.

Another problem was the rapid clearance of liposomes from circulation by uptake into the cells of the mononuclear phagocyte system (MPS), predominantly in the liver and spleen (Juliano and Stamp, 1975). The rapid uptake of liposomes into the MPS substantially reduced their distribution to other tissues of the body, and were also implicated in toxicities to the MPS organs (Ellens et al., 1982). Initially, attempts were made to increase the circulation half-life of liposomes by MPS blockade using large pre-doses of liposomes that contained no drug ('empty' liposomes). Also the reduction in vescicle size modestly improved the half life circulation (Hwang et al., 1987). The opsonization of liposomes by serum proteins was suggested as a likely mechanism for the rapid clearance of liposomes into the liver and spleen (Hoekstra et al., 1981), and modifications of the membrane surface led to improvements in their circulation half-lives. Early research focused on identifying differences between plain or unmodified phospholipid membranes and biological membranes with a surface layer rich in carbohydrates. Addition of the monosialoglyprotein (GM1) to liposomes composed of egg phosphatidylcholine (egg PC), in combination with cholesterol for membrane rigidity, resulted in the first long-circulating liposomes that did not require MPS blockade to achieve the effect. Substitution of sphingomyelin for egg PC resulted in even longer circulation half-lives, and lower uptake of liposomes into the liver (Allen and Chonn, 1987). The mechanism was postulated to be due to increases in the surface hydrophilicity of the liposomes imparted by the gangliosides; these long-circulating liposomes were termed 'Stealth' liposomes, a term subsequently adopted to apply to liposomes sterically stabilized with polymers such as polyethylene glycol (PEG). Indeed, research pointed the way towards a simpler way of increasing the circulation half-life of liposomes. The covering of liposomes surface with the synthetic neutral polymer PEG led to the formation of a protective hydrophilic layer and resulted in substantial reductions in the rapid clearance of liposomes into the MPS (Klibanov et al., 1990).

Moreover, the use of liposomes conjugated with a specific ligand, which is able to recognize a specific expression pattern of membrane associated proteins such as receptors or membrane transport system, has been proposed to achieve an active-targeting (Zalba and Garrido, 2013).

Immunoliposomes combining the specificity of monoclonal antibodies (mAb) with the properties of liposomes in drug delivery have been described as the most specific targeted formulations (Pasquetto et al., 2011). Although the most common ligands reported in the literature coupled to nanoparticles are folate, transferrin and galactosamine, they are not considered tumor-specific, contrary to mAb used against tumor cells (Pasquetto et al., 2011). For this therapy, a high density of the antigen or receptor in the surface of the tumor cells is necessary.

Few targeted liposomes for platinum derivatives have been reported in the literature. Indeed, the techniques for producing ligand-targeted liposomes are

tedious, difficult to control, expensive, and lead to poorly defined systems that are often rapidly cleared from the circulation (Allen and Cullis, 2013).

These advanced techniques have indeed led to several liposomal formulations in clinical use, with AmBisome® (Astellas Pharma US Inc, Northbrook, IL, USA) and Doxil® (Johnson and Johnson, New Brunswick, NJ, USA) being the most successful examples. Doxil, a pegylated liposomal formulation of doxorubicin, is the first liposomal anticancer formulation approved by the US Food and Drug Administration (FDA); it received the approval in 1995 for the treatment of chemotherapy refractory acquired immune deficiency syndrome (AIDS)-related Kaposi's sarcoma (Immordino et al., 2006). In human studies, Doxil was found to have pharmacokinetics dramatically different to those of doxorubicin. Doxil has a half-life of approximately 90 hours, whereas doxorubicin has an initial distribution half-life of approximately 5 minutes followed by a terminal half-life of 20-48 hours. More importantly, as the very first proof of the enhanced permeability and retention effect observed in humans, Doxil was found to accumulate preferentially in tumor tissue through passive targeting (Gabizon et al., 1994). The differential pharmacokinetic profiles between Doxil and doxorubicin also led to differing toxicity profiles. Doxil has significantly reduced cardiotoxicity, allowing prolonged and repeated drug treatments that were previously not possible with doxorubicin. In addition to optimized biodistribution, tumor accumulation, and reduced cardiac toxicity, superior efficacy was observed in Kaposi's sarcoma and recurrent ovarian cancer, and equivalent efficacy was observed in metastatic breast cancer and multiple myeloma (Safra et al., 2000).

Currently, there are more than twenty liposome-based drugs approved for clinical use (Table 3.1) and more are in various stages of clinical trials.

Table 3.1 Liposomal formulation currently used in clinical application.

Product	Drug	Indications	Company
Doxil™/Caelyx™	Doxorubicin	Kaposi's sarcoma	Sequus Pharmaceutical
Myocet®	Doxorubicin	Metastatic breast cancer	Sopherion Therapeutics
DaunoXome™	Daunorubicin	Kaposi's sarcoma, breast and lung cancer	NeXstar Pharmaceuticals
Amphotec™	Amphotericin-B	Fungal infections, Leishmaniasis	Sequus Pharmaceutical
Fungizone®	Amphotericin-B	Fungal infections, Leishmaniasis	Bristol-Squibb, Netherland
AmBisome®	Amphotericin-B	Fungal infections	NeXstar Pharmaceuticals
Abelcet®	Amphotericin-B	Fungal infections	The Liposome Co.
VENTUS™	Prostaglandin-E_1	Systemic inflammatory diseases	The Liposome Co.
ALEC™	Dry protein-free powder of DPPC-PG	Expanding lung diseases in babies	Britannia Pharmaceuticals
Topex-Br	Terbutaline sulfate	Asthma	Ozone
Depocyt	Cytarabine	Cancer therapy	Skye Pharmaceuticals
Novasome®	Smallpox vaccine	Smallpox	Novavax
Avian retrovirus vaccine	Killed avian retrovirus	Chicken pox	Vineland Laboratories
Epaxal–Berna vaccine	Inactivated hepatitis-A virions	Hepatitis A	Swiss Serum and Vaccine Institute
Doxil®	Doxorubicin Hcl	Refractory ovarian cancer	ALZA
Evacet™	Doxorubicin	Metastatic breast cancer	The Liposome Co.
VincaXome	Vincristine	Solid Tumors	NeXstar
Mikasome®	Amikacin	Bacterial infection	NeXstar
Autragen™	Tretinoin	Kaposi's sarcoma	Aronex Pharmaceutical
Shigella Flexneri 2A vaccine	*Shigella flexneri* 2A	*Shigella flexneri* 2A infections	Novavax
Nyotran™	Nystatin	Systemic fungal infections	Aronex Pharmaceutical

Liposomes have been extensively studied as drug carriers in the pharmaceutical and medical fields.
For instance, Epaxal and Inflexal V are both vaccine products using the virosome-based antigen delivery system for commercial use. Virosomes are reconstituted virus liposomes, constructed without the genetic information of the virus making them unable to replicate or cause infection. The incorporation of viral membrane proteins or peptide antigens into liposomes has been shown to potentiate cell-mediated and humoral immune response, and generate solid and durable immunity against the pathogen (Zalba and Garrido, 2013).

3.3.1 Liposomal formulations for cisplatin

It is in the case of anticancer drugs that the liposome system represents an interesting challenge regarding the improvement of their therapeutic activity by reducing the side effects or/and increasing the antitumor efficacy (Gabizon, 2002). Within this type of drugs, platinum derivatives have been widely investigated in this field, especially cisplatin, due to its significant toxicity in patients. However, at the moment there are no formulations for this drug approved by the FDA, although some of them are being evaluated in Phase III clinical trials (Zalba and Garrido, 2013).
SPI-007 (Alza Corp., California, CA, USA) is the first liposomal formulation of cisplatin. It is a sterically stabilized, PEGylated, long circulating liposome, encapsulating cisplatin. The bilayer consists of hydrogenated soy phosphatidylcholine (HSPC), cholesterol (CH) and DSPE-PEG2000 (Newman et al., 1999). The half-life was estimated to be 16 hours in mice, compared with cisplatin which has a half-life of 0.24 hours. In addition to a longer blood circulation time, SPI-77 exhibits a 60-fold larger plasma area under the curve (AUC, area under the plasma drug concentration-time curve reflects the actual body exposure to drug after administration of a dose of the drug; it is expressed in mg*h/L), three-fold higher peak plasma levels, a four-fold reduction in the amount of platinum delivered to the kidneys, and a 28-fold higher tumor AUC compared with cisplatin (Newman et al., 1999). Despite its superior pharmacokinetic properties, SPI-77 did not demonstrate enhanced therapeutic efficacy over cisplatin in preclinical experiments in a separate study of M-109 lung carcinoma, J-6456 lymphoma, C-26 colon carcinoma, and A-375 melanoma (Bandak et al., 1999).
To explain this lack of *in vivo* efficacy, Zamboni et al. developed a microdialysis study in mice (Zamboni et al., 2004). They found a high tumor accumulation of liposomes associated with a low antitumor effect, suggesting a very slow release of cisplatin from this formulation. Indeed, they also found low DNA-adduct concentration after liposome administration, in accordance with the poor antitumor efficacy. *In vitro* release experiments showed that less than 10% of cisplatin was released from the liposomes (Zalba and Garrido, 2013).

The lack of efficacy of SPI-007 has also been demonstrated in clinical trials. For example, in a Phase I study in pediatric patients, a range of doses between 40 and 420 mg/m^2 applied every 4 weeks, showed no significant therapeutic response. In this study total platinum clearance of SPI-077 displayed a value $\leq$ 20 ml/h, dramatically lower than the value reported for cisplatin, 10-20 l/h/m^2. Regarding the urine excretion, only 4% of the applied dose of SPI-077 was found at 72 hours, while for the free drug it was between 27 and 35% at 48 hours (Veal et al., 2001).

Similar results were found in adults (Harrington et al., 2001). Indeed, in several Phase II studies of patients with inoperable head and neck cancer, advanced non-small-cell lung cancer (NSCLC), or platinum-sensitive recurrence of ovarian cancer SPI-77 did not produce significant clinical response rates, even though the formulation was shown to be well tolerated (Harrington et al., 2001). SPI-77 did not induce any of the toxicities commonly associated with platinum-based chemotherapy, such as nephrotoxicity and neutropenia. Side effects include mild gastrointestinal toxicity and mild anemia and muscle weakness. However, the lack of therapeutic efficacy was likely due to slow and inefficient release of platinum from SPI-77, as shown in preclinical studies. On this basis, Harrington et al. concluded in their Phase I/II study that a change or reformulation of SPI-077 should be taken into consideration before continuing with its development (Harrington et al., 2001).

Lipoplatin^{TM} (Regulon, Inc., Athens, Greece) is one of the most promising liposomal formulations for cisplatin. It is a PEGylated formulation that differs from SPI-77 in several ways. First, the loading method used in lipoplatin is based on formation of reverse micelles between cisplatin and dipalmitoyl phosphatidyl glycerol, while the mechanism of cisplatin encapsulation in SPI-77 is totally passive. Second, the lipoplatin formulation uses anionic dipalmitoyl phosphatidyl glycerol lipid and neutral soy phosphatidylcholine lipid, whereas SPI-77 uses only neutral lipids. Third, the cisplatin to total lipid ratio is around 1:10 in the case of lipoplatin, and much lower in SPI-77, 1:70 (Stathopoulos and Boulikas, 2012; Veal et al., 2001). Results in several Phase II and III trials seem to be encouraging (more details in section 3.3.2.).

pH-Sensitive liposomal formulation (SpHL-CDDP) is a long circulating and pH-sensitive liposome formulation for cisplatin. These liposomes have been prepared with dioleoylphosphatidylethanolamine (DOPE) and an unsaturated phosphatidylethanolamine (PE), which presents fusogenic properties to enhance the drug release into the cytosol. The formulation also includes cholesteryl hemisuccinate (CHEMS) and DSPE-PEG 2000. The incorporation of DOPE and CHEMS in the formulation leads to liposome destabilization and rapid release at acid pH (De Oliveira et al., 1998). Under this condition the release of the entrapped drug is very fast, representing an advantage in the case of the tumor site, where the environment reaches acid pH values. Although the results for SpHL-CDDP seem to be very promising, there are currently few articles in the literature regarding this formulation. One of the main objectives for these

liposomes was focused on the improvement in cisplatin release, because this was the major point responsible for SPI-077 failure (Zalba and Garrido, 2013).
The release of encapsulated drugs from liposome carriers upon their deposition in tumor tissues is critical to confer antitumor activity. LiPlaCis®, a novel liposomal formulation of cisplatin, is designed to be degraded by secretory phospholipase A_2. Given that secretory phospholipase A_2 is relatively abundant in tumor sites, triggered drug release in tumor tissue is expected. Although LiPlaCis was designed to be decomposed by secretory phospholipase A_2 specifically, other factors also contributed to the degradation of the particles because no correlation between the baseline levels of secretory phospholipase A_2 and the initial half-life of LiPlaCis was observed in patients. In addition, renal toxicity was not prevented by treatment by LiPlaCis and acute infusion reactions were observed in many patients even with premedication. The poor safety profile of LiPlaCis led to early cessation of this particular formulation in the Phase I stage and LiPlaCis requires reformulation to enable further development (Liu et al., 2013).
SPI-077 B103 (Alza Corp., USA) represents a modification of SPI-077. The difference between the two formulations is in the replacement of the HSPC by other unsaturated phospholipids to enhance the release of cisplatin from these new liposomes. However, preclinical studies did not suggest a great improvement with regard to SPI-077 (Zamboni et al., 2004).
Thermosensitive liposomes (LTSL) of cisplatin were developed by Woo et al. (Woo et al., 2008). The composition of LTSL is dipalmitoylphosphatidylcholine (DPPC), monostearoylphosphatidylcholine (MSPC) and DSPE-PEG2000. MSPC is a lysolipid that confers a rapid release of the drug when liposomes are heated at 40°-42°C. At this temperature the lysolipid is able to stabilize the pores formed at the melting temperature allowing a release of 95% of the entrapped drug within the first 5 minutes (Hossann et al., 2012). However, in the first approach in preclinical *in vivo* studies the formulation presented poor stability. This might be due to the presence of some components in blood, such as plasma proteins. They can interact with the lipids of the formulation increasing the drug leakage. Thus, albumin and IgG, the major protein components in blood, influence the stability of LTSL, representing an important issue for the efficacy of this formulation (Hossann et al., 2012). ThermoDox which is currently in Phase III is the most advanced clinical and commercial TSL formulation (Manzoor et al., 2012).
New technologies and novel systems with improved encapsulation efficiency, drug loading capacity, and active targeting capability have been reported. Although many of these platforms are still in the early development stage (Liu et al., 2013).

3.3.2 Lipoplatin

Lipoplatin™ is a liposomal formulation of the FDA approved cisplatin, produced by the biopharmaceutical company Regulon. Regulon Inc. with headquarters in

Mountain View (California), and R&D in Alimos, Athens (Greece), is a biotechnology company focusing on the discovery, testing and commercialization of anticancer drugs and with demonstrated abilities in the liposomal encapsulation of toxic drugs (Stathopoulos et al., 2005).

Liposomes of lipoplatin are composed of dipalmitoyl phosphatidyl glycerol (DPPG), soy phosphatidyl choline (SPC-3), cholesterol and methoxypolyethylene glycol-distearoyl phosphatidyl-ethanolamine (mPEG2000-DSPE). Lipoplatin is composed of 8.9% cisplatin and 91.1% lipids (w/w). It has an opaque appearance reflecting its liposomal nature and is being provided in 50-ml glass vials of 3 mg/ml (concentration refers to cisplatin) (Figure 3.8). Lipoplatin is stored at 0-4°C and has an expiration date of three years. The concentration of 3 mg/ml of cisplatin in lipoplatin exceeds the solubility of the free drug, cisplatin, usually provided as a 0.5 -1 mg/ml solution for intra venous infusion. Non-PEGylated liposomes are taken up by liver macrophages and destroyed with a half-life in body fluids of 20 minutes (Martin et al., 1998). On the contrary, PEGylated liposomes such as those of lipoplatin display a half-life of 120 hours in body fluids (Stathopoulos et al., 2005).

A

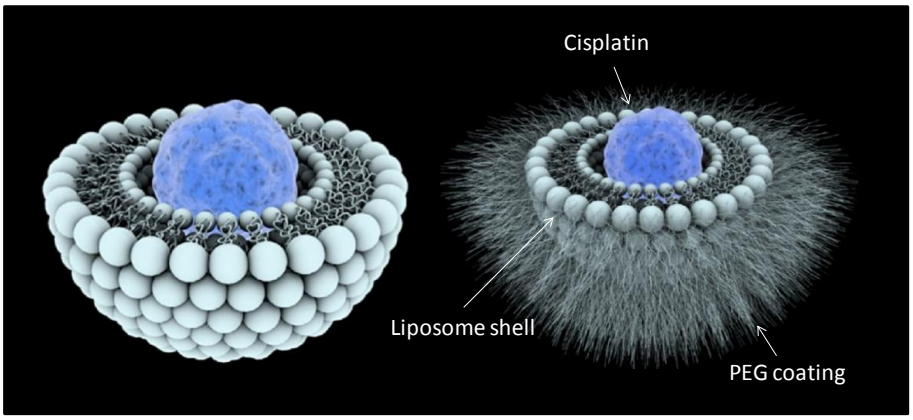

B

Figure 3.8 Depiction of a lipoplatin nanoparticle **(A)**. The model shows the lipid bilayer and the cisplatin molecules in its lumen (blue spheres) with the PEG molecules on its surface (white hair-like structures) coating the particle with a hydrophilic inert polymer giving the ability to escape detection from macrophages and evade immune surveillance. **(B)** Lipoplatin 50/ml glass vial.

Lipoplatin formulation is based on the formation of reverse micelles between cisplatin and DPPG under special conditions of pH, ethanol, temperature, ionic strength and other parameters. Cisplatin-DPPG reverse micelles are subsequently converted into liposomes by interaction with neutral lipids. This process, involving various steps sensitive to temperature, ethanol concentration, pH, ionic strength, type of salt, type of lipid and other sensitive parameters leads to very high encapsulation efficiencies (95-97%). About 15 repeated extrusions are performed using a Thermobarrel Extruder through membranes of 0.2, 0.1, 0.08 and 0.05 mm pore sizes under pressure in ultra pure nitrogen to an average size of 110 nm. Particles of larger sizes (100-150 nm) might display a better extravasation to tumors over normal tissue compared to smaller particles (60-100 nm) (Boulikas, 2007).

The lipoplatin formulation uses several advancements in its liposome encapsulation: i) the anionic lipid DPPG gives lipoplatin its fusogenic properties presumably acting at the level of entry of the drug through the cell membrane after reaching the target tissue; ii) the total lipid to cisplatin ratio is low (10:1 mg lipid/mg cisplatin) in lipoplatin, which means that less lipid is injected into the patient; and iii) the PEG polymer coating used on lipoplatin is meant to give the drug particles the ability to pass undetected by the macrophages and immune cells, to remain in the circulation of body fluids and tissues for long periods, to extravasate preferentially and to infiltrate solid tumors and metastatic tissue through the altered and often compromised tumor vasculature (Boulikas, 2007).

Although the mechanism of entry of lipoplatin nanoparticles into cells has not been deciphered, tumor cells were proposed to uptake more avidly lipoplatin particles because of:

- their tendency to uptake nutrients from the environment;
- the proposed fusion of liposomes with the tumor cell membrane;
- the higher concentration of the drug into tumors (Boulikas, 2009).

Lipoplatin nanoparticles were proposed to diffuse to the extracellular space and to be taken up more avidly by the cell membrane of the tumor cell compared to normal cell (five times more). This is supposed to arise from the avidity of tumor cells for nutrients (the lipid shell of lipoplatin composed of lipids is mistaken as a nutrient).

The fusion between liposomes and the cell membrane was suggested based on the fusogenic properties of DPPG and lipids integrated into the shell of lipoplatin (Figure 3.9).

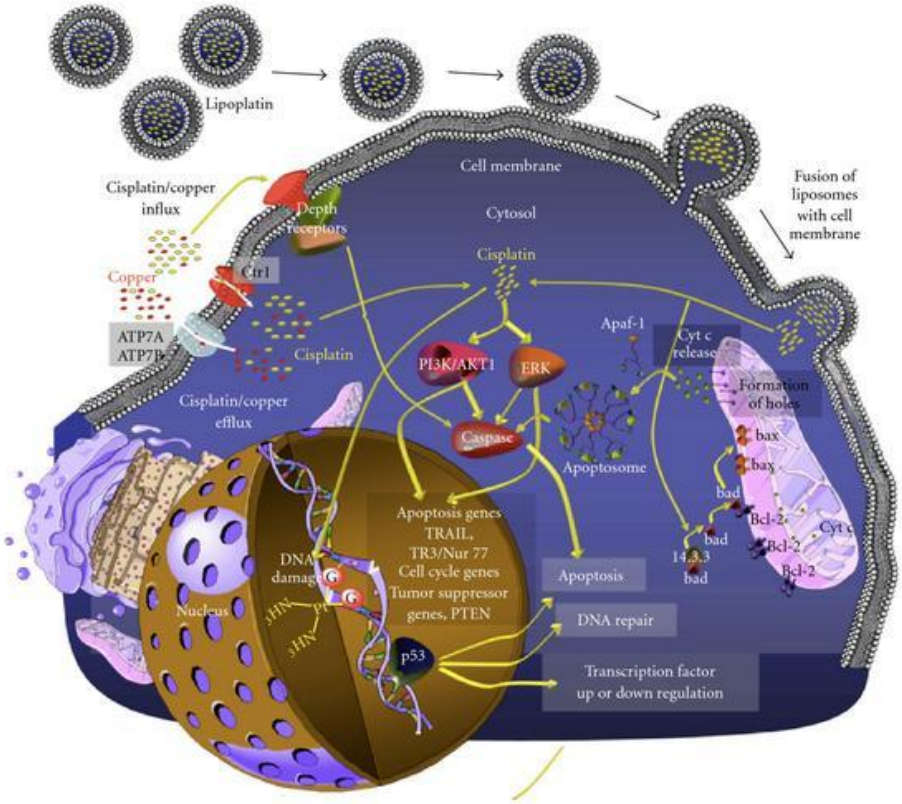

Figure 3.9 Penetration of lipoplatin nanoparticles through the cell membrane of tumor cells.

Subsequent cell culture studies, where the lipids of the lipoplatin nanoparticle were labelled with fluorescein isothiocyanate (FITC), established the rapid uptake and internalization of the nanoparticles. In these studies the fluorescent nanoparticles were incubated with MCF-7 breast cancer cells in culture for various times, ranging from 5 minutes to 24 hours. The study has provided proof that the lipids of lipoplatin are transferred initially (in less than 5 minutes) to the cell membrane of MCF-7 cells in culture and are then (from 5 minutes to 24 hours) docked to the interior of the cell. The implications of this process are profound because lipoplatin demonstrated to deliver its toxic payload readily (within 5 min after reaching its cancer cell target), resulting in the destruction of the cancer cell; the membrane fusion is proposed to modulate signalling, an important process for cancer cell proliferation; moreover, lipoplatin could be used in patients previously treated with other platinum compounds (oxaliplatin, carboplatin, cisplatin) who have developed resistance to these drugs at the level of the cell membrane, bypassing this major type of resistance. Cells of patients in such tumors are impermeable to platinum drugs because of downregulation of the membrane cisplatin transporters (Ctr1). Provided that the platinum drugs in the market (cisplatin, oxaliplatin, carboplatin) are used in over 50% of human cancers and the fact that resistance is a major hurdle of chemotherapy, lipoplatin offers hopes to treat resistant tumors (Stathopoulos and Boulikas, 2012).

Due to its particle size lipoplatin has the ability to target tumors and metastasis following intravenous administration, using the compromised endothelium of the

tumor vasculature sprouted during neoangiogenesis; this process, known as extravasation (Figure 3.10) has been demonstrated injecting in an immunodeficient mouse, implanted with MCF-7 human breast tumor cells, liposomes, with the same shell structure as lipoplatin, carrying the reporter β-galactosidase gene to reveal the sites of transgene expression after relocalization of the gene vehicles. Preferential staining of the tumors, especially of the vascular system around the tumors, was shown. Even more important, the subcutaneous vasculature developed to supply the tumor with nutrients had a more pronounced staining indicating that cells (presumably endothelial cells) of tumor vasculature are the targets for entry of the liposome and expression of the foreign gene. This observation leads to the conclusion that lipoplatin not only kills tumor cells but also cells of the tumor vasculature. It could therefore be classified also as an anti-angiogenesis agent. (Boulikas, 2007). Also in surgical specimens from patients, lipoplatin showed an enhanced concentration in tumors and metastases, at levels up to 200-fold higher compared to the adjacent normal tissue (Stathopoulos and Boulikas, 2012).

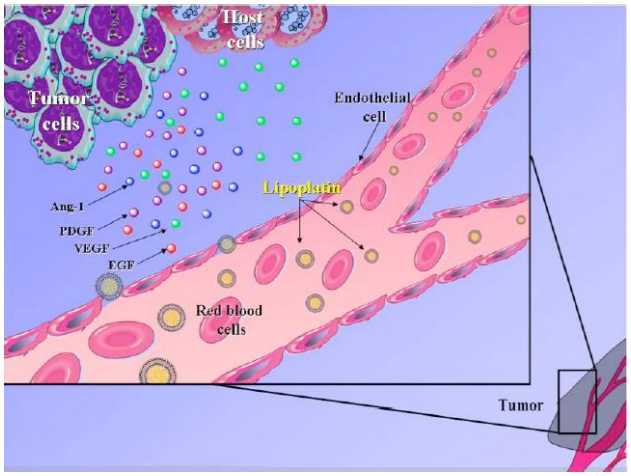

Figure 3.10 Lipoplatin nanoparticles extravasation process.

Furthermore, lipoplatin showed reduced adverse side effects compared with its parental compound, cisplatin. Preclinical study compared lipoplatin and cisplatin cytotoxicity *in vitro* in established cell lines derived from NSCLC, renal cell carcinoma, and in normal hematopoietic cell precursors. The results showed a superior cytotoxicity in all tumor cell models and a much lower toxicity in normal cells for lipoplatin compared with cisplatin, suggesting a higher therapeutic index for the liposomal compound (Arienti et al., 2008). Preclinical studies on nude mice, rats, and severe combined immunodeficiency mice have highlighted the milder adverse effects, especially to the kidney, of lipoplatin compared with cisplatin, confirming *in vitro* results (Boulikas, 2004; Devarajan et al., 2004). In subsequent studies, mice and rats injected with cisplatin developed renal insufficiency with clear evidence for tubular damage, but those injected with the same dose of lipoplatin were almost completely free of kidney injury. Treatment

of dogs with lipoplatin led to the conclusion that the drug can be safely administered to clinically normal dogs at dosages of up to 150 mg/m^2 without the need for concurrent hydration protocols. The maximum tolerated dose (MTD) of unencapsulated cisplatin in dogs has been establishe as 70 mg/m^2. Therefore, lipoplatin would allow the safe and repeated administration of doses higher than the MTD of unencapsulated cisplatin (Marr et al., 2004).
Moreover, the intrapleural administration of lipoplatin in an animal model seems to offer a more effective therapeutic index while improving tolerability. Wistar rats were treated with doses of 10 mg/kg lipoplatin (intravenously) versus 10 or 20 mg/kg lipoplatin (intrapleurally) corresponding to 60 and 120 mg/m^2, respectively, in humans. The authors noted minor fibrotic changes in the pleura of rats injected intrapleurally, and mild kidney changes in rats injected intravenously, as expected (Froudarakis et al., 2011).

3.3.2.1 Clinical trials Phase I studies

There are more than 16 trials concerning lipoplatin.
The human testing of this new agent primarily required pharmacokinetics studies and the definition of toxicity by investigating the MTD as well as the dose-limited toxicity (DLT) (Stathopoulos and Boulikas, 2012).
A Phase I study of 27 patients with different malignancies was performed (19 pancreatic carcinomas, 6 renal cell carcinomas, 1 gastric cancer and 1 squamous cell carcinoma of the head and neck (SCCHN)). Lipoplatin was administered as an 8 h infusion diluted in 1 L 5% dextrose, repeated every two weeks. The intravenous infusion was slow to reduce side effects (~25 mg/(m^2 hours)). There was no need for pre- or post-hydration of the patient with lipoplatin. This is in contrast to cisplatin chemotherapy that requires admittance of the patient the night before infusion for hydration, as well as extended stay in the hospital after infusion for post hydration, to reduce the nephrotoxicity of the drug. Interestingly, the maximum tolerated dose (MTD) was not reached even when the dose was increased up to 350 mg/m^2 in one patient as a single infusion. The highlights of this study were that lipoplatin had mild hematological and gastrointestinal toxicity, did not show any nephro-, neuro- and oto-toxicity, did not cause hair loss and was void of most other side effects characteristic of cisplatin treatment. Grade 1 and 2 myelotoxicity (neutropenia), and grade 1 and 2 gastrointestinal tract toxicity (vomiting) were observed only at the dose of 125 mg/m^2. No other toxicity was observed even with repeated doses. A further finding was the long circulation of lipoplatin, a property necessary for its preferential extravasation through the leaky vasculature of tumors. Indeed, the half-life of total platinum in human plasma was determined to be 60-117 hours depending on the dose. At the dose of 100 mg/m^2 the half-life was 117 hours (about 5 days) compared to ~6 hours for cisplatin (Stathopoulos et al., 2005). Although measurement of the response rate was not a primary goal of the study, 3 (11.1%) of 27 patients were

recorded to have achieved a partial response; of the remaining 24 patients, 14 (51.9%) achieved stable disease and clinical benefit in a follow-up of 2-5 months (Stathopoulos et al., 2005). Provided that all patients had failed previous chemotherapy, that they all were at stage IV of their disease and had a rather poor performance status, this finding was very encouraging.

In a different Phase I study, lipoplatin dose-escalated at 100 mg/m^2 by increments of 10%, was combined with gemcitabine 1000 mg/m^2 in 13 patients with refractory or resistant NSCLC. The dose of 120 mg/m^2 of lipoplatin was defined as the MTD in its combination with gemcitabine (Froudarakis et al., 2008). The drug was also successfully used for mesothelioma by the same group (Karpathiou et al., 2007). The small number of 13 patients was not efficacious enough to determine ample data concerning toxicity. In both these aforementioned studies, there was also a defect in that all of the patients had undergone chemotherapy pretreatment when they were recruited and the efficacy of lipoplatin was tested.

A proper third Phase I trial was eventually performed. The main objective of this study was to determine the DLT and MTD of lipoplatin tested as a single agent and in combination with a second cytotoxic agent. The selected second agent was paclitaxel. Sixty-six patients with NSCLC were recruited. Thirty-nine patients comprised the group that received lipoplatin monotherapy, and 27 patients were given lipoplatin in combination with paclitaxel. It was determined that 350 mg/m^2 was the DLT and 300 mg/m^2 the MDT. The results of the combined treatment evaluation determined the DLT as 250 mg/m^2 and the MTD, 200 mg/m^2. Nausea, vomiting, fatigue, and neutropenia were not higher than grade 1-2, and other adverse reactions in a small percentage of patients reached grade 3. In the combined modality, other side effects, such as neurotoxicity, were observed, and this was attributed to paclitaxel. Grade 1 nephrotoxicity was observed in a small percentage of patients, but this was only temporary (Stathopoulos et al., 2010).

Intravenous infusion of lipoplatin results in tumor targeting in four independent patient cases (one with hepatocellular adenocarcinoma, two with gastric cancer and one with colon cancer) who underwent lipoplatin infusion followed by a prescheduled surgery ~20 hours later. Direct measurement of the platinum levels in specimens from the excised tumors and normal tissues showed that the total platinum levels were on average 10-171 times higher in malignant tissue compared to the adjacent normal tissue specimens; most effective targeting was observed in colon cancer, with an accumulation up to 200-fold higher in colon tumors compared to normal colon tissue (Boulikas et al., 2005).

3.3.2.2 Clinical trials Phase II studies

A pilot Phase II study using lipoplatin at dose levels of 75, 100, 125 mg/m^2 every 14 days in combination with gemcitabine 1000 mg/m^2 was tested on 26 patients (19 patients with pancreatic cancer and 7 with NSCLC). All patients were resistant to previous first- or second-line chemotherapy and lipoplatin plus

gemcitabine was given as a third-line treatment. No renal toxicity, neuropathy, ototoxicity, hepatotoxicity, cardiotoxicity or allergic reactions were observed. Lipoplatin at 125 mg/m^2 induced grade III and IV neutropenia and grade III nausea and vomiting. Six (23%) patients showed partial response. Stable disease was seen in 65.3% of the patients and clinical benefit in 42.3% (Stathopoulos et al., 2002).

A Phase I-II cohort, dose escalation trial of lipoplatin and gemcitabine was conducted on 24 advanced-stage pretreated pancreatic cancer patients who were refractory to previous chemotherapy. Preliminary objective response rate data showed a partial response in 2 (8.3%) patients, disease stability in 14 (58.3%) patients for a median duration of 3 months (range 2-7 months), and clinical benefit in 8 (33.3%) patients. At the end of the study, 7 (29.2%) patients were still alive. Taking into account that all of the patients were refractory or in disease progression while on a previous treatment including gemcitabine, the response rate produced were attributed to the addition of lipoplatin (Stathopoulos et al., 2006).

Recently a Phase II study of lipoplatin 120 mg/m^2 and gemicitabine 1000 mg/m^2 versus cisplatin 100 mg/m^2 and gemcitabine 1000 mg/m^2 has been completed on 88 patients with NSCLC. The lipoplatin/gemcitabine treatment was better tolerated, with myelotoxicity as the main side effect. The overall response rate across all histological subtypes of NSCLC was 31.7% in the lipoplatin/gemcitabine arm versus 25.6% in the cisplatin/gemcitabine arm, but not statistically significant (p value = 0.411). However, a preliminary efficacy of lipoplatin/gemcitabine versus cisplatin/gemcitabine in the adenocarcinoma histological subtype of NSCLC showed 83.3 versus 54.2% response/stabilization rates (Mylonakis et al., 2010). This was an exciting finding proposed to be investigated further in a Phase III on non-squamous NSCLC.

The cisplatin/vinorelbine combination has been studied recently in patients with breast cancer and an overall response rate of 64% was obtained. Nevertheless, the use of cisplatin was limited by the frequently induced nausea, vomiting and nephrotoxicity. The aim of the Phase II study was to evaluate the efficacy and safety of the lipoplatin/vinorelbine combination as first-line treatment in advanced breast cancer patients. Twenty patients with HER2/neu negative advanced or metastatic breast cancer, with no previous treatment, were treated with 30 mg/m^2 vinorelbine and 120 mg/m^2 lipoplatin. Sixteen patients were evaluable for response. An objective tumor response was achieved in 8 (50%) patients, with complete response in 2 (13%) patients. Six (38%) patients had stable disease. All patients (20) were evaluable for toxicity. Most adverse events were mild to moderate. The new combination of lipoplatin and vinorelbine showed promising activity and good tolerance as first-line treatment for HER2/neu negative advanced or metastatic breast cancer (Farhat et al., 2011).

A Phase II trial is evaluating response and toxicity in advanced NSCLC patients who underwent previously cisplatin-based chemotherapy; thus, this trial is

addressing the efficacy of lipoplatin plus gemcitabine in patients whose disease is refractory to classical cisplatin chemotherapy.

Patients were treated with lipoplatin 120 mg/m^2 plus gemcitabine 1000 mg/m^2. Twenty-seven (77.8%) patients were assessable for response and toxicity according to the World Health Organization (WHO) criteria. Partial response was observed in 6 (22.2%), stable disease in 5 (18.5%) and progressive disease in 16 (59.2%) patients. Grade 3-4 neutropenia was observed in six (22.2%) patients, grade 3 thrombocytopenia in one (3.7%) patient and grade 3 anemia in one (3.7%) patient. Other toxicities included grade 3-4 nausea/emesis in nine (33.3%) patients, grade 3 fever in nine (33.3%) patients, and grade 3 nephrotoxicity in one (3.7%) patient. Further toxicities such as rush, constipation and peripheral neuropathy were rare and/or mild. Median overall time to tumor progression was 14 weeks (3-50).

The preliminary results of this continuing Phase II trial were encouraging in terms of response rate and toxicity (Anevlavis et a., 2008). Especially important is the fact that lipoplatin seems to have activity in cisplatin-resistant tumors, something predicted previously from the liposomal nature of the drug; lipoplatin was proposed to be able to treat cisplatin-resistant tumors with resistance arising at the cell membrane level and not at the level of DNA repair (Boulikas, 1998).

Patients with locally advanced gastric cancer or gastric cancer inoperable for medical reasons or recurrent carcinomas were recruited. The objective of this Phase II study was to investigate the toxicity, response rates, and overall survival of lipoplatin radio-chemotherapy in locally advanced gastric adeno-carcinomas, in those unable to undergo surgery and to test the radiosensitizing ability of lipoplatin because of the concentration of its nanoparticles in tumors. Lipoplatin was given at a dose of 120 mg/m^2, 5-fluorouracil (5-FU) at 400 mg/m^2, while radiotherapy was given through 3.5 Gy fractions. The response rates assessed with CT-scan, endoscopy and biopsies confirmed 33% (2/6) complete remission and 3 (50%) of 6 partial response in patients treated with four cycles and 4 (80%) of 5 complete remission in patients treated with five cycles (Koukourakis et al., 2010).

Pancreatic cancers (>230,000 cases worldwide) are very hard to diagnose because they grow in the absence of alarming symptoms; about 85% of the patients are usually diagnosed at an advanced stage and have bad prognosis. Lipoplatin received the orphan drug status by the European Medicines Agency (EMEA). A multi-center Phase II/III registrational clinical study is in progress using lipoplatin plus gemcitabine as first-line treatment in inoperable, locally advanced or metastatic pancreatic cancer with the involvement of 20 oncology centers of excellence in various EU countries. During Phase II, 61 patients will receive i.v. lipoplatin 120 mg/m^2 plus gemcitabine 1000 mg/m^2. During Phase III, 328 patients will be randomized (164 in each arm) to compare the same schedule of lipoplatin plus gemcitabine as in Phase II with i.v. gemcitabine 1000 mg/m^2 (Boulikas, 2009).

3.3.2.3 Clinical trials Phase III studies

A randomized multi-center Phase III non-inferiority clinical study compared lipoplatin 120 mg/m^2, plus gemcitabine 1000 mg/m^2 with cisplatin 100 mg/m^2 plus gemcitabine 1000 mg/m^2 as first-line treatment in patients with NSCLC. The primary end points were overall survival; secondary end points were toxicity, overall response rates, progression-free survival, and quality of life. Fiftynine patients were included, of whom 33 received the lipoplatin/gemcitabine regimen and 26 the cisplatin/gemcitabine one. Particularly important might be the significantly lower neuro- and nephro-toxicity of the lipoplatin arm and its administration on an outpatient basis with clear pharmacoeconomic benefits; lipoplatin was administered without pre- and post-hydration as a 6-hours infusion (Boulikas, 2009). An interim analysis of this trial on 101 patients of whom 60 received the lipoplatin/gemcitabine and 41 the cisplatin/gemcitabine regimen, with a stratification for histological subtypes of NSCLC, showed there was a significant reduction in nephrotoxicity, nausea/vomiting, neurotoxicity and asthenia in the lipoplatin/gemcitabine compared to cisplatin/gemcitabine treatment arms (Kosmas et al., 2009). In this study, that recruited more than 280 patients, lipoplatin, under the name Nanoplatin, received in 2009 the consent of EMEA to be tested as first line against non-squamous NSCLC mainly composed of adenocarcinomas.

The use of a taxane in combination with a platinum compound has become an acceptable standard as first-line treatment for patients with advanced or metastatic NSCLC (Kim et al., 2003). This randomized Phase III used 200 mg/m^2 lipoplatin plus 135 mg/m^2 paclitaxel (Arm A) and 75 mg/m^2 cisplatin plus 135 mg/m^2 paclitaxel (Arm B). The main objective of the study was to show that lipoplatin was not inferior to cisplatin when combined with paclitaxel as first-line treatment, as assessed by overall survival in a randomized group of patients with NSCLC at stage IIIB/IV (with locally advanced or metastatic disease), but that patients in the lipoplatin/paclitaxel arm had a better toxicity profile and showed a better quality of life. Secondary objectives of the study were to compare the time to tumor progression, 1-year survival, and response rate between the two arms.

It was concluded that the response rate was similar but toxicity, and in particular nephrotoxicity, neurotoxicity, and myelotoxicity were significantly lower in the lipoplatin arm (Stathopoulos et al., 2011). This Phase III was terminated successfully after treating 229 patients; the data showed the non-inferiority of the lipoplatin/paclitaxel combination compared to cisplatin/paclitaxel in the schedule described above but with statistically significant lower toxicities in the lipoplatin/paclitaxel arm for nephrotoxicity, grade 3 and 4 leukopenia, grade 2 and 3 neuropathy, asthenia (fatigue) and gastrointestinal toxicity (nausea/vomiting). There was no significant difference in median and overall survival (Boulikas, 2009).

A randomized, multi-center Phase III trial against SCCHN was designed, in which conventional cisplatin or lipoplatin were used in combination with 5-FU, to

compare efficacy and safety profiles of both treatment arms. This study is used treatment with 100 mg/m^2 lipoplatin plus 1000 mg/m^2 day 5-FU (Arm A). The comparative arm (Arm B) used 100 mg/m^2 cisplatin with pre- and post-hydration. An interim analysis was reported (Jehn et al., 2008) on 46 evaluable patients, 25 in the lipoplatin/5-FU and 21 in the cisplatin/5-FU arm, respectively, after at least two cycles in both arms. The main end points for this interim analysis were hemato- and nephro-toxicity. Seven patients had to stop cisplatin therapy due to severe toxicity as compared to one patient in the lipoplatin treatment arm. Severe hematotoxicity was more frequent in the cisplatin arm, with grade III and IV toxicity occurring in 31.7% of the patients treated with the cisplatin-based regimen versus 12% in the lipoplatin-based regimen. Grade IV leucopenia occurred in 22.2% of the patients treated with cisplatin/5-FU, whereas in the lipoplatin/5-FU arm 0% grade IV leukopenia occurred. One of the most debilitating toxic side effects and a great impingement on the quality of life of cisplatin-based chemotherapies is neuropathy. Lipoplatin seems to reduce neuro-toxicity profoundly. A total of 67% of the patients treated with the cisplatin regimen experienced grade I and II neuropathy compared to 27% in the lipoplatin arm. The renal toxicity profile of both drugs also showed marked differences: 23.8% of the treated patients suffered a significant reduction in kidney function. A high rate of stable disease was observed in the lipoplatin versus cisplatin arms (64 versus 50%); also the clinical benefit rate (stable disease plus partial remission) was similar for the cisplatin (88.5%) and lipoplatin combinations (83%), although there were more objective responses seen in the cisplatin arm (Jehn et al., 2008).

One of the serious adverse reactions with the administration of chemotherapeutical agents is renal failure. In general, when the level of creatinine/glomerular filtration data is high, chemotherapy involving almost all cytotoxic agents is avoided or the dosage is reduced. In the present trial, lipoplatin was tested as monotherapy and in combination with gemcitabine or paclitaxel or 5-FU-leucovorin, mainly in lung and bladder cancer patients with renal insufficiency. The primary objective of the present study was to investigate the administration of lipoplatin in patients with renal insufficiency and secondly, to determine the response of patients with bladder cancer, the majority of whom received the present treatment as first-line therapy. Forty-two patients (14 with NSCLC, 2 with squamous cell carcinoma non-small-cell lung cancer, 16 with bladder cancer, and 10 gastrointestinal tract cancer) were included. Lipoplatin and gemcitabine were administered to patients with bladder cancer, paclitaxel plus lipoplatin were administered to lung cancer patients, and patients with gastrointestinal tract cancer received 5-FU and leucovorin plus lipoplatin. Serum creatinine was 1.6 mg/dl to 4.0 mg/dl (median 2.4 mg/dl). No serum creatinine increase was observed in any of the patients. Grade 1-2 myelotoxicity and anemia were observed in 28.57% and 50% of the patients, respectively. Results showed that lipoplatin may favorably be considered as the treatment solution for cancer patients with renal insufficiency (Stathopoulos et al., 2012).

3.3.2.4 Pharmacoeconomics

Lipoplatin is being administered on an outpatient basis without pre- or post-hydration and with clear pharmacoeconomic benefits over cisplatin that requires admittance of the patient to the hospital a day before and a day after treatment for pre- and post-hydration. Hospitalization costs are usually $1000/day in most Western countries. In addition, there is less healthcare requirements for the recovery of patients from adverse reactions, especially nephro- and neuro-toxicity as well as less use of the expensive hematopoietic factors GM-CSF after administration of lipoplatin compared to cisplatin. The expected increase in overall survival and improvement in the quality of life suggested from preliminary results are also considered important benefits. Although lipoplatin has not received marketing authorization yet, its pricing takes into consideration its affordability for establishing it as a drug able to replace cisplatin in all world markets (Boulikas, 2009).

3.4 Tumor models

3.4.1 Cervical cancer

Cancer of the cervix uteri is the second most frequent cancer in women in the world (529,409 new cases in 2008) and the third greatest cause of death from cancer in women. Many more women die of cervical cancer in the developing world than in wealthier countries. Of the estimated 274,883 deaths from cervical cancer every year, more than 85% occur in developing countries (Sanjosé et al., 2012). Before the introduction of screening and vaccination programs the incidence of cervical cancer in many of the more developed countries was similar to that in less developed countries today. Between 1955 and 1992, cervical cancer death rate declined by almost 70%. The main reason for this change was the increased use of the Pap test. The Pap smear test (Papanicolaou test) is a screening test for cervical cancer in which cells are scraped from the cervix and looked at under a microscope. Screening should start at age 21. Most of the time, cervical cancer develops very slowly and follow-up Pap smears should identify worrisome changes in time for treatment (Bradford and Goodman, 2013). The high mortality rate from cervical cancer globally could be reduced by effective screening and treatment programs also in developing countries.

Cervical cancers start in the cells on the surface of the cervix. There are two types of cells on the surface of the cervix, squamous and columnar. The majority of cases are squamous cell carcinoma and adenocarcinomas are less common. From 2006 to 2010, the median age at diagnosis for cancer of the cervix uteri was 49 years of age.

Cervical cancer is almost always caused by human papillomavirus (HPV) infection.

HPV is a very common virus that can affect the cells of the cervix. It is mainly passed on during sex. Having sex at an early age and having several sexual partners can increase the risk of catching HPV and developing cervical cancer.

There are more than 100 different types of HPV, many of which are harmless. However, some types of HPV can disrupt the normal functioning of the cells of the cervix and can eventually trigger the onset of cancer. At present, there are two HPV vaccines, a bivalent (Cervarixc) and a quadrivalent (Gardasilc) HPV vaccine (Cutts et al., 2007). Both vaccines are composed of HPV L1 proteins that spontaneously self assemble into Virus-like particles (VLPs). Cervarixc was designed to prevent infection by HPV16 and 18, the two types that cause 70% of cervical cancer. Gardasilc targets the same two cancer causing types and, in addition, is intended to prevent infection by HPV6 and 11, which cause 75-90% of external genital warts. The vaccine is given as a series of three shots. It is recommended for girls and women ages 9 - 26. Both vaccines are prophylactic but not therapeutic, so cervical screening programs are still needed for women already infected or unimmunized with the potential for future infection (Kahn, 2009).

HPV is a necessary cause of cervical cancer, but it is not a sufficient cause. Other cofactors are necessary for progression from cervical HPV infection to cancer:

- Giving birth to many children.
- Having many sexual partners.
- Having first sexual intercourse at a young age.
- Smoking cigarettes.
- Using oral contraceptives ("the Pill").
- Having a weakened immune system.

Cancer of the cervix is not infectious and can’t be passed on to other people (Deacon et al., 2000).

If cervical cancer is diagnosed at an early stage it is usually possible to treat it using surgery. In some cases it is possible to leave the womb in place, but it may need to be removed. The surgical procedure used to remove the womb is called a hysterectomy.

Radiotherapy is an alternative to surgery for some women with early stage cervical cancer. In some cases it is used alongside surgery. More advanced cases of cervical cancer are usually treated using a combination of chemotherapy and radiotherapy. Drugs most often used to treat cervical cancer include: cisplatin, carboplatin, paclitaxel (Taxol®), topotecan, and gemcitabine (Gemzar®). Some other drugs can be used as well, such as docetaxel (Taxotere®), ifosfamide (Ifex®), 5-fluorouracil (5-FU), irinotecan (Camptosar®), and mitomycin. Often combinations of these are used (Yee et al., 2013).

Based on phase III results, the combination of cisplatin and paclitaxel remains the standard of care for treatment of recurrent cervical cancer, although clinical benefit is limited. Indeed, although cisplatin is the most effective agent for metastatic cervical cancer, prolonged treatment induces multiple mechanisms of tumor resistance and is associated with significant toxicity (Leath and Straughn, 2013). Therefore, the development of new cisplatin formulations to overcome

both resistance and toxicity remains a high priority and is crucial for a better treatment and a more prolonged survival.

3.4.2 Ovarian cancer

The term "ovarian cancer" includes several different types of cancer. Epithelial ovarian cancer (EOC) accounts for about 70% of all ovarian cancers. It is generally thought of as one of three types of cancer that include ovarian (epithelial ovarian cancer), fallopian tube, and primary peritoneal cancer that all behave, and are treated the same way, depending on the type of cell that causes the cancer. There are also less common forms of ovarian cancer that come from within the ovary itself, including germ cell tumors and sex cord-stromal tumors (N et al., 1998). The four most common cell types of epithelial ovarian cancer are serous, mucinous, clear cell, and endometrioid. These cancers arise due to DNA changes in cells that lead to the development of cancer. Serous cell type is the most common variety. It is now thought that many of these cancers actually come from the lining in the fallopian tube, and fewer of them from the lining on the surface of the ovary, or the peritoneum. However, it is often hard to identify the sources of these cancers when they present at advanced stages, which is very common (Bell, 2005).

The median age at presentation of ovarian cancer is 63 years (Cannistra, 2004).

Worldwide, the estimated annual incidence of ovarian cancer is 204,000, with 125,000 deaths, identifying ovarian carcinoma as the fifth leading cause of cancer-related death among women (Jemal et al., 2008). The high mortality of this tumor is largely explained by the fact that the majority (75%) of patients are diagnosed with advanced stage, with widely metastatic disease within the peritoneal cavity. This is mostly due to the lack of definite symptoms at the early stages of development of the disease process.

There is a close correlation between stage at presentation and survival; therefore, early detection of ovarian cancer represents the best hope for mortality reduction and long-term disease control. However, so far there are no effective ovarian cancer screening tests. The cancer antigen 125 (CA-125) has become well established as tumor marker for epithelial ovarian cancer, but its sensitivity and specificity is known to be poor. It is only raised in approximately 50% of stage I epithelial ovarian cancers and in 75% to 90% of patients with advanced disease (Jacobs and Bast, 1989).

Most women diagnosed with ovarian cancer have the sporadic variety; however, a subset of ovarian cancer cases occur in a familiar fashion. For this subset, a strong family history of ovarian or breast cancer is the most important risk factor. Overall, hereditary predisposition accounts for at least 10% of all epithelial ovarian cancers. Mutations in the BRCA genes account for approximately 90% of these cases, with most of the remaining 10% attributable to Lynch syndrome (hereditary nonpolyposis colorectal cancer (HNPCC)) (Chen et al., 2006). The

cumulative lifetime risk of ovarian cancer is 40% to 50% for BRCA1 mutation carriers and 20% to 30% for BRCA2 mutation carriers. The cumulative risk of ovarian cancer in HNPCC families is more than 12%. Nulliparity, early menarche, late menopause, and increasing age are also associated with increased risk, whereas oral contraceptive use, pregnancy, lactation, and tubal ligation are associated with reduced risk (Hankinson et al., 1993).

The standard initial management of epithelial ovarian cancer consists of aggressive surgical cytoreduction, to remove all visible disease in the abdomen, including total abdominal hysterectomy (surgery to remove the uterus and the cervix) and bilateral salpingo-oophorectomy (a surgical procedure to remove both ovaries and both fallopian tubes), and platinum/taxane combination chemotherapy (Cannistra, 2004).

There are two ways to give chemotherapy in ovarian cancer. Traditionally, it is given into the vein intravenously (IV). Another way of giving the chemotherapy is to place it directly into the abdomen (intraperitoneal or IP). In many studies, intraperitoneal administration has been shown to significantly increase survival. This is most often used after optimal surgical debulking. When initially diagnosed, the two most common drugs are carboplatin and paclitaxel. Currently, the drugs used are cisplatin and paclitaxel. There are studies that are looking at substituting carboplatin for cisplatin, because the side effects are less. Unfortunatly, recurrence is very frequent. When epithelial ovarian cancer recurs the type of drugs used for second line chemotherapy are determined by how long it has been since the last time a patient has taken a drug containing platinum. If it has been less than 6 months, then the patient is termed platinum-resistant. If it has been more than 6 months since the last day of platinum-based chemotherapy, then often a platinum-containing drug will be used again. If the patient is platinum-resistant it will receive a non-platinum drug that can be pegylated liposomal doxorubicin, docetaxel, paclitaxel, topotecan, gemcitabine, etoposide, and bevacizumab (Wp and Rf, 1998).

Unlike most other cancers, ovarian carcinoma rarely disseminates through the vasculature. However, pelvic and/or para-aortic lymph nodes can be involved (Eisenkop and Spirtos, 2001). Ovarian carcinoma metastasizes either by direct extension from the ovarian/fallopian tumor to neighboring organs (bladder/colon) or when cancer cells detach from the primary tumor (Figure 3.11).

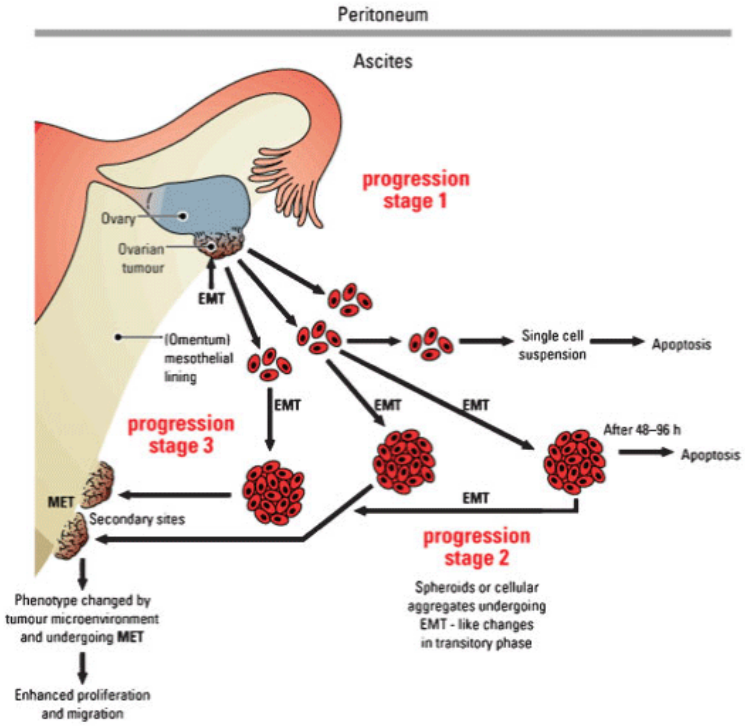

Figure 3.11 Model of ovarian cancer progression.

Invasion of the mesothelium is an early step of ovarian carcinoma metastasis. Indeed, exfoliated tumor cells from the primary tumor can subsequently attach to the mesothelial cell lining and invade, forming metastatic outgrowths. Late stage cancers are frequently associated with ascites, and tumor cells can be shed into the ascites fluid either as single cells or multicellular aggregates called spheroids (A Farghaly, 2013). It is not clear whether single cells detach and then aggregate to form spheroids, or if the cells detach as cell clumps that stay together while floating in ascites (Figure 3.11). However, several *in vitro* studies have explored the possibility that spheroids are less susceptible to chemotherapy than single cells. This raises the possibility that spheroids are implicated as factor in disease persistence or recurrence (Lengyel, 2010).

Despite advances in the treatment of ovarian cancer, effective screening, early detection, and cure remain elusive for most women.

4. MATERIALS AND METHODS

4.1 Drugs

Lipoplatin™, the liposomal formulation of cisplatin, was generously provided by Regulon (Regulon, Athens, Greece); cisplatin was purchased from Mayne Pharma (Napoli, Italy); abraxane (Celgene Corporation, Milano, Italy); doxorubicin (Pfizer, Latina, Italy); docetaxel (Hospira, Napoli, Italy); and paclitaxel (Actavis, Milano, Italy). Drugs were dissolved in medium at the indicated concentrations immediately before use.

4.2 Cell lines and culture conditions

Human ovarian epithelial adenocarcinoma derived cancer cell lines A2780 (Sigma-Aldrich), the parent cisplatin-resistant A2780cis (Sigma-Aldrich), MDAH 2774 (ATCC CRL-10303), OVACR-3 (ATCC HTB-161), OVACR5 (NIH), SKOV-3 (ATCC HTB-77), TOV21G (ATCC CRL-11730), and the highly invasive cervical cancer-derived HeLa (ATCC CCL-2), ME-180 (ATCC HTB-33) (HPV+) cell lines were purchased from the American Type Culture Collection (ATCC, Rockville, MD, USA). The cisplatin-resistant variant R-ME-180 was generated by weekly selection and maintained in 1 μM cisplatin. Cell lines used in the study were further authenticated for their origin by BMR Genomics (Padova, Italy). Ovarian cancer cell lines were cultured in RPMI medium (Sigma-Aldrich-Italy), cervical cancer cell lines in DMEM medium (Sigma-Aldrich-Italy) supplemented with 10% heat-inactivated Fetal Bovine Serum (FBS; Gibco), 0.2 mg/ml penicillin/streptomycin (Cambrex) and 0.1% (w/v) L-glutamine (Cambrex) at 37°C in a 5% CO_2 fully humidified atmosphere.

4.3 Cytotoxicity assay

$4.0x10^3$ cells were plated in 96-well flat-bottomed plates and allowed to adhere for 24 hours, then exposed to increasing concentrations of lipoplatin (2.5-100 μM) or cisplatin (2.5-100 μM) at 37ºC for 72 hours. Triplicate cultures were established for each treatment. Cytotoxicity was measured by using MTT assay. Following drug treatment, the 3-(4,5-Dimethylthiazol-2-yl)-2,5-diphenyltetrazolium bromide (MTT) solution was added to the culture medium and the culture further incubated for 4 hours at 37 °C. The degree of cell survival was determined by checking conversion of MTT to formazan. The absorbance was measured at 570/630 nm using a plate reader (Sunrise, TECAN) and the cytotoxicity percentage was calculated. IC_{50} values (representing the concentration of a substance required for 50% growth inhibition *in vitro*) were calculated using the CalcuSyn software (Biosoft, Ferguson, MO, USA)(Chou and Talalay, 1984).

4.4 Experimental Design for Drug Combinations and Chou–Talalay analysis for synergy

Methods for assessing synergy were used as described earlier (Chou, 2006). In particular, we used the diagonal constant ratio combination design proposed by Chou and Talalay (1984), in which a small number of data points were combined so that the contributions of effects of each drug to the combination were almost equal (Table 4.1). We first determined the IC_{50} for abraxane, docetaxel, doxorubicin, and paclitaxel for OVCAR5 and SKOV3. Then 4.0×10^3 cells/well, plated in 96-well, were incubated with each drug alone or in combination with lipoplatin for 72 hours, and cell viability was evaluated by MTT assay.
Calcusyn (version 2.0), a Windows®-based computer program automating the multiple-drug-effect analysis of Chou and Talalay, based on the median-effect principle (Chou and Talalay, 1984), was used to calculate combined drug effects. The combination index (CI) was then used to determine synergy, additivity or antagonism. Combination indices of <1, =1 and >1 represent synergy, additivity and antagonism, respectively.

Table 4.1 A proposed experimental design showing the outlay of dose range and dose density of two drugs for drug combination analysis.

			Drug 1				
	0	0 Control $(f_a)_0$	$0.25 \times (ED_{50})_1$ $(f_a)_1$	$0.5 \times (ED_{50})_1$ $(f_a)_1$	$(ED_{50})_1$ $(f_a)_1$	$2 \times (ED_{50})_1$ $(f_a)_1$	$4 \times (ED_{50})_1$ $(f_a)_1$
Drug 2	$0.25 \times (ED_{50})_2$ $(f_a)_2$		$(f_a)_{1,2}$				
	$0.5 \times (ED_{50})_2$ $(f_a)_2$			$(f_a)_{1,2}$			
	$(ED_{50})_2$ $(f_a)_2$				$(f_a)_{1,2}$		
	$2 \times (ED_{50})_2$ $(f_a)_2$					$(f_a)_{1,2}$	
	$4\times (ED_{50})_2$ $(f_a)_2$						$(f_a)_{1,2}$

4.5 Evaluation of cell cycle progression and apoptosis

Effects on the cell cycle were evaluated by propidium iodide (PI) staining. $5x10^5$ cells cultured in a 10 ml petri dish were treated 72 hours with 30 µM lipoplatin. Cells were fixed and permeabilized 15 minutes in ice with 70% ethanol. Afterwards they were incubated 1 hour at room temperature with PI solution (PI 1mg/ml, NP40 1%, RNAsi 10mg/ml in sodium citrate 0.1%) Data analysis was performed by ModFit LT™ software (Variety Software House, Topsham, ME, USA).
To assess Annexin-V binding, DNA fragmentation, features of mitochondrial apoptotic pathway, mitochondrial reactive oxygen species (ROS) formation, $1.0x10^5$ cervical and $5.0x10^4$ ovarian tumor cells were incubated for 72 hours on 6-well plates in complete medium in the presence of lipoplatin or cisplatin. All the cells were harvested.
Annexin-V was assessed incubating fluoresceine isothiocyanate (FITC) Annexin-V (Becton-Dickinson [BD]-Pharmingen, San Jose, CA, USA) for 15 minutes in

Annexin-V Binding Buffer. 0.7 µg/ml of propidium iodide was added and sample were analyzed by flow cytometry.
DNA fragmentation within cells was detected using the *Apo-Direct* kit (BD Pharmingen) following the manufacturer's instructions.
To evaluate the dissipation of the mitochondrial membrane potential, 200 nM Chloromethyl-X-rosamine (CMXRos) (Molecular Probes, Eugene, OR, USA) (Pendergrass et al., 2004) was added to the cell culture for 30 minutes, then the cells were washed twice and analyzed by flow cytometry.
For B-cell lymphoma/leukemia-2 (Bcl-2), B-cell lymphoma-extra large (Bcl-xL) and Bcl-2 associated x protein (Bax) analysis, fixed and permeabilized cells (FIX & PERM cell fixation and permeabilization kit, Invitrogen) were incubated with 10 mg/l FITC-conjugated mouse anti-human Bcl-2 (clone 124) (DAKO Citomation, Milan, Italy), with rabbit anti-human Bcl-xL (54H6) (Cell Signalling, Danvers, MA, USA) (1:400) followed by goat anti-rabbit immunoglobulin (IgG) FITC-coniugated (BD), and with 1 µg/ml of mouse anti-Bax generated from Bax-alpha (BD), followed by 10 µg/ml phycoerythrin (PE)-conjugated goat anti-mouse IgG (BD).
Cytochrome-c (Cyt-c) release was assessed, as explained elsewhere (Campos et al., 2006), with minor modifications. Briefly, tumor cells were permeabilized with 100 µg/ml digitonin (Sigma) and fixed with 4% paraformaldehyde in PBS for 20 minutes at room temperature. After washing twice with PBS, the cells were incubated in labeling medium (2% FBS, 0.2% sodium azide, 0.5% Triton X-100 in PBS) for 10 minutes, then with 1 µg/ml of mouse anti-Cytochrome-c antibody (BD), and finally with PE-conjugated goat anti-mouse IgG (BD).
For mitochondrial ROS evaluation, cells were incubated with 5 µM of MitoSox reagent working solution (Molecular Probes, Invitrogen, Milan, Italy) for 30 minutes at 37º C. Red fluorescence was immediately analyzed by flow cytometry.
Caspase activity was ascertained with the fluorochrome-labeled inhibitors of caspases (FLICA), CaspaTagTM caspase-3/7 (FAM-DEVD-FMK) and caspase-9 (FAM-LETD) (FITC-IETD-FMK) (Chemicon International, Milan, Italy). Cells were treated with 30 µM of lipoplatin or cisplatin for 0, 24 and 48 hours, then harvested, washed, resuspended in warmed complete medium supplemented with FLICA for 1 hours at 37°C under 5% CO_2, and immediately analyzed by flow cytometry.
Viable antibody-labeled cells were identified according to their forward and right-angle scattering, electronically gated. Data were collected and analyzed on a FACScan flow cytometer (BD) using CellQuest software (BD).

4.6 Thioredoxin Reductase (TrxR) enzyme activity assay

TrxR activity was assessed using the Thioredoxin Reductase Assay Kit (Sigma-Aldrich), according to the manufacturer's instructions: $1.0x10^5$ cells were treated with 20 and 30 µM lipoplatin or cisplatin and, after 72 hours, cells were lysed

with lysis buffer (50 mM Tris-HCl, 0.1% Triton X-100, 0.9% NaCl, pH 7.6) and incubated for 30 minutes on ice. Total protein content was analyzed with the protein assay dye reagent (Bio-Rad Laboratories, Hercules, CA, USA). The cell lysates were then incubated in 100 mM of potassium phosphate with 10 mM ethylenediaminetetraacetic acid (EDTA) and 0.24 mM nicotinamide adenine dinucleotide phosphate (NADPH) with and without a TrxR inhibitor. The reaction was started by adding dinitrothiocyanobenzene (DNTB) and was monitored spectrophotometrically at 412 nm.

4.7 Cell migration assay

Cell migration was assessed using the scratch wound healing assay, as described elsewhere (Liang et al., 2007). Briefly, cells were grown to confluence in tissue culture dishes, then 10 µM of lipoplatin, cisplatin or medium alone were added. After 72 hours treatment, the cells were washed twice with PBS and scraped up using a sterile pipette tip, then washed again and cultured in DMEM with 0.5% FCS. The percentage of cell migration was evaluated by the Image Tool Software measuring the area of the scratch covered by the migrated cells after 24 and 48 hours (http://ddsdx.uthscsa.edu/dig/itdesc.html; San Antonio, TX, USA).

4.8 Cell invasion assay

Cervical cancer cell lines were treated 12 hours with 30 µM lipoplatin, ovarian cancer cells were treated 72 hours with 10 µM lipoplatin . Invasion was assessed by FATIMA assay as previously described (Spessotto et al., 2009). Briefly, after drug treatment viable cells ($1.0x10^5$ cells/insert), tagged with the lipophylic dye Fast DiI (Molecular Probes), were seeded in 150 µl SF medium in the upper side of collagen type I-coated Boyden chamber inserts. Migration was then monitored at different time intervals for 24 hours, using a computer-interfaced GeniusPlus microplate reader. FATIMA software determined the percentage of transmigrated cells out of the total amount introduced into the system. Complete medium 20% FCS was used as chemoattractants. Each experiment was performed at least three times, in duplicate.

4.9 Expression of Epithelial Growth Factor Receptor (EGFR)

$1.0x10^5$ cervical and $5.0x10^4$ ovarian tumor cells were incubated for 72 hours on 6-well plates in complete medium in the presence of lipoplatin or cisplatin (20 and 30 µM). After fixing cells (FIX & PERM cell fixation and permeabilization kit, Invitrogen), the surface expression of the EGFR was analyzed by flow cytometry using the PE mouse anti-human EGFR antibody, as indicated in the manufacturer's instructions (20 µl per test).

4.10 Identification of cancer stem cells (CSCs)

CSCs were identified by alcohol dehydrogenase (ALDH) and CD133 stem cell markers.
To detect ALDH enzymatic activity I used the Aldeflour reagent based (Stem Cell Technologies, Vancouver, Canada) flow cytometry method according to the manufacturer's instructions. This method relies on the increased ALDH activity of CSCs. Briefly, adherent cells were trypsinized and washed with phosphate buffered saline (PBS). Cells ($2x10^5$ cell/ml) were then suspended in cell suspension buffer provided in the kit. Aldeflour reagent was then added to the cell suspension followed by the incubation for 40 minutes at 37°C. For each cell type tested, a negative control comprising cells treated with ALDH-inhibitor diethylamino-benzaldehyde (DEAB) was also included. Cells were recovered by centrifugation finally resuspended in ice cold cell suspension buffer. Cell analysis were carried out using a FACSCalibur flow cytometer (BD). ALDH+ cells were quantified by calculating the percentage of total cells that displayed greater fluorescence compared with the negative control.
$5.0x10^4$ ovarian tumor cells were incubated for 72 hours on 6-well plates in complete medium in the presence of lipoplatin. All the cells were harvested and fixed (FIX & PERM cell fixation and permeabilization kit, Invitrogen). The surface expression of CD133 was assessed using the antibody anti-human CD133/1(AC133)-PE (Miltenyi Biotec), as indicated in the manufacturer's instructions, (diluition 1:11) and analyzed by flow cytometry.

4.11 Multicellular tumor spheroid formation assays

To obtain multicellular tumor spheroids *in vitro*, 24-well plates were coated twice with poly(2-hydroxyethyl methacrylate) 20 mg/ml (poly-HEMA; Sigma, Inc., St. Louis, MO, USA) (Ivascu and Kubbies, 2006) in 95% ethanol and washed once with PBS before cell seeding. Spheroids were obtained plating $5x10^4$ R-ME-180 or SKOV3 cells in complete medium in the presence of 10, 25 or 50 µM of lipoplatin or cisplatin. To evaluate apoptosis or ALDH activity, spheroids treated for 72 hours were trypsinized in a single cell suspension. To obtain a second generation, formed spheroids (72 hours) were dissociated and then replated on poly-HEMA coated wells for other 72 hours.

4.12 Spheroid volume growth kinetic and spheroid cell viability

Tumor spheroid growth kinetics and treatment with test compounds was performed as reported. For single spheroid generation 100 µl/well of SKOV-3 cell suspension at optimized density ($1.0x10^4$) were dispensed into poly-HEMA coated round-bottom 96-well. Plates were incubated for 4 days at 37°C, then spheroids were treated with increasing concentrations of lipoplatin (10-100 µM).

Spheroid size was measured up to 15 days after initiation. A 50% medium replacement was performed on days 3, 7, 10 and 15. Responses were evaluated by spheroid volume measurements at regular intervals (Bandekar et al., 2012) using inverted microscope (Eclipse TS/100, Nikon) magnification 4x with the photomicrographic systems DS Camera Control Unit DS-L2. Spheroid volume was calculated according to the formula: (width^2 x length x 3.14)/6 (Liu et al., 2005), and the percentage of volume change was calculated as Vt/V0x100 where Vt is the calculated volume at time t of at least three single spheroids and Vo the mean spheroid volume right before the start of incubation with drug treatment.
To assess spheroid cell viability, single spheroids were incubated for 30 minutes with 2 µg/ml propidium iodide before being observed under the fluorescence microscope (DMI 600013, Leica) (original magnification 4×).

4.13 Tumor spheroid-based migration assay on matrix protein

To assess cell dissemination I used a spheroid adhesion and migration assay. Spheroids were grown in poly-HEMA coated round-bottom 96-well as described above. The disaggregation assay was performed in 96-well plates coated with collagene (10 µg/ml) I and blocked with BSA (1 mg/ml) for 2 hours. Plates were washed with PBS and 3-5 spheroids suspended in complete medium were layered on the wells in absence or presence of 25 and 50 µM lipoplatin. Spheroids were sized and photographed at 0, 24 and 48 hours. The pixel area of the cells was determined using Adobe Photoshop by outlining the entire area of the dispersed cells with the lasso tool. The fold change in area was then calculated by dividing the pixel area of the spheroid at 24 and 48 hours by the pixel area at time 0.

4.14 Tumor xenograft experiments

Six-week-old female athymic nu/nu (nude) mice were purchased from Charles River (Lecco, Italy) and 2.5x10^6 R-ME-180 and 2.7x10^6 OVCAR5 cells suspended in 0.1 ml of matrigel (1:3 in PBS) were inoculated in the right flank of each mouse. When cervical tumors reached ~32 mm^3 and ovarian tumors ~44 mm^3 in volume, mice were divided randomly into two groups of 5 and 8 mice each, for cervical and ovarian tumors, respectively. Mice were treated every other day. Tumor size was measured over time using a caliper, and volumes were calculated according to a standard formula: (width^2 x length x 3.14)/6. Mice carrying cervical cancer cells were treated with intraperitoneal injection of 10 mg/kg lipoplatin or drug-free vehicle, and were sacrificed after 28 days of treatment, when control tumors had reached a volume of ~600 mm^3.
Mice carrying ovarian cancer cells were treated with intraperitoneal injection of 20 mg/kg lipoplatin or drug-free vehicle. At day 39 the treatment was suspended.

After 14 days, when control tumors had reached a volume of ~1000 mm^3, mice were sacrificed.
The mouse organs were excised and fixed in formalin for tissue toxicity analyses. Sections were cut and counterstained with haematoxilin and eosin according to standard procedures.
To estimate the equal sample size for the mouse study groups, the experiment was designed to be able to detect a 0.60 difference with 0.90 power and an α error of 0.05.

4.15 Software and statistical analysis of data

Graphs were generated using Microsoft Office Excel (Microsoft Italia, Segrate, Italy) and SigmaPlot software (Systat Software Inc., San Jose, CA, USA). Values are presented as the mean with the standard error of not less than three measurements (unless otherwise stated) (mean ± SEM). Statistical analysis was performed using GraphPad Prism 6 Software (GraphPad, San Diego, CA, USA). The statistical significance of differences was determined by Student's *t*-test for comparison between two groups. Analysis of variances (ANOVA) was used to evaluate the correlation of data among three or more groups; consecutive multiple comparison analysis was performed using Dunnett's or Tukey's tests. Differences were considered statistically significant at $P<0.05$.

5. RESULTS

5.1 Lipoplatin activity on cervical cancer cells

5.1.1 Lipoplatin inhibited cervical cancer cell proliferation and induced apoptosis

I compared the *in vitro* cytotoxic effects of lipoplatin (Fig. 5.1A) on cervical cancer derived tumor cells HeLa, ME-180, and its cisplatin-resistant clone R-ME-180. Treatment with increasing concentrations of lipoplatin or cisplatin (2.5-100 μM) induced a dose-dependent inhibition of cell proliferation, as evaluated by MTT cell viability assay (Fig. 5.1). IC_{50}, the concentration of drug that inhibits 50% of cell proliferation, was calculated using the CalcuSyn software (Table 5.1).

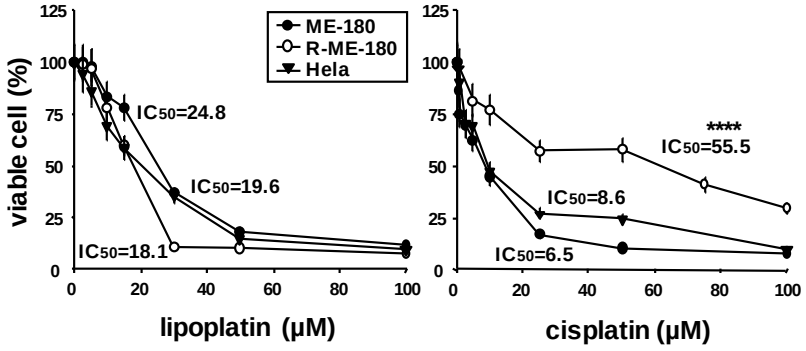

Figure 5.1 Lipoplatin inhibits cell growth. Cells were exposed to lipoplatin or cisplatin (2.5-100 μM). After 72 h the viable cell number was evaluated by MTT staining. IC_{50} values (i.e. the concentration of drug that reduces cell growth by 50%) were calculated using the Calcusyn software. Results represent the mean ± SEM of three replicate wells from three independent experiments.

Table 5.1 Growth inhibition of ME-180, R-ME-180 and HeLa cells by lipoplatin and cisplatin.

	IC_{50} (μM)		
	ME-180	R-ME-180	HeLa
Lipoplatin	**24.8±2.3**	**18.1±1.7**	**19.6±1.8**
Cisplatin	6.5±0.7	55.5±5.1	8.6±0.8

IC_{50} values are mean ± SEM from 3 independent experiments.

The IC_{50} of cisplatin in the cisplatin-resistant cell line R-ME-180 was about 9-fold higher than in ME-180 cisplatin-sensitive cells (Table 5.1).

Interestingly, the IC_{50} of lipoplatin was similar in both cell lines, and even 3-fold lower than the IC_{50} of cisplatin in R-ME-180 cells. A similar IC_{50} for lipoplatin was also obtained in HeLa cells.

Cisplatin affects tumor cell proliferation by activating the process of programmed cell death (Brozovic et al., 2010).

One of the early events of apoptosis is the loss of plasma membrane asymmetry: in apoptotic cells, the membrane phospholipid phosphatidylserine (PS) is translocated from the inner to the outer leaflet of the plasma membrane. Annexin-V protein has a high affinity for PS, and binds to cells with exposed PS. Viable cells with intact membranes exclude the fluorescent dye propide iodide (PI), whereas the membranes of dead and damaged cells are permeable to PI. Cells that are Annexin-V positive and PI negative are considered in early apoptosis, cells that are both Annexin-V and PI positive are considered in late apoptosis or necrotic cells.

I evaluated apoptosis induction by lipoplatin in ME-180 and its cisplatin-resistant clone R-ME-180, including cisplatin as reference drug.

Increasing lipoplatin concentrations (10, 20, 30 µM) correlated with an increase of apoptotic cells. At the highest concentration (30 µM) lipoplatin demonstrated a significant apoptosis induction in both cell lines. Lipoplatin treated R-ME-180 cells showed a higher amount of Annexin-V/PI positive cells (late apoptosis) than ME-180 cells. On the contrary, cisplatin used at the same concentrations, did not induce apoptosis in R-ME-180 cells (Figure 5.2).

Moreover, I evaluated DNA fragmentation, one of the later steps in apoptosis, a process which results from the activation of endonucleases during the apoptotic program.

APO-DIRECT™ is a single-step staining method for labeling DNA breaks to detect apoptotic cells by flow cytometry. An increase of fluorescence signal is associated with the presence of DNA breaks.

Apoptosis induction by lipoplatin (30 µM for 72 hours) was further confirmed in both cell lines by the presence of DNA damage (Figure 5.3A). Cisplatin induced a remarkable DNA fragmentation only in cisplatin-sensitive ME-180 cells, as showed in the representative flow cytometry histograms (Figure 5.3A).

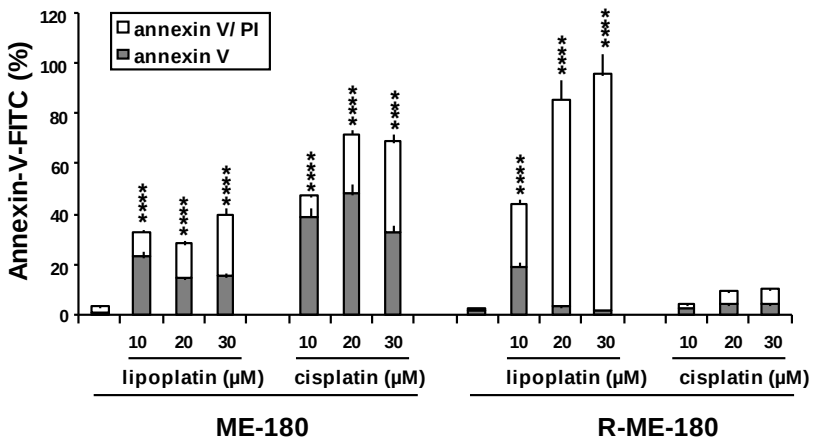

Figure 5.2 Lipoplatin induces apoptosis. FACS analysis of cells after 72 h incubation at 37 °C with different concentrations of either lipoplatin or cisplatin (10, 20, and 30 µM) and double stained with Annexin-V-FITC and PI. Values in the bar graph represent the mean ± SEM of three different experiments. ****P < 0.0001 drug *vs* medium.

5.1.2 Lipoplatin activated mitochondrial apoptotic pathway

Apoptosis induction by cisplatin is mediated by various signals including the activation of mitochondrial pathways (Brozovic et al., 2010).

The mitochondrial or intrinsic apoptotic pathway is characterized by mitochondrial outer membrane permeabilization (MOMP), cytochrome-c release, apoptosome assembly, and activation of the caspase cascade through caspase 9, which subsequently activates effector caspase 3. Permeability of the outer mitochondrial membrane is regulated via the opposing activities of the pro- and anti-apoptotic members of the Bcl-2 family. The balance between these competing activities determines cell fate (Adams and Cory, 1998; Mayer and Oberbauer, 2003).

ME-180 and R-ME-180 were treated with lipoplatin (30 µM) for 72 hours. Then I assessed the activation of the mitochondrial apoptotic pathway by flow cytometry.

Chloromethyl-X-rosamine (CMXros) is a fluorescent dye that stains mitochondria in live cells and its accumulation is dependent upon membrane potential (Pendergrass et al., 2004).

The treatment with lipoplatin led to a decline in the mitochondrial membrane potential, revealed by the decreased fluorescent signal of CMXros, and to the release of cytochrome-c, evaluated by antibody staining, in both ME-180 and R-ME-180 cell lines (Figure 5.3A).

Moreover, lipoplatin treatment increased the expression of the pro-apoptotic molecule Bax, while it decreased the expression of the anti-apoptotic molecules Bcl-2 and Bcl-xL (Figures 5.3B).

Consistently, I found the activation of caspases 9 and 3 in both cell lines after 48 hours of lipoplatin treatment (Figure 5.3C).

Taken together these results suggested that lipoplatin activated the mitochondrial apoptotic pathway in both cell lines. On the contrary, cisplatin, at the same experimental conditions, induced apoptosis only in ME-180 cisplatin-sensitive cells (Figures 5.3A, B and C).

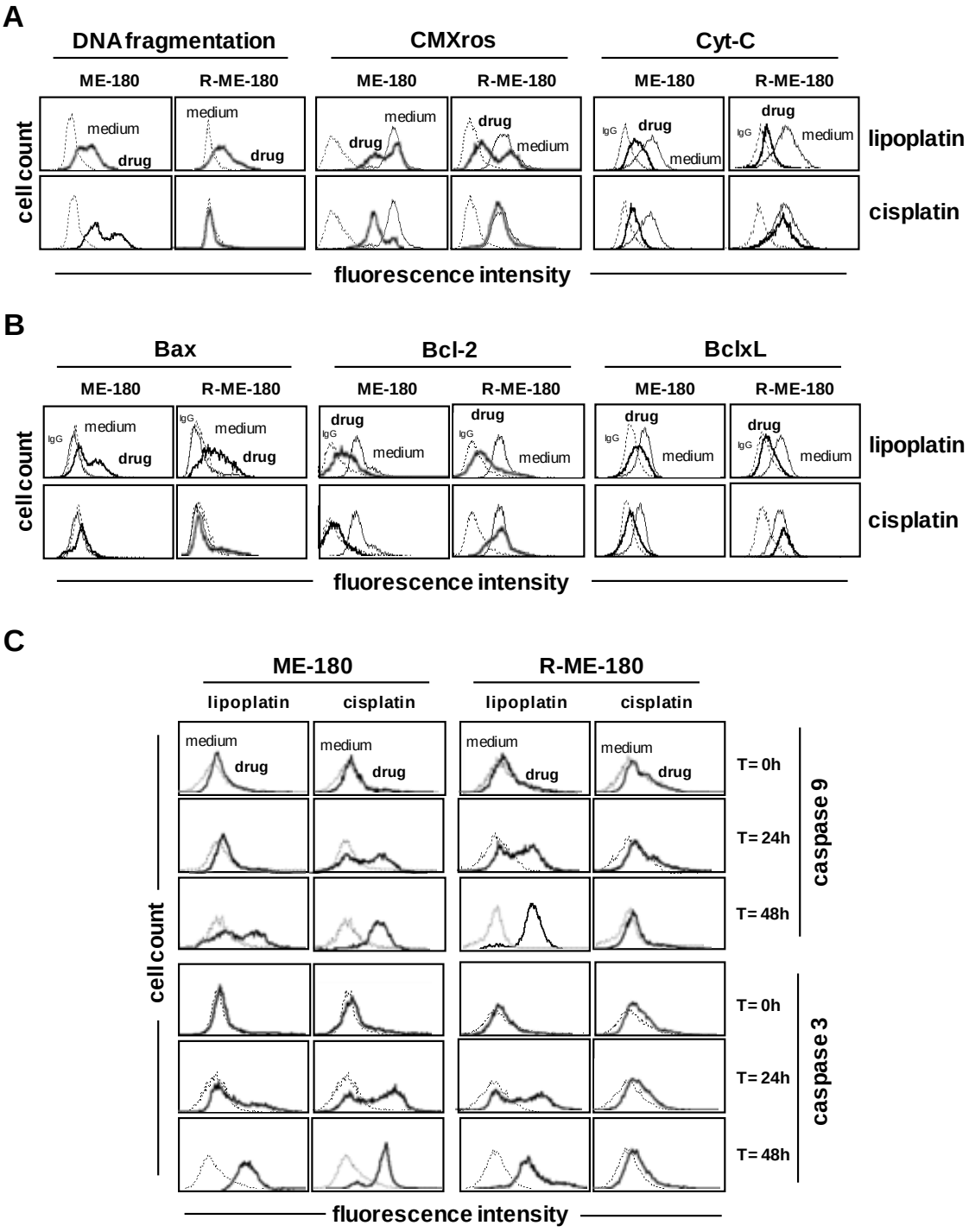

Figure 5.3 Lipoplatin induces mitochondria-mediated apoptosis and modulates Bax, Bcl-2 and Bcl-xL expression. **(A)** DNA fragmentation, mitochondrial membrane permeabilization (CMXRos), and cytochrome-c release were assessed by flow cytometry after treatment for 72 h with either lipoplatin or cisplatin (30 μM). **(B)** Analysis of Bax, Bcl-2 and Bcl-xL expression.

Cells were incubated with either lipoplatin or cisplatin (30 μM). After 72 h, Bax, Bcl-2, and Bcl-xL expression was assessed by flow cytometry. **(C)** Analysis of caspases activation after incubating cells with either lipoplatin or cisplatin (30 μM) for 24 and 48 h. Cells were harvested, washed and resuspended in complete medium supplemented with FLICA for 1 h at 37 °C, then washed again and analyzed by flow cytometry. Dotted lines indicate background fluorescence of cells. X- and Y-axes indicate the logarithms of the relative fluorescence intensity and relative cell number, respectively. FACS histograms are representative of one of three different experiments.

5.1.3 Lipoplatin induced ROS formation and affected TrxR activity

Several mechanisms are believed to mediate cisplatin-induced apoptosis including the generation of reactive oxygen species (ROS) (Brozovic et al., 2010).
Consistently, induced ROS formation after lipoplatin treatment was observed in both cell lines (ME-180 = 21% and R-ME-180 = 39% ROS positive cells), while cisplatin induced ROS formation only in the cisplatin-sensitive ME-180 cells (Figure 5.4A). Representative flow cytometry dot plots are shown in Figure 5.4B.
Thioredoxin reductase (TrxR) is a selenoenzyme essential to maintain the balance of the cellular redox status and to protect the cells against oxidative damage due to ROS accumulation (Mahmood et al., 2013). R-ME-180 cells expressed higher enzymatic activity of TrxR than ME-180 cells (about 3-fold) (Figure 5.4C). Both lipoplatin and cisplatin reduced TrxR activity in a dose-dependent manner (20 and 30 μM) in both cell lines, but only lipoplatin (30 μM) was able to reduce TrxR activity in R-ME-180 cells to levels lower than those of sensitive ME-180 cells.
These results suggested that reduced enzymatic activity of TrxR by lipoplatin could be involved in ROS accumulation and consequent apoptosis induction.

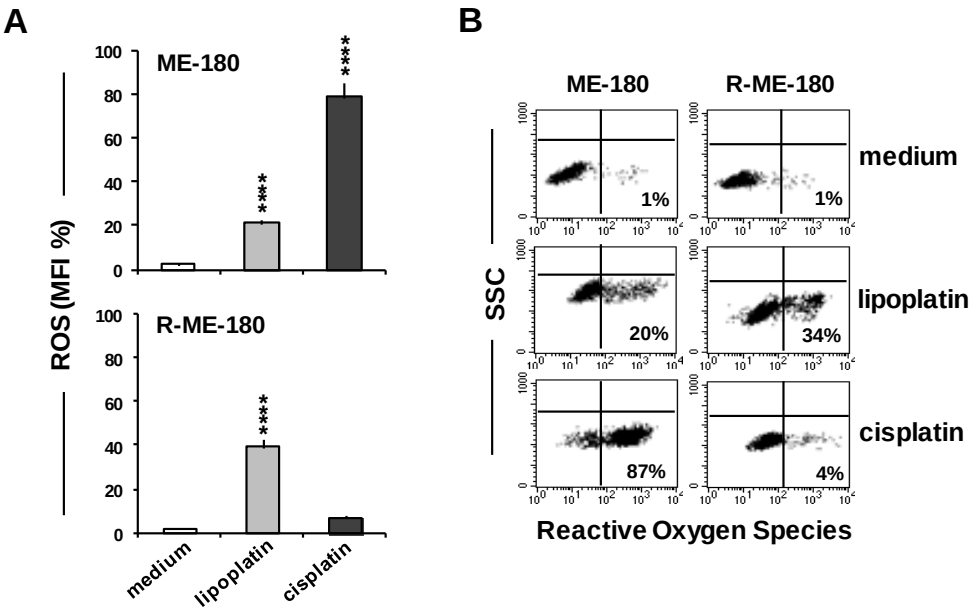

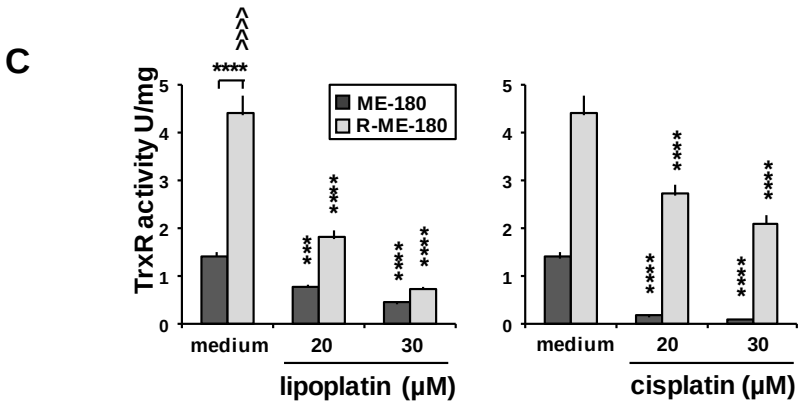

Figure 5.4 Lipoplatin induces ROS accumulation and inhibition of TrxR activity. Cells were treated with either lipoplatin or cisplatin (30 μM) for 72 h. **(A)** ROS production was analyzed with MitoSox reagent; the bar graphs represent the percentage of ROS (MFI = mean fluorescence intensity) as the mean ± SEM of three different experiments. **(B)** Representative FACS dot plots of one of three independent experiments showing ROS formation. **(C)** TrxR enzymatic activity evaluated with the Thioredoxin Reductase Assay Kit after 72 h treatment with lipoplatin (20 and 30 μM). Values in the bar graph represent the mean ± SEM of three different experiments. ***P < 0.001, ****P < 0.0001 drug *vs* medium, ^^^^P < 0.0001 R-ME-180 *vs* ME-180.

5.1.4 Lipoplatin inhibited cancer cell migration, invasion and down-modulated EGFR expression

Metastasis is a multistep process where tumor cells disseminate from the primary tumor and colonize distant organs. To achieve this, cell motility and cell invasion of basement membranes and of surrounding tissues are crucial (Bravo-Cordero et al., 2012).

I evaluated the effect of lipoplatin on cancer cell migration using the scratch wound healing assay and the FATIMA assay for cell invasion.

Cells were treated 72 hours with low drug concentration (10 μM) to avoid cell death. To exclude that in untreated cells a higher migration rate could be attributable to an increased cell proliferation, cells were cultured in the presence of low serum concentration.

After 48 hours untreated control cells almost closed the wound, while the migration rate (the percentage of the surface area covered by tumor cells after the scratch) of lipoplatin treated cells was 57% in ME-180 and 60% in R-ME-180. At the same experimental conditions cisplatin reduced cell migration only in ME-180 cells (Figures 5.5A and B).

In subsequent experiments, I assessed invasion of tumor cells, treated for a short time (12 hours) with 30 μM lipoplatin, through a type I collagen-coated Boyden chamber. Invasion was evaluated after 5 and 24 hours. R-ME-180 cells exhibited enhanced invasive properties compared to ME-180 cells (Figure 5.5C). At 24 hours lipoplatin decreased the invasion rate of about 35% in ME-180 and 50% in R-ME-180 cells (Figure 5.5C).

Epithelial growth factor receptor (EGFR), also known as Her or ErbB, is over-expressed in approximately 85% of invasive cervical tumors, it is associated with higher stages and poor prognosis, and its inhibition significantly decreases tumor cell metastases (Soonthornthum et al., 2011).

I evaluated the surface expression of EGFR in ME-180 and R-ME-180 cells by flow cytometry. R-ME-180 (mean fluorescence intensity (MFI) = 387.26 ± 42) expressed higher amounts of EGFR than ME-180 cells (MFI = 201.68 ± 30). Lipoplatin (30 μM) decreased EGFR expression in both cell lines, while cisplatin, used at the same concentration, remarkably down-modulated EGFR in ME-180 cells and only minimally affected R-ME-180 cells (Figure 5.5D). A representative experiment is shown in Figure 5.5E.

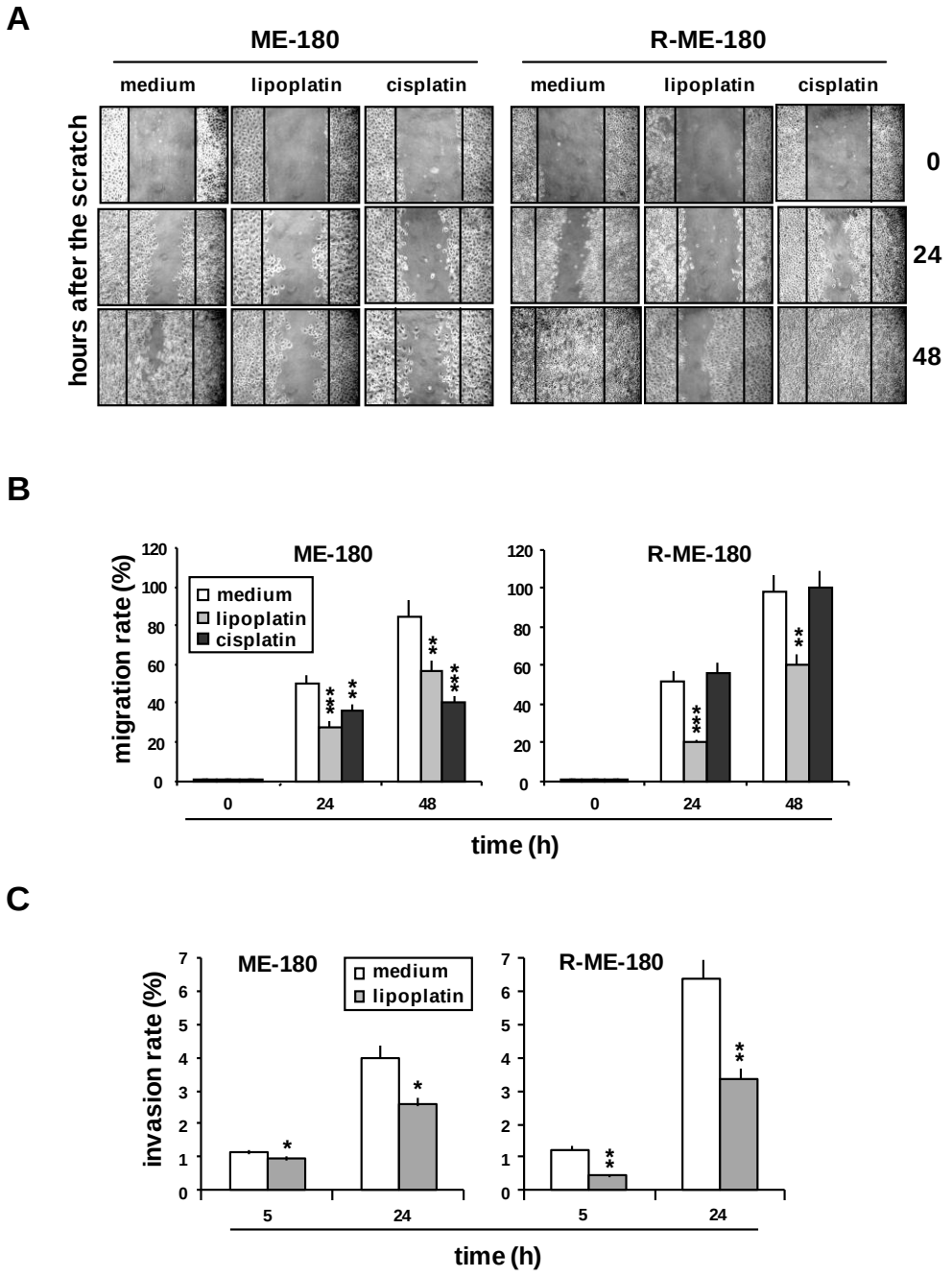

D

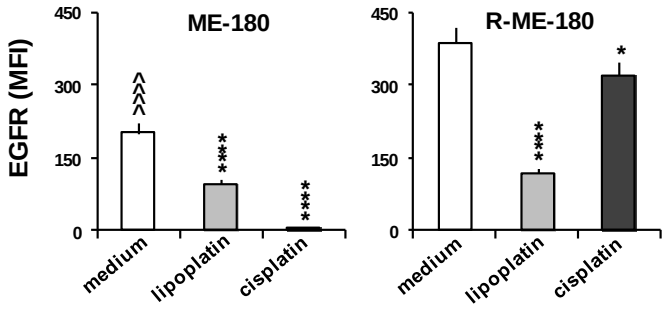

E

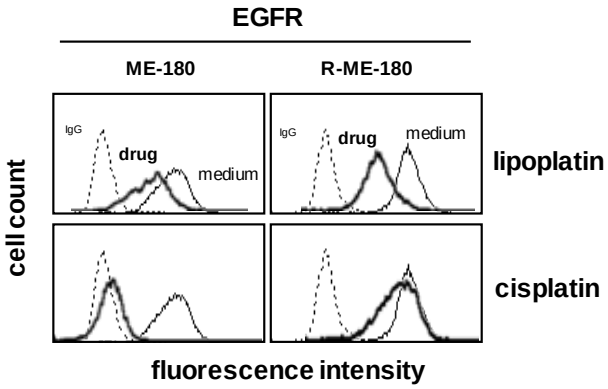

Figure 5.5 Lipoplatin inhibits cell migration and decreases EGFR expression. Cells were treated with lipoplatin or cisplatin at 10 μM for 72 h. Then cell confluent monolayers were scraped up three times and cultured in low serum medium for additional 48 h: **(A)** representative scratch test analysis of cell migration (phase contrast microphotographs, original magnification 10×); **(B)** migration rate represented as the distance between the edges of the wound (defined by the lines), indicating the surface area occupied by the migrating cells after 24 and 48 h. Values in the bar graph represent the mean ± SEM of three different experiments. **(C)** Migration of cervical cancer cells through a collagen type I-coated Boyden chamber (invasion) after treatment for 12 h with 30 μM lipoplatin. *P < 0.05, **P < 0.01, ***P < 0.001 drug *vs* medium. **(D)** Cells were treated for 72 h with either lipoplatin or cisplatin (30 μM). Then EGFR surface expression was analyzed by flow cytometry using the anti-EGFR mAb 528. Mean fluorescence intensity (MFI) values in the bar graph represent the mean ± SEM of three different experiments. *P < 0.05, ****P < 0.0001 drug *vs* medium. ^^^^P < 0.0001 R-ME-180 *vs* ME-180. **(E)** Representative FACS histograms of one of three independent experiments showing EGFR expression after drug treatment.

5.1.5 Spheroids-forming efficiency and ALDH are increased in R-ME-180 cells: lipoplatin inhibited spheroid formation and reduced ALDH(+) cells

Spheroids represent a three-dimensional *in vitro* system that more closely resembles the *in vivo* tumor microenvironment. A greater ability to form spheroids (Sugihara and Saya, 2013) and the expression of Aldehyde Dehydrogenase

(ALDH) enzyme (López et al., 2012) usually indicate an increase in the Cancer Stem Cell (CSC) population.

Cisplatin-resistant R-ME-180 cells, but not ME-180, spontaneously formed spheroids when cultured in non-adherent conditions (poly-HEMA coated wells). Consistently, R-ME-180 expressed a higher amount of ALDH(+) cells than ME-180 when cultured as monolayer. The percentage of ALDH(+) cells increased in R-ME-180 cultured as spheroids (I gen). Then, to further select ALDH(+) cells I dissociated the first generation of spheroids to single cells and replated them under non-adherent conditions (II gen). In this second generation of spheroids I found an enriched ALDH(+) cell population compared to the first generation spheroids.

ALDH activity was about 0.2% in ME-180 and 0.51% in R-ME-180 cells grown as monolayer. The percentage of ALDH(+) cells in R-ME-180 cultured as spheroids was 4.45-fold (I gen) and 6.82-fold (II gen) higher than R-ME-180 cultured as monolayer (Figure 5.6A). A representative FACS dot plot showing ALDH expression is shown in Figure 5.6B.

Then, I investigated whether lipoplatin could affect spheroid formation and the amount of ALDH(+) cells.

Lipoplatin (10, 25, 50 μM) inhibited spheroid formation in poly-HEMA coated wells. After 72 hours R-ME-180 cells formed several large and dense spheroids, whereas lipoplatin treated cells formed small spheroids with dead cells interspersed among cell aggregates (Figure 5.7A). At the highest lipoplatin concentration (50 μM) I detected only dead cells (Figure 5.7A).

Then, I dissociated R-ME-180 spheroids and evaluated apoptosis and ALDH(+) enzymatic activity by flow cytometry.

Lipoplatin induced apoptosis (Figure 5.7B), evaluated by Annexin-V/PI staining, and decreased the percentage of ALDH(+) cells in a dose-dependent manner (Figure 5.7C). Representative flow cytometry dot plots of ALDH activity are shown in Figure 5.7D.

Under the same experimental conditions cisplatin did not affect spheroid formation and only slightly induced apoptosis (Figures 5.7A and B).

A

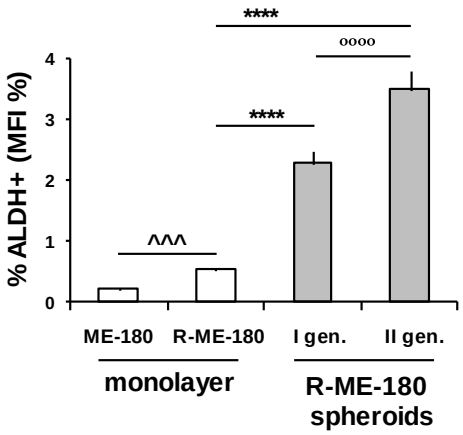

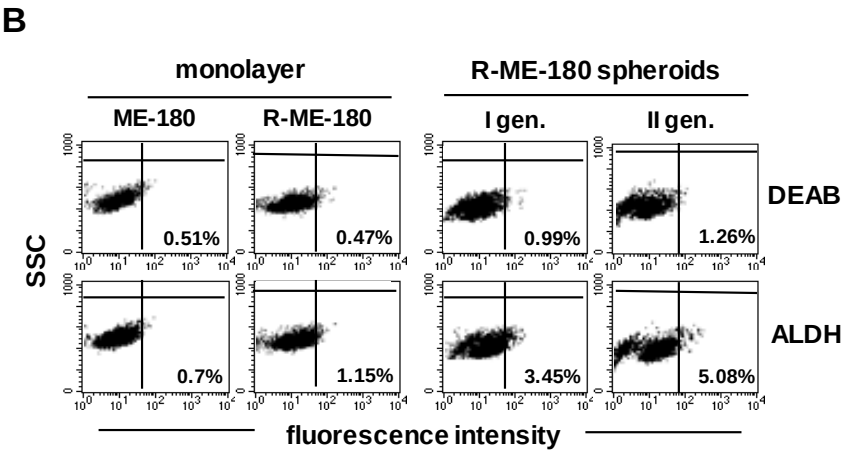

Figure 5.6 Spheroid-forming efficiency and ALDH are increased in R-ME-180 cells. **(A)** ALDH expression was evaluated by flow cytometry in ME-180 and R-ME-180 monolayers and in first (I gen.) and second generation (II gen.) spheroids. Values in the bar graph, reported as the percentage of ALDH positive cells, represent the mean ± SEM of three different experiments. ^^^P < 0.001ME-180 *vs* R-ME-180 monolayer; ****P < 0.0001 R-ME-180 monolayer *vs* I and II gen. spheroids, °°°°P < 0.0001 I gen. *vs* II gen. spheroids. **(B)** Representative FACS dot plots of one of three independent experiments showing ALDH expression.

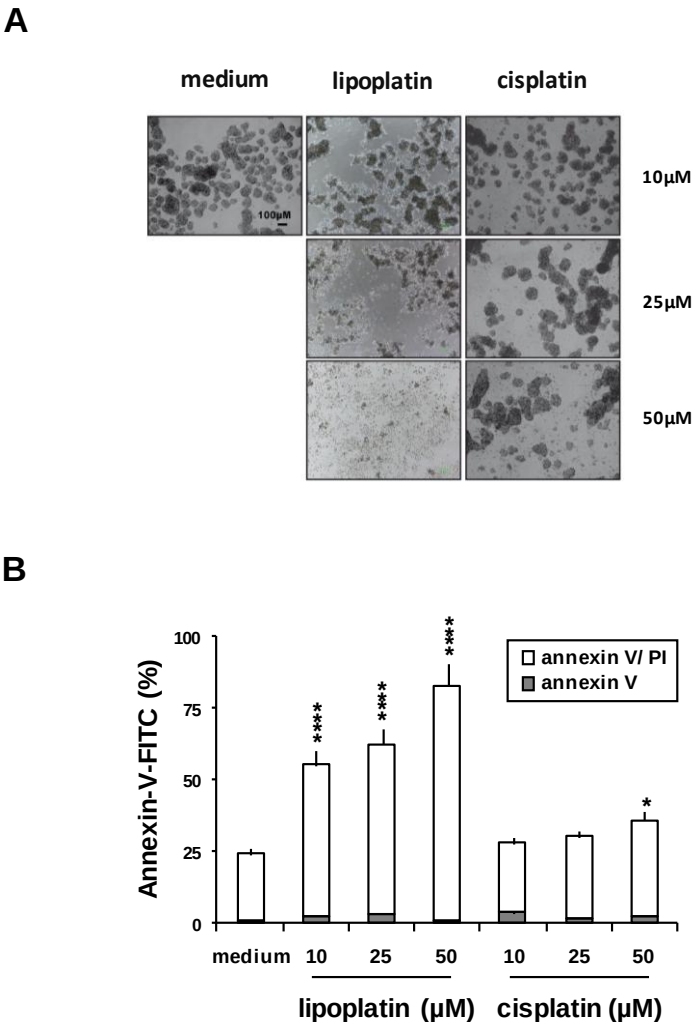

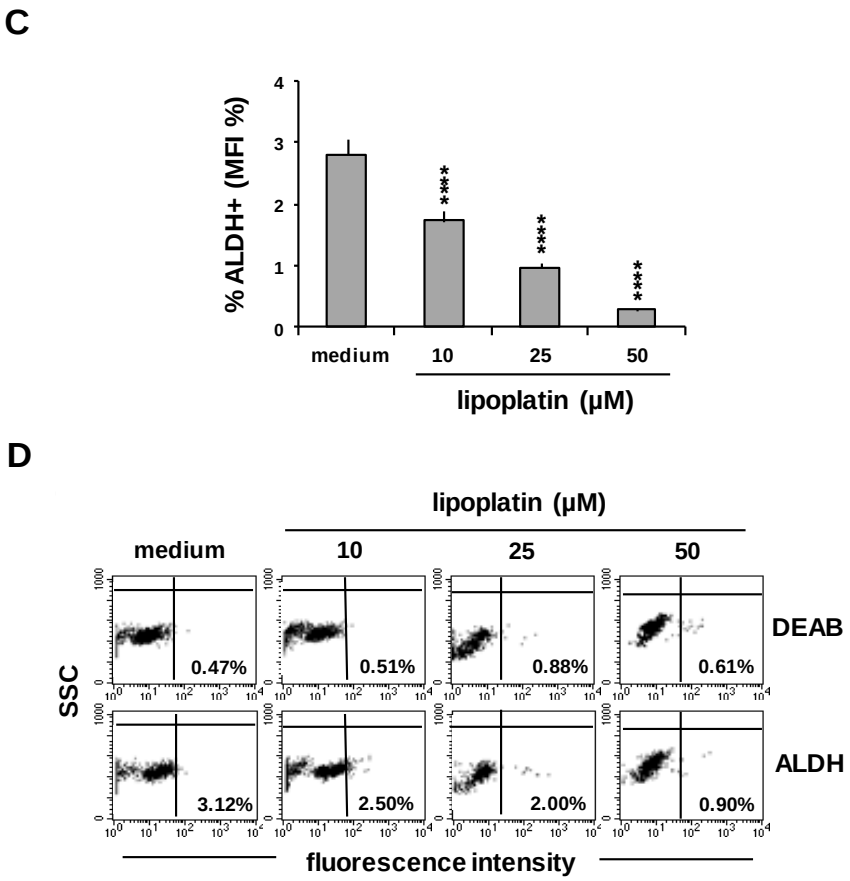

Figure 5.7 Lipoplatin inhibits spheroid formation and reduces ALDH(+) cells. **(A)** R-ME-180 cells, cultured on plates covered with poly- HEMA (2-hydroxyethyl methacrylate), were treated with lipoplatin or cisplatin (10, 25, 50 μM). After 72 h spheroids were photographed (phase contrast microphotographs, original magnification 4×) and then disrupted to evaluate apoptosis **(B)** or ALDH expression **(C-D)**. **(B)** The graph indicates the mean ± SEM values of the percentages of apoptotic cells evaluated by Annexin-V/PI staining from three independent experiments, each performed in duplicate. **(C)** The graph represents ALDH quantification, as MFI percentage, after spheroid treatment with lipoplatin. Data are expressed as mean ± SEM of three separate experiments. **(D)** Representative FACS dot plots of one of three independent experiments showing ALDH expression (% of positive cells).

5.1.6 Lipoplatin inhibited the growth of cervical cancer xenografts

Finally, I evaluated lipoplatin anticancer activity *in vivo*.

Cisplatin-resistant R-ME-180 cells (2.5×10^6) were injected into the right flank of 6-week-old female athymic nude mice. After 4 days (tumor size of about 32 mm^3) mice were randomly divided in two groups (5 mice per group) and treated intraperitoneally either with 10 mg/kg lipoplatin or with vehicle. Treatment for 28 days resulted in a significant ($P<0.01$) tumor growth inhibition, approximately 70%. The tumors of the untreated control group grew to a mean tumor size of 615.4 ± 50 mm^3, while in lipoplatin treated mice tumors reached a mean size of 192 ± 15 mm^3 (Figure 5.8). There was no histological detectable cytotoxicity

involving the animals' heart, spleen, liver, and kidney, whereas treatment with the same concentration of cisplatin was lethally toxic for mice (data not shown).

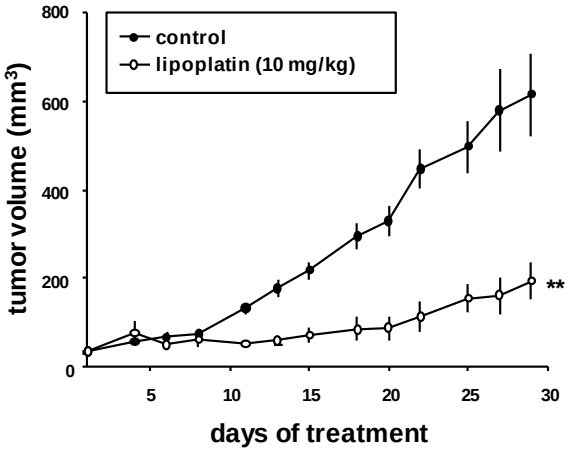

Figure 5.8 *In vivo* anticancer activity of lipoplatin (xenograft). Tumor volume was measured in female athymic nude mice after intraperitoneal (i.p.) injection of either drug-free medium or containing 10 mg/kg lipoplatin, three times a week using a caliper. Points represent the mean ± SEM of five animals per group. **P < 0.01 lipoplatin *vs* control.

5.2 Lipoplatin activity on ovarian cancer cells

5.2.1 Lipoplatin inhibited ovarian cancer cell proliferation and induced apoptosis and cell cycle modifications

I evaluated the antiproliferative activity of lipoplatin in a panel of ovarian cancer cell lines of different histotypes and with various degrees of cisplatin sensitivity: A2780, A2780cis, MDAH, OVCAR-5, OVCAR-3, SKOV-3, and TOV-21G.
Seventy-two hours treatment with increasing concentrations of lipoplatin or cisplatin (2.5-100 μM) induced a dose-dependent inhibition of cell proliferation, as evaluated by MTT cell viability assay. Using the CalcuSyn software I calculated the IC_{50}.
All the ovarian cancer cell lines expressed similar sensitivity to lipoplatin. The IC_{50} of lipoplatin was about 17 μM for all cell lines, excluding OVCAR3 cells (32 μM), while the IC_{50} for cisplatin was very different, ranging from 1.5 μM to 11.9 μM, with OVCAR5 being the less sensitive cell line (Table 5.2).
Also A2780 cells and its parental cisplatin-resistant cell line, A2780cis, showed a comparable sensitivity to lipoplatin (Table 5.2). On the contrary, the IC_{50} of cisplatin was about 7-fold higher in the cisA2780 (IC_{50} = 10.4 μM) compared to the parental cisplatin-sensitive cell line A2780 (IC_{50} = 1.5 μM).

Table 5.2 Growth inhibition by lipoplatin and cisplatin in a panel of ovarian cancer cell lines.

	IC_{50} (μM)						
	A2780	A2780cis	MDAH	OVCAR3	OVCAR5	SKOV3	TOV21G
Lipoplatin	**17.8±1.6**	**17.2±1.5**	**14.6±1.4**	**32.1±3.3**	**16.9±1.5**	**17.1±1.5**	**17.8±1.7**
Cisplatin	1.5±0.1	10.4±0.9	4.3±0.3	5.9±0.6	11.9±1.2	5.4±0.6	3.2±0.2

IC_{50} values are mean ± SEM from 3 independent experiments.

Then, I evaluated apoptosis induction after lipoplatin treatment. For this purpose I used the most cisplatin-resistant cell line OVCAR5, and SKOV3 cells, capable to generate tumor spheres (Ma et al., 2010).
Lipoplatin induced apoptosis in a dose-depent manner in both OVCAR5 and SKOV3 cells, as evaluated by Annexin-V and PI staining (Figure 5.9A).
Apoptosis induction after lipoplatin treatment (30 μM for 72 hours) was also confirmed by the presence of DNA fragmentation, a late event in apoptosis (Figure 5.10A).
It is known that cisplatin affects cell cycle progression (Liu et al., 2000).

Lipoplatin treatment (30 µM for 24 hours) determined an arrest of the cell cycle in the G2/M phase in SKOV3 cells, and an increase in S and G2/M phase in OVCAR5 cells (Figure 5.9B).

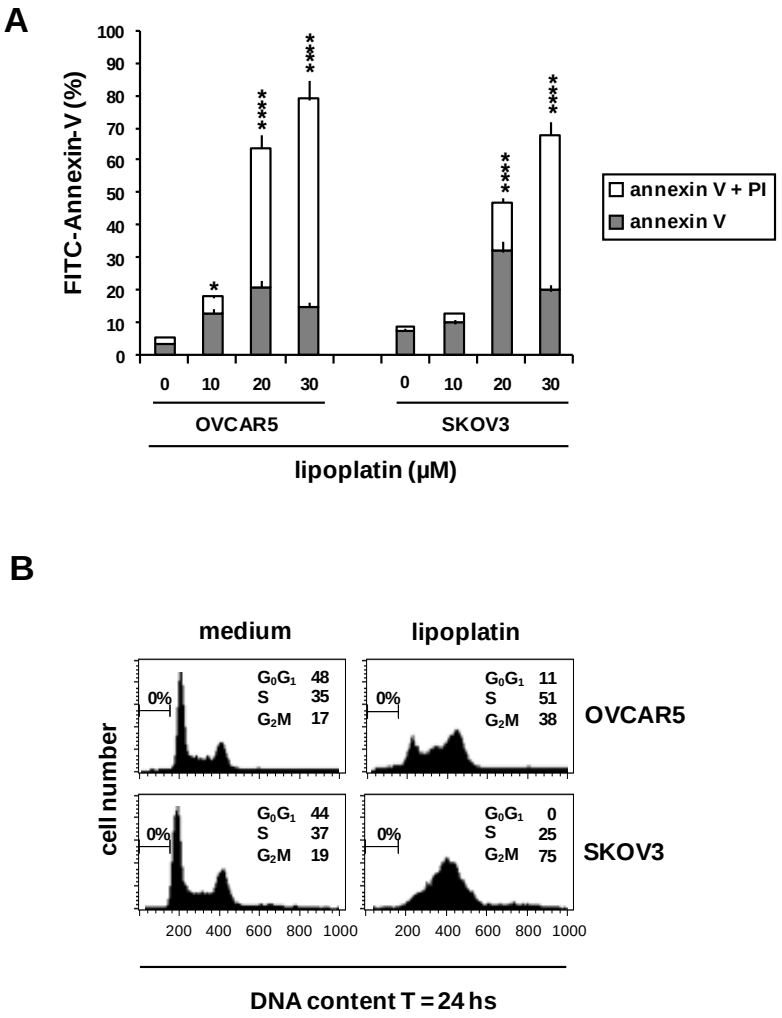

Figure 5.9 Lipoplatin induces apoptosis and cell cycle modifications. **(A)** FACS analysis of cells, double stained with Annexin-V-FITC and PI, after 72 h incubation at 37 °C with different concentrations of lipoplatin. Values in the bar graph represent the mean ± SEM of three different experiments. ****P < 0.0001 drug *vs* medium. **(B)** FACS histograms showing cell cycle progression. Cells were treated 24 h with 30µM lipoplatin and stained with PI. The percentages of cells in the G0/G1 phase, S phase, and G2M phase are reported, as well as the percentage of sub-G1 cells. FACS histograms are representative of one of three different experiments.

5.2.2 Lipoplatin affected mitochondrial functions, ROS formation and TrxR activity

Similarly to the results obtained with cervical cancer cells, lipoplatin treatment (30 μM for 72 hours) led to a decline in the mitochondrial membrane potential, revealed by the decreased fluorescent signal of CMXRos, and to the release of cytochrome-c, as evaluated by flow cytometry, in both OVACR5 and SKOV3 cells (Figure 5.10A). Moreover, after lipoplatin treatment the expression of the pro-apoptotic molecule Bax remarkably increased, whereas the anti-apoptotic molecule Bcl-2 decreased. The expression of Bcl-xL did not change (Figure 5.10A and B). Consistently, lipoplatin determined the activation of caspases 9 and 3, in both cell lines (Figure 5.10C and D).

Lipoplatin (20 and 30 μM for 72 hours) let to a dose-dependent induction of ROS in both cell lines (Figures 5.11A). At concentration 30 μM ROS accumulation remarkably increased. Representative FACS dot plots of ROS formation are shown in Figure 5.11B.

Subsequently, I evaluated the enzymatic activity of the ROS scavenger TrxR. OVCAR5 cells expressed higher amounts of TrxR than SKOV3 cells (OVCAR5 U/mg = 276 and SKOV3 U/mg = 217) (Figure 5.11C). Lipoplatin treatment reduced TrxR activity in a dose-dependent manner (20 and 30 μM for 72 hours) in both cell lines. At the highest concentration, lipoplatin reduced TrxR activity to less than 20% of control (Figure 5.11C).

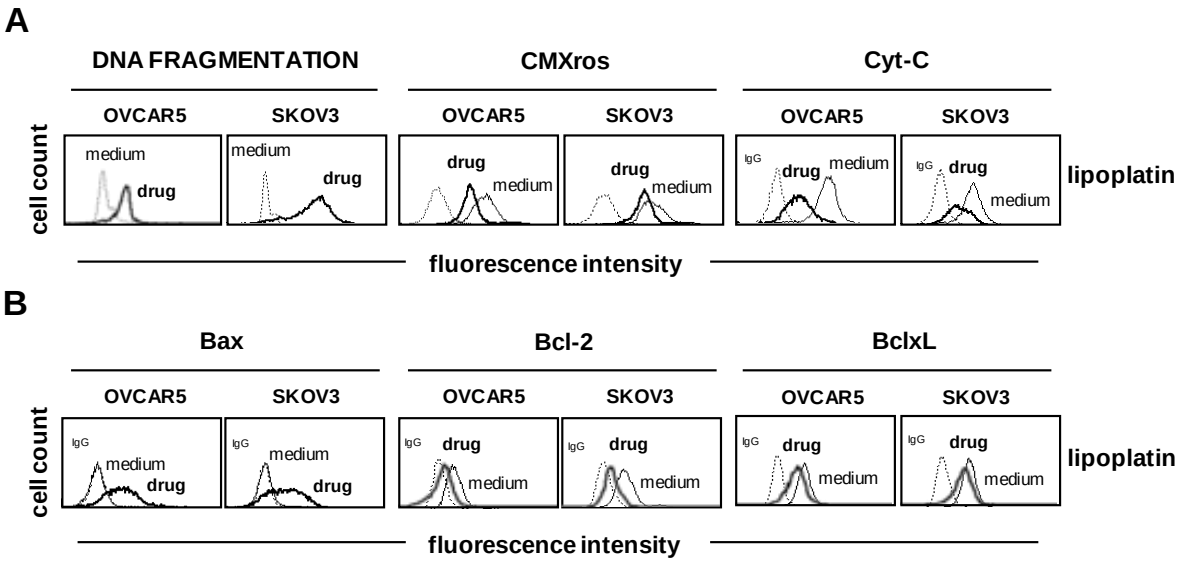

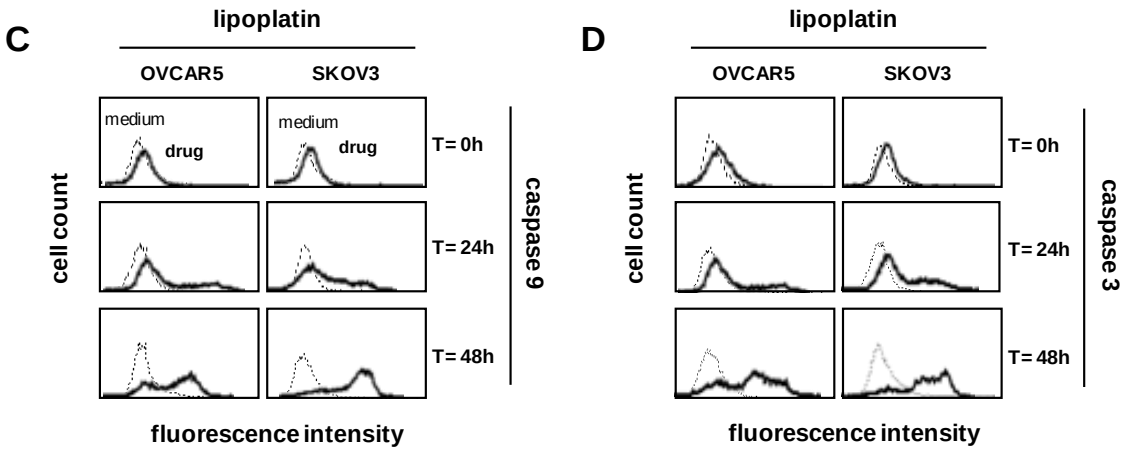

Figure 5.10 Lipoplatin induces mitochondria-mediated apoptosis and modulates Bax and Bcl-2. **(A)** DNA fragmentation, mitochondrial membrane permeabilization (CMXRos), and cytochrome-c release were assessed by flow cytometry after treatment for 72 h with lipoplatin (30 μM). **(B)** Analysis of Bax, Bcl-2 and Bcl-xL expression. Cells were incubated with lipoplatin (30 μM). After 72 h, Bax, Bcl-2, and Bcl-xL expression was assessed by flow cytometry. **(C)** Analysis of caspases activation after incubating cells with lipoplatin (30 M) for 24 and 48 h. Cells were harvested, washed and resuspended in complete medium supplemented with FLICA for 1 h at 37 °C, then washed again and analyzed by flow cytometry. Dotted lines indicate background fluorescence of cells. X- and Y-axes indicate the logarithms of the relative fluorescence intensity and relative cell number, respectively. FACS histograms are representative of one of three different experiments.

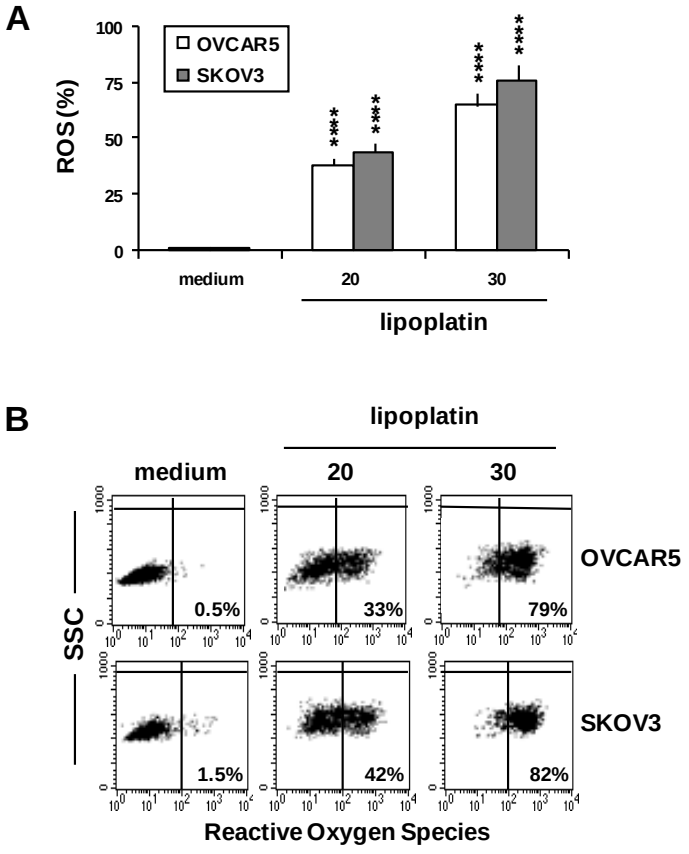

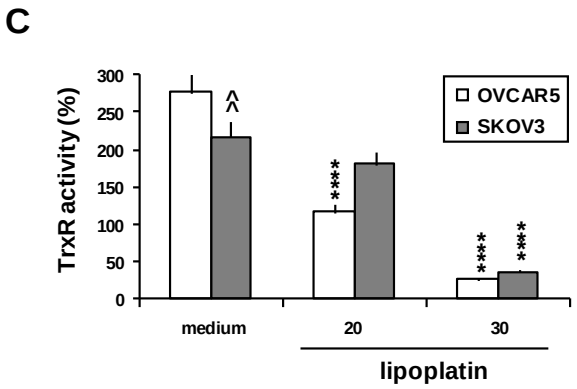

Figure 5.11 Lipoplatin induces ROS accumulation and inhibition of TrxR activity. Cells were treated with lipoplatin (20 and 30 μM) for 72 h. **(A)** ROS production was analyzed with MitoSox reagent; the bar graphs represent the percentage of ROS as the mean ± SEM of three different experiments. **(B)** Representative FACS dot plots of one of three independent experiments showing ROS formation. Percentage of ROS positive cells are shown. **(C)** TrxR enzymatic activity evaluated with the Thioredoxin Reductase Assay Kit. Values in the bar graph represent the mean ± SEM of three different experiments. ****P < 0.0001 drug *vs* medium, ^^P < 0.0001 OVCAR5 *vs* SKOV3.

5.2.3 Lipoplatin inhibited cancer cell invasion and down-modulated EGFR expression

I evaluated the effect of lipoplatin on cancer cell invasion through a type I collagen-coated Boyden chamber using the FATIMA assay. Cells were treated 72 hours with low drug concentration (10 μM) to avoid apoptosis.

Lipoplatin decreased cell invasion of both cell lines of more than 40% (Figure 5.12A).

EGFR is involved in ovarian cancer cell invasion, representing an attractive target in the treatment of epithelial ovarian cancer (Gui and Shen, 2012; Jeong et al., 2013).

Cells were treated with lipoplatin (20 and 30 μM) for 72 hours. OVCAR5 cells expressed a higher level of EGFR (MFI = 818 ± 73) than SKOV3 cells (MFI = 639 ± 57) (Figure 5.12B). At the concentration of 20 μM lipoplatin decreased EGFR surface expression to less than 20% of control in both cell lines (Figure 5.12B). Representative flow cytometry histogram plots are shown in Figure 5.12C.

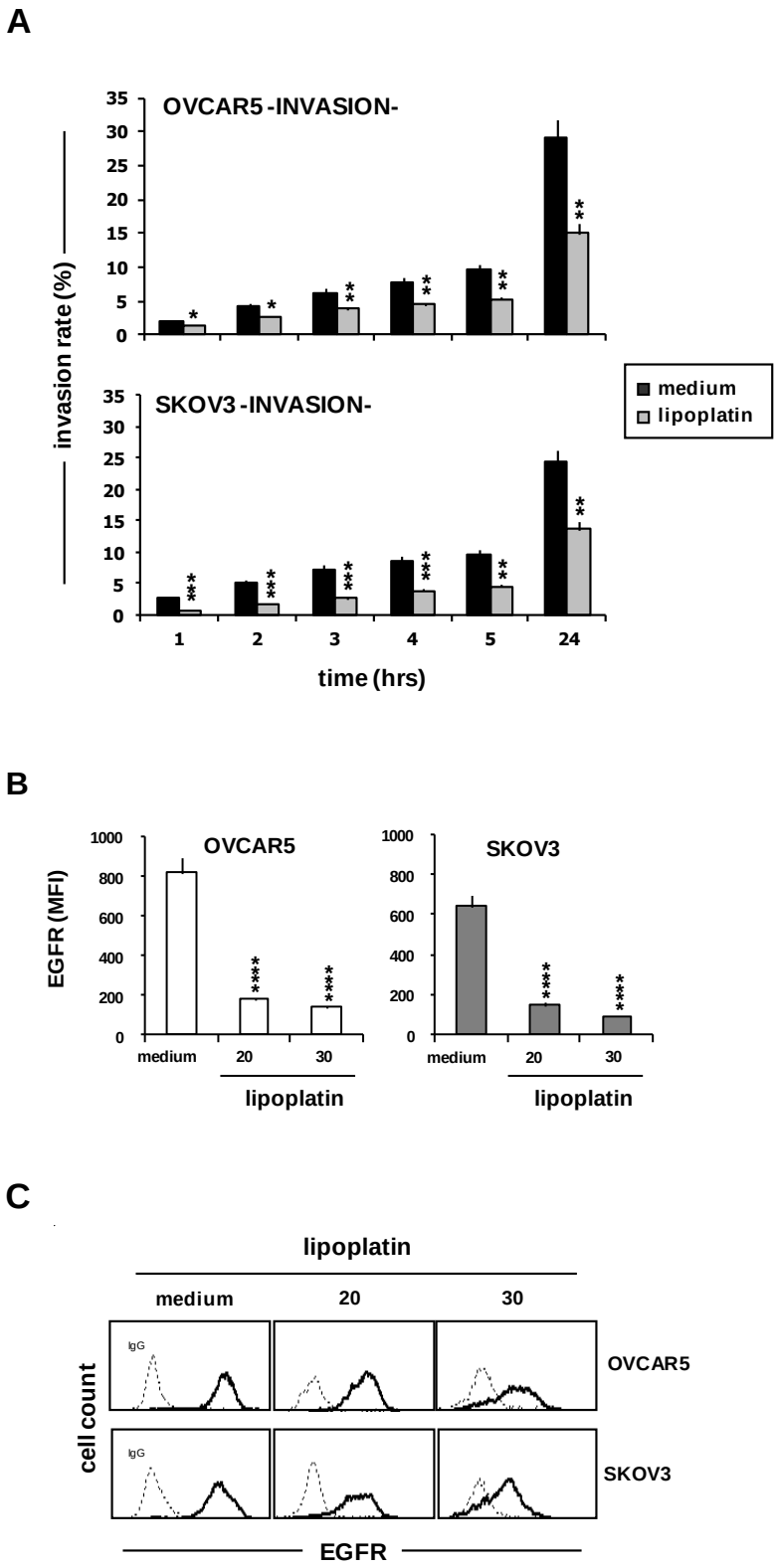

Figure 5.12 Lipoplatin inhibits cell invasion and decreases EGFR expression. **(A)** Invasion of ovarian cancer cells through a collagen type I-coated Boyden chamber after treatment for 72 h with 10 μM lipoplatin. **P < 0.01drug *vs* medium. **(B)** Cells were treated for 72 h with lipoplatin (20 and 30 μM), then EGFR surface expression was analyzed by flow cytometry using the anti-

EGFR mAb 528. Values in the bar graph represent the mean ± SEM of three different experiments. ****P < 0.0001 drug *vs* medium. ^^P < 0.0001 OVCAR5 *vs* SKOV3. **(C)** Representative FACS histograms of one of three independent experiments showing EGFR expression after drug treatment.

5.2.4 Lipoplatin drug combination

Synergy occurs when drugs can interact in ways that their combined effect is greater than the sum of their individual effects. Drug combination is widely used in treating cancer. The main aims are to achieve synergistic therapeutic effect, dose and toxicity reduction, and to minimize or overcome the induction of drug resistance (Chou, 2010).
I combined lipoplatin with the most commonly drugs used to treat ovarian cancer: abraxane, docetaxel, doxorubicin, and paclitaxel.
OVCAR5 and SKOV3 cells were cultured in the presence of a single chemotherapeutic agent or in combination with lipoplatin. After 72 hours treatment, I assessed cell viability using the MTT assay and determined the possible synergistic activity calculating the combination index (CI) using the Calcusyn software. Values of CI less than 1 indicate synergy, CI over 1 indicate antagonism, and CI about 1 indicate additive effect (Table 5.3) (Bijnsdorp et al., 2011).

Table 5.3 Table showing the combination index values and their indication.

CI		Synergism/antagonism
<0.1	+++++	Very strong synergism
0.1–0.3	++++	Strong synergism
0.3–0.7	+++	Synergism
0.7–0.85	++	Moderate synergism
0.85–0.9	+	Slight synergism
0.9–1.1		Nearly additive
1.1–1.2	–	Slight antagonism
1.2–1.45	––	Moderate antagonism
1.45–3.3	–––	Antagonism
3.3–10	––––	Strong antagonism
>10	–––––	Very strong antagonism
Simplified CI values and their indication		
<0.8		Synergism
0.8–1.2		Additive
>1.2		Antagonism

The combination of lipoplatin and abraxane showed synergistic activity against OVCAR5 and SKOV3 cells with CI minor than 0.7 at low drug concentrations. At high concentrations an additive or even antagonistic effect was observed (Figure 5.13B and C). A representative synergy effect of lipoplatin and abraxane on cell viability is shown in Figure 5.13A.
OVCAR5 cells were less sensitive to doxorubicin compared to SKOV3 cells (IC_{50} = 0.87 ng/ml and IC_{50} = 0.13 ng/ml, respectively). The combination of lipoplatin

and doxorubicin showed synergism at IC_{50} concentrations in both OVCAR5 and SKOV3 cell lines (Figure 5.13D and E). An additive or even antagonistic effect was observed at the extremes of the dose-response curves in SKOV3 cells and at the highest concentration in OVCAR5 (Figure 5.13F).
In OVCAR5 cells the combination of lipoplatin with docetaxel was moderate or additive (Figure 5.14B and C). Similar results were obtained also in SKOV3 cells, even if docetaxel did not reach an IC_{50} (Figure 5.14B and C). A representative growth-inhibitory effect of lipoplatin and docetaxel on cell viability is shown in Figure 5.13A.
Interestingly, IC_{50} of paclitaxel was 25.27 ng/ml in OVCAR5 and 136.45 ng/ml in SKOV3 cells, whereas the calculated IC_{50} of abraxane, the albumin-bound paclitaxel formulation, was almost similar in both cell lines. The combination of lipoplatin and paclitaxel showed a moderate synergism or an additive effect in both cell lines, with CI of about 0.7 (Figure 5.14D, E and F).

A

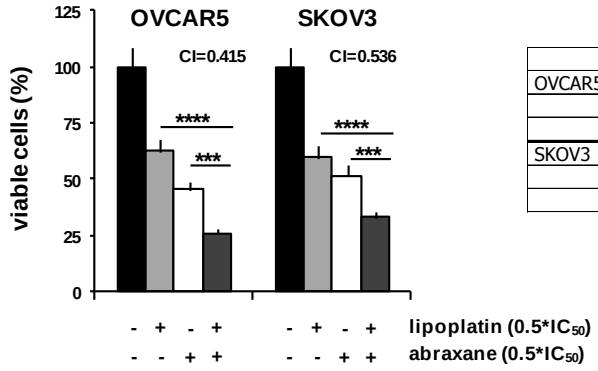

B

	Lipoplatin (µM)	ABX (ng/ml)	**C.I.**
OVCAR5	4.23	8.42	**0.687**
	8.46	16.84	**0.415**
	*16.93	*33.68	**0.325**
SKOV3	4.27	11.76	**0.381**
	8.53	23.52	**0.536**
	*17.06	*47.05	**0.507**

C

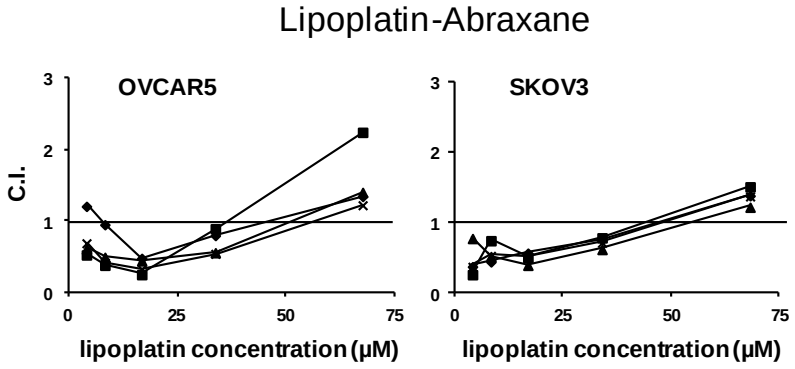

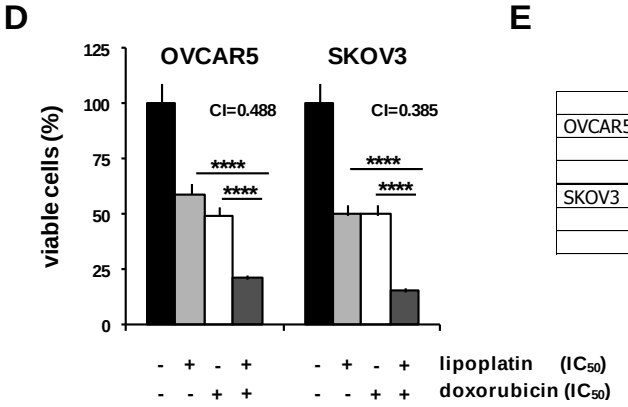

E

	Lipoplatin (μM)	DOXO(ng/ml)	C.I.
OVCAR5	8.46	0.43	**0.839**
	*16.93	*0.87	**0.488**
	33.86	1.73	**0.718**
SKOV3	8.53	0.06	**0.877**
	*17.06	*0.13	**0.385**
	34.12	0.26	**0.586**

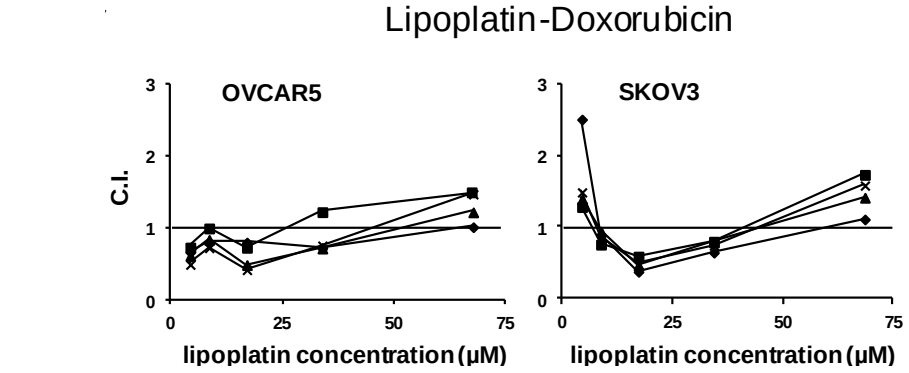

Figure 5.13 Combination of lipoplatin with abraxane and doxorubicin. OVCAR5 and SKOV3 cells were incubated with each drug alone or in combination for 72 h and cell viability was determined by the MTT assay. Synergy was determined by calculating the combination index (CI) analyzed by Calcusyn software. Each value represents a mean of 3 independent experiments performed in triplicate (± SEM). ***P < 0.001, ****P < 0.0001 single drug *vs* combination treatment. Representative experiments demonstrating synergistic effects on cell viability of lipoplatin with abraxane **(A)** and doxorubicin **(D)**.

Synergy between lipoplatin and abraxane (ABX) **(B)**, doxorubicin (DOXO) **(E)** using a range of drug concentrations. CI<1 denotes synergism, CI=1 additivity and CI>1 antagonism. * indicates drug IC_{50}.

CI for lipoplatin combined with abraxane **(C)** and doxorubicin **(F)**. The horizontal dashed line highlights CI=1.

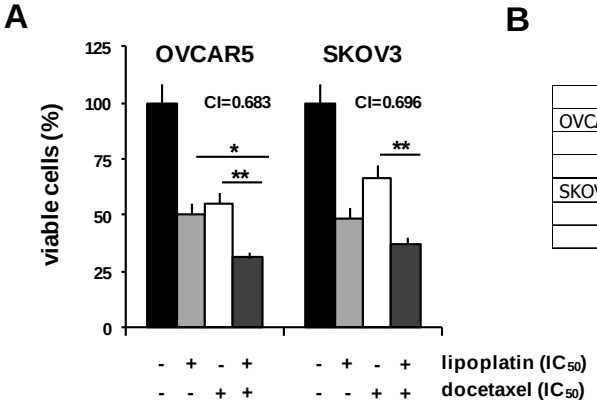

B

	Lipoplatin (μM)	DTX (nM)	C.I.
OVCAR5	8.46	9.02	**1.105**
	*16.93	*18.04	**0.683**
	33.86	36.08	**0.729**
SKOV3	8.53	20.45	**0.728**
	*17.06	40.90	**0.696**
	34.12	81.80	**0.636**

C

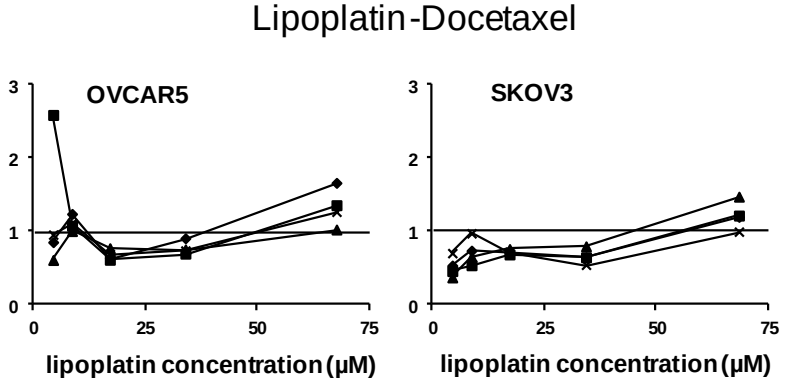

D

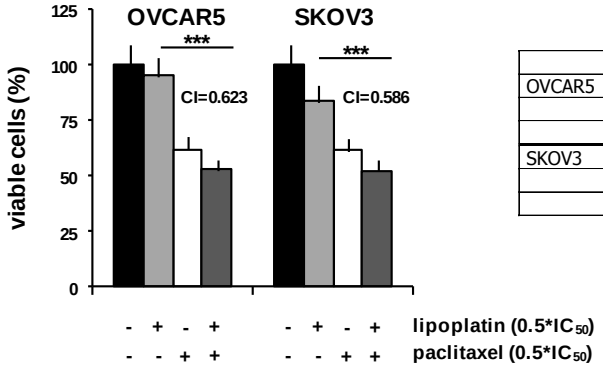

E

	Lipoplatin (µM)	PTX (ng/ml)	**C.I.**
OVCAR5	8.46	12.64	**0.623**
	*16.93	*25.27	**0.752**
	33.86	50.54	**0.808**
SKOV3	8.03	68.23	**0.586**
	*17.06	*136.45	**0.706**
	34.12	272.90	**0.617**

F

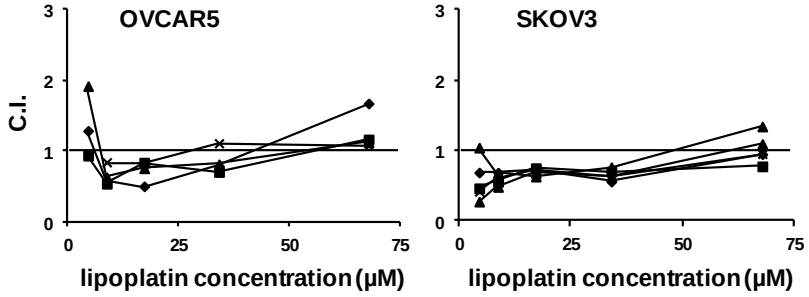

Figure 5.14 Combination of lipoplatin with docetaxel and paclitaxel. OVCAR5 and SKOV3 cells were incubated with each drug alone or in combination for 72 h and cell viability was determined by the MTT assay. Synergy was determined by calculating the combination index (CI) analyzed by Calcusyn software. Each value represents a mean of 3 independent experiments performed in triplicate (± SEM). *P < 0.05, **P < 0.01, ***P < 0.001 single drug *vs* combination treatment. Representative experiments demonstrating synergistic effects of lipoplatin with docetaxel **(A)** and paclitaxel **(D)**.

Synergy between lipoplatin and docetaxel (DTX) **(B)**, paclitaxel (PTX) **(E)** using a range of drug concentrations. CI<1 denotes synergism, CI=1 additivity and CI>1 antagonism. * indicates drug IC_{50}.

CI for lipoplatin combined with docetaxel **(C)** and paclitaxel **(F)**. The horizontal dashed line highlights CI=1.

5.2.5 Lipoplatin decreased cancer stem cell markers and prevented tumor spheroid formation

Cancer seems to be driven by tumor-initiating cells, popularly known as cancer stem cells (CSC). CSC are characterized by their ability to form tumor spheres and are involved in drug resistance and disease recurrence (Shank et al., 2012). Markers identifying CSC in ovarian cancer include CD133 and the aldehyde dehydrogenase (ALDH) enzyme activity. Drugs that are able to target CSC may offer a great promise to improve the therapeutic outcome (Silva et al., 2011).

I evaluated by flow cytometry ALDH enzymatic activity and CD133 surface expression in both, OVCAR5 and SKOV3 cells, after lipoplatin treatment. OVCAR5 cells showed a 2-fold higher level of ALDH positive cells compared to SKOV3 cells (ALDH+ = 7.96% and 4.08%, respectively) (Figure 5.15A), whereas CD133 expression was almost similar in both cell lines (CD133+ = 5.4% and 5.6%, respectively) (Figure 5.15C). The treatment of OVCAR5 and SKOV3 cells with increasing concentrations (10, 20, and 30 μM) of lipoplatin for 72 hours reduced ALDH (Figure 5.15A) and CD133 (Figure 5.15C) positive cells in a dose-dependent manner.

Representative flow cytometry dot plots of ALDH(+) cells (Figure 15B) and histogram plots of CD133 surface expression (Figure 5.15D) are shown.

It is known that in the ascites of a patient with advanced ovarian cancer there is the presence of multicellular tumor aggregates or spheroids that are believed to make a significant contribution to chemoresistance and intraperitoneal spread (Lengyel, 2010).

SKOV3 cells spontaneously produced compact spheroids when cultured under non-adherent conditions. The spheroids obtained with the poly-HEMA technique were similar to those I observed in the ascites of patients with ovarian cancer (Figure 5.16A). Lipoplatin (10, 25, and 50 μM) reduced in a dose-dependent manner spheroid formation. At the highest lipoplatin concentration (50 μM) I only detected dead cells, as confirmed by the Annexin-V/PI staining (Figure 5.16B and C) performed on dissociated spheroids.

Taken together, these results demonstrated that lipoplatin decreased two markers of ovarian cancer stem cells and spheroids formation.

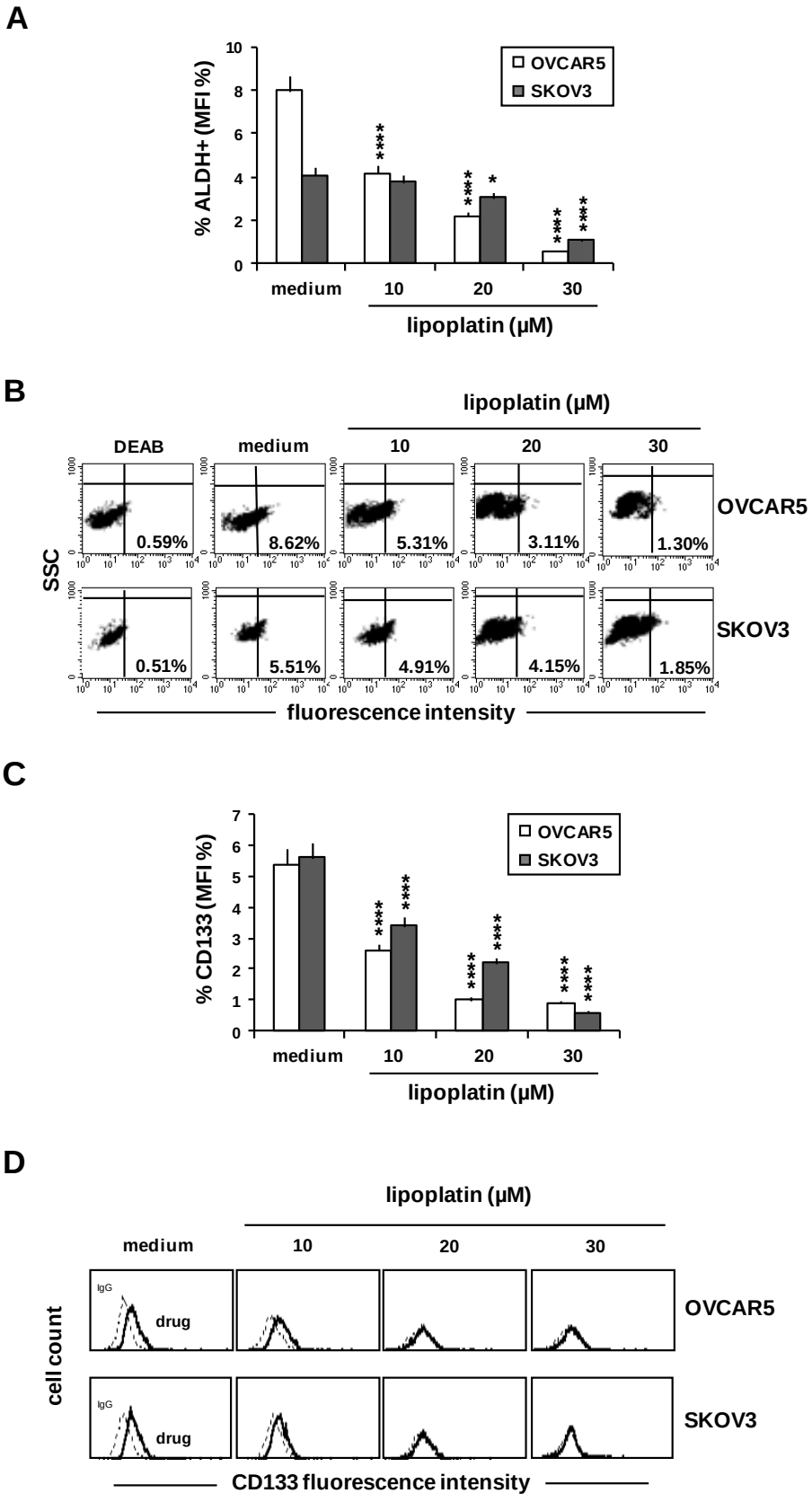

Figure 5.15 Lipoplatin decreases cancer stem cell markers. ALDH enzymatic activity and the surface expression of CD133 was evaluated by flow cytometry in OVCAR5 and SKOV3 after 72h

treatment with lipoplatin (10, 20, and 30 μM). **(A)** Values in the bar graph, reported as the percentage of ALDH positive cells, represent the mean ± SEM of three different experiments. *P < 0.05, ****P < 0.0001 drug *vs* medium. **(B)** Representative FACS dot plots of one of three independent experiments showing ALDH expression. **(C)** Graph representing CD133 quantification as percentage of positive cells. Data are expressed as mean ± SEM of three separate experiments. ****P < 0.0001 drug *vs* medium. **(D)** Representative FACS histogram plots of one of three independent experiments showing CD133 expression.

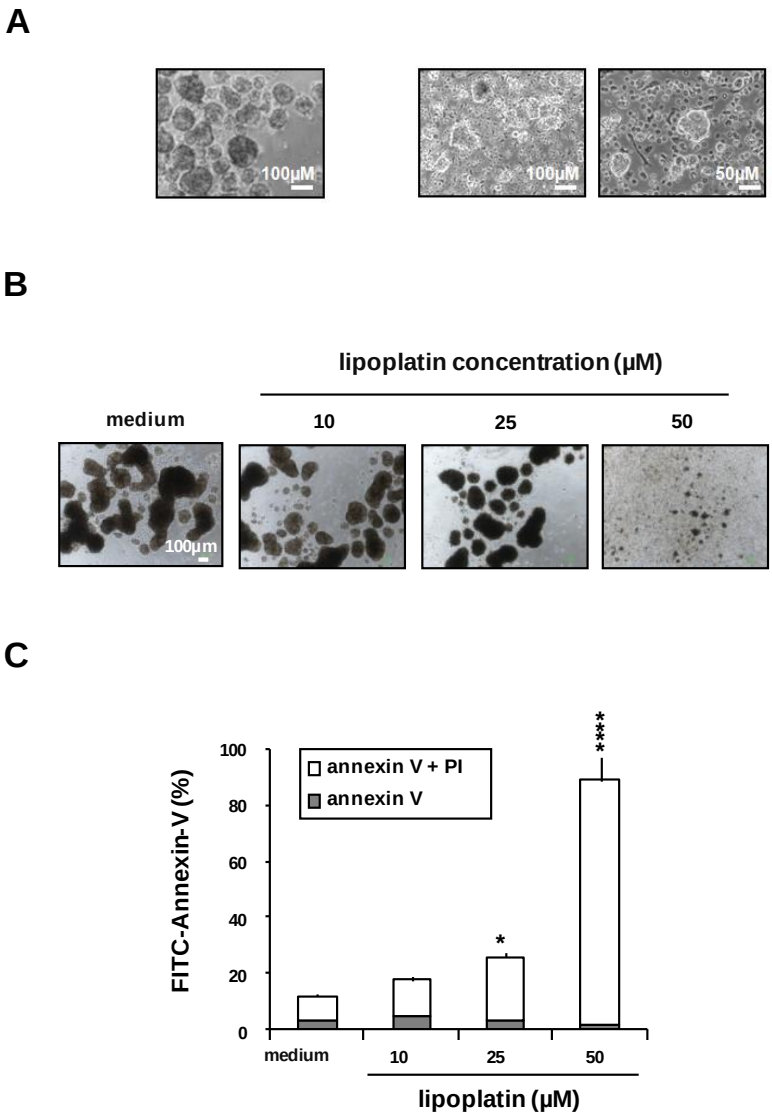

Figure 5.16 Lipoplatin inhibits spheroid formation. **(A)** Phase contrast microphotographs (original magnification 4×, 10×, 20×) SKOV3 generated tumor spheroids on poly-HEMA (left) and patient ascites derived multicellular aggregates (right). **(B)** SKOV3 cells, cultured on plates covered with poly- HEMA were treated with (10, 25, 50 μM) lipoplatin. After 72 h spheroids were photographed (phase contrast microphotographs, original magnification 4×) and then disrupted to evaluate apoptosis **(C)**. **(C)** The graph indicates the mean ± SEM values of the percentages of apoptotic cells evaluated by Annexin-V/PI staining from three independent experiments, each performed in duplicate. *P < 0.05, ****P < 0.0001 drug *vs* medium.

5.2.6 Lipoplatin affected SKOV3 spheroid volume growth, cell viability and dissemination

Spheroids have been used as models for evaluation of drug activity in ovarian cancer and are typically more resistant to chemo-and radiotherapies compared to cells cultured as 2-D monolayers (Soriţău et al.,2010; Mehta et al., 2012).
I evaluated lipoplatin activity using single spheroids of defined size. SKOV3 spheroids of four days, with a volume of ~100 $\mu m^3 * 10^5$, were treated with increasing concentrations of lipoplatin (10-100 µM). I determined spheroid growth by calculating the volume at time 0, 3, 7, 10 and 15 days (Figure 5.17A).
Lipoplatin inhibited in a dose-dependent manner spheroid growth, evaluated as spheroid volume. The volume of spheroids treated with 25 µM lipoplatin did not change compared to the initial volume (time 0). At higher lipoplatin concentrations (50 and 100 µM) spheroids volume even significantly decreased (Figure 5.17A and B). Figure 5.17C shows representative tumor spheroid growth in the presence of 25 or 50 µM lipoplatin.
To detect dead cells interspersed into lipoplatin treated spheroids (25 and 50 µM), I used the PI staining. After 3, 7, 10, and 15 days PI positive cells were recorded using a fluorescent microscope. Consinstently with the observed growth inhibition, treatment with lipoplatin increased in a time- and dose-dependent manner PI positive cells. Moreover, cells surrounding spheroids also were positive for PI staining (Figure 5.17D).
Taken together these results demonstrated that lipoplatin affects spheroid volume growth exerting a cytotoxic effect.

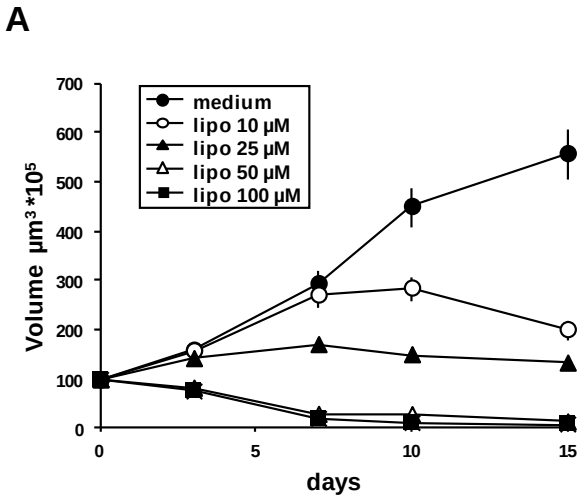

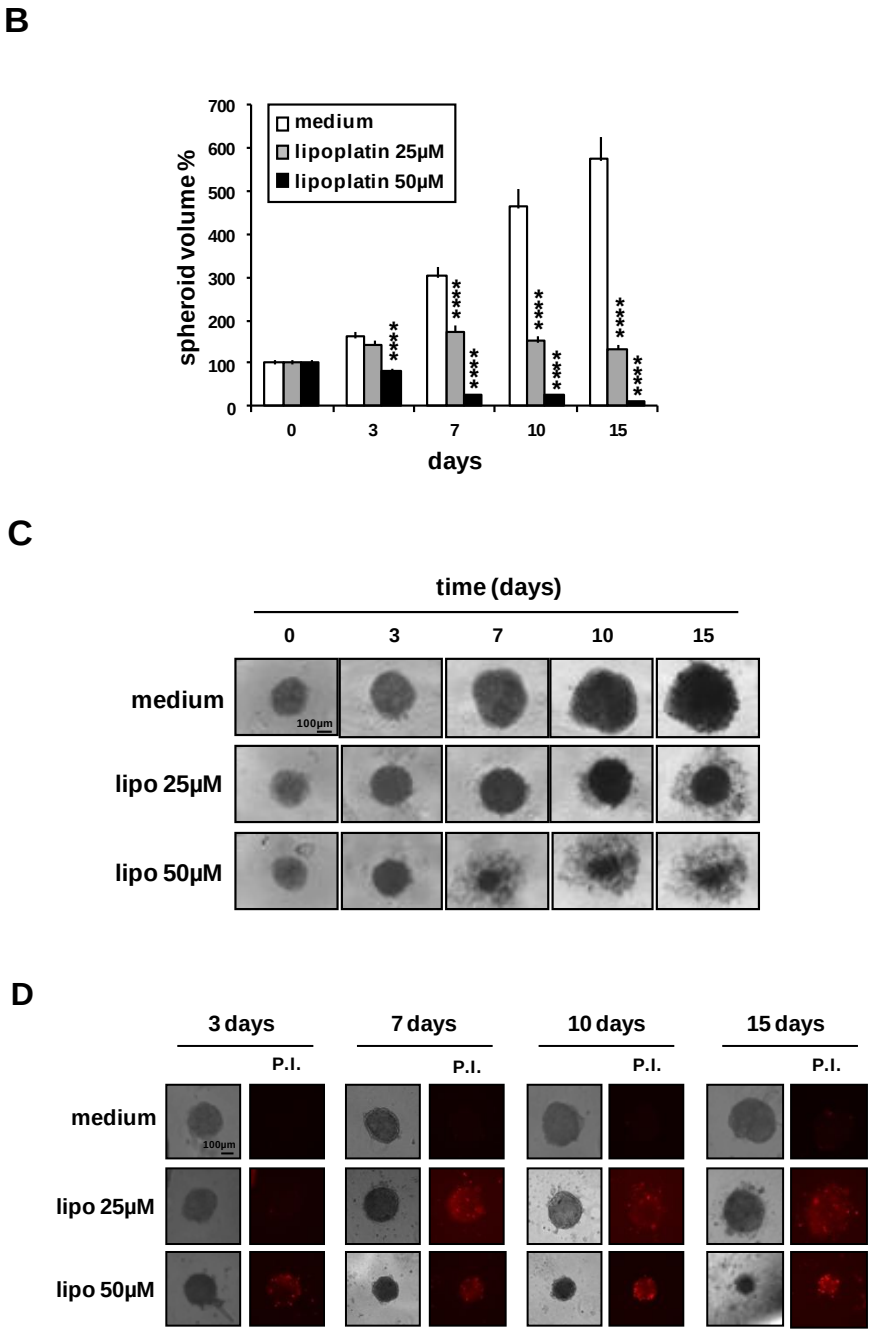

Figure 5.17 Lipoplatin activity on tumor spheroid volume growth and viability. SKOV3 single spheroids (four days old) of defined size, ~100 $\mu m^3 * 10^5$, were treated with increasing concentrations of lipoplatin (0, 10, 25, 50, 100 µM) and after 0, 3, 7, 10, and 15 days their size was recorded and the volume calculated. **(A)** Graph represents the curve of spheroids volume growth of at least three spheroids per condition. **(B)** Values in the bar graph were reported as the percentage of increased volume compared to T0 volume. They represent the mean ± SEM of three independent spheroids. ****P < 0.0001 drug *vs* medium. **(C)** Representative microphotographs (original magnification 4×) showing the volume growth of one of three independent lipoplatin (25, 50 µM) treated spheroids. **(D)** Representative microphotographs (original magnification 4×) showing cell viability using PI staining of at least three independent lipoplatin (25, 50 µM) treated spheroids.

Then, I evaluated lipoplatin activity on spheroids with larger volume (~300 $\mu m^3 * 10^5$). SKOV3 spheroids of four days were treated with increasing concentrations of lipoplatin (10-100 µM). I determined spheroid growth by calculating the volume at time 0, 3, 7, 14 and 17 days (Figure 5.18A).
In these spheroids lipoplatin used at 10 and 25 µM did not significantly affect the volume growth. A growth inhibition was obtained at higher concentrations. The concentration of lipoplatin to achieve a volume growth arrest was 50 µM. A volume growth reduction was observed at 75 or 100 µM (Figures 5.18B and C).
Representative microphotographs of tumor spheroids treated with 50 or 100 µM lipoplatin are shown in figure 5.17G.

A

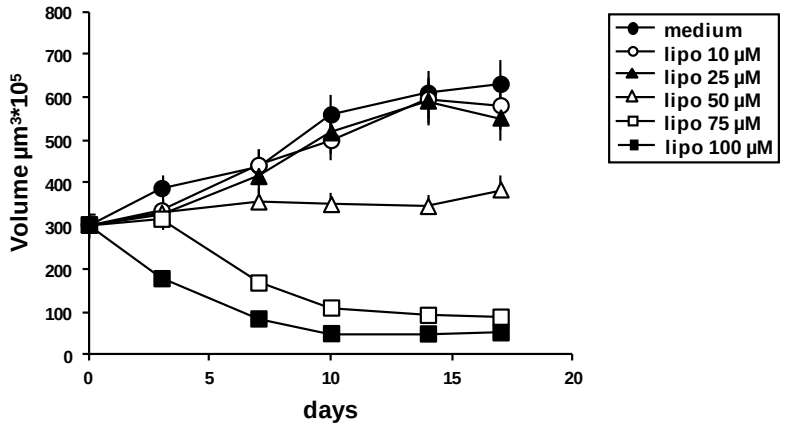

B

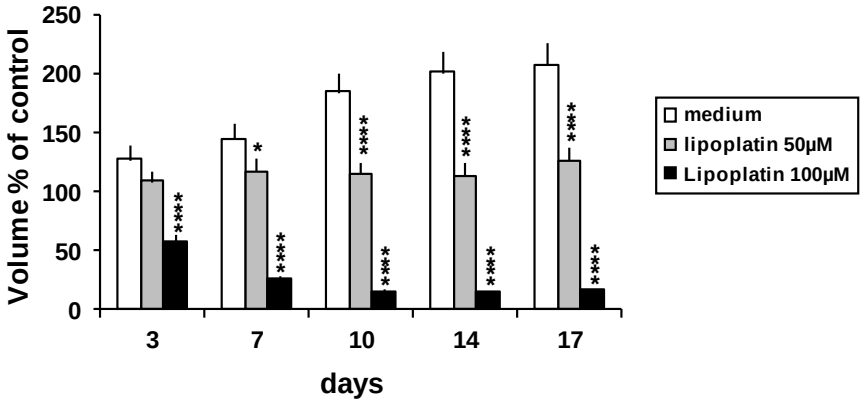

C

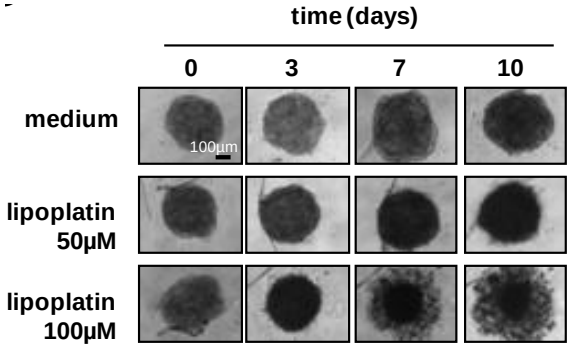

Figure 5.18 Lipoplatin activity on tumor spheroid. SKOV3 single spheroids (four days old) of defined size, ~300 $\mu m^3 * 10^5$, were treated with increasing concentrations of lipoplatin (0, 10, 25, 50, 75, 100 µM) and after 0, 3, 7, 10, 14 and 17 days their size was recorded and the volume calculated. **(A)** Graph represents the curve of spheroids volume growth of at least three spheroids per condition. **(B)** Values in the bar graph were reported as the percentage of increased volume compared to T0 volume. They represent the mean ± SEM of three independent spheroids. *P < 0.05, ****P < 0.0001 drug *vs* medium. **(C)** Representative microphotographs (original magnification 4×) showing the volume growth of one of three independent lipoplatin (50, 100 µM) treated spheroids.

I used a tumor spheroid-based assay migration *in vitro* to mimic tumor cell dissemination from a solid microtumor or micrometastasis. Cell spreading was evaluated onto an extracellular matrix coated surface (Vinci et al., 2012).
I transferred single formed SKOV3 spheroids onto collagene-I coated wells. Then spheroids were cultured in the presence or absence of lipoplatin (25 and 50 µM). Within a few hours tumor cells disseminated from the spheroid over the coated surface, as shown in the representative microphotographs in Figure 5.19B. After 24 and 48 hours, I recorded the leading edge of the migrating cells and calculated the covered area in fold increase compared to time 0 area of each sample.
The migration rate of SKOV3 cells, evaluated after 24 and 48 hours, decreased of about 50% in lipoplatin treated spheroids (25 and 50 µM) (Figure 5.19A).

A

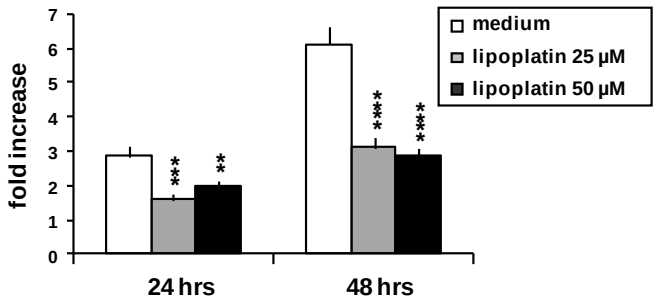

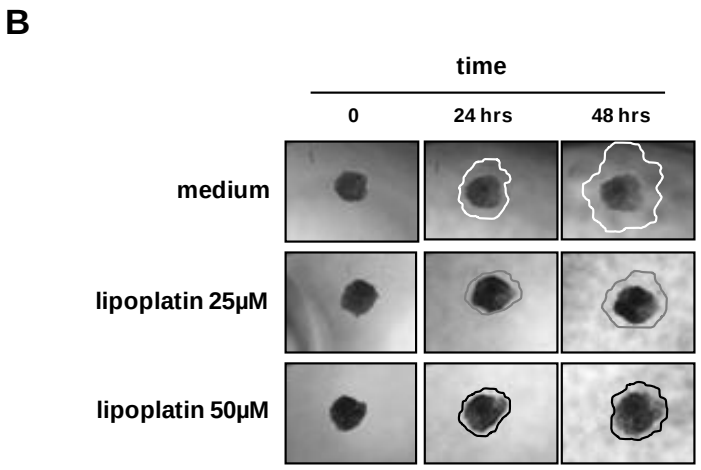

Figure 5.19 Lipoplatin inhibits tumor cell dissemination. Day 4 SKOV3 spheroids were placed on collagene-I coated plates and treated with lipoplatin (25 and 50 μM). Images were captured at time 24 h and 48 h using an inverted microscope (phase contrast microphotographs, original magnification 4×). **(A)**Values shown represent the average fold change in pixel area compared to T0 area. **P < 0.01, ***P < 0.001, ****P < 0.0001 drug *vs* medium. **(B)** Representative images of one of three separate experiments are shown.

5.2.7 Lipoplatin inhibited the growth of ovarian cancer xenografts

OVCAR5 (2.7×10^6) were injected into the right flank of 6-week-old female athymic nude mice. After 3 days (tumor size of about 44 mm^3) mice were randomly divided in two groups, including 7 mice/group, and were treated intraperitoneally with either 20 mg/kg lipoplatin or vehicle. Treatment for 41 days resulted in a significant ($P<0.01$) tumor growth inhibition, approximately 82% of control. The tumors of the untreated control group grew to a mean tumor size of about 417.2 mm^3, while the lipoplatin treated tumors reached a mean size of about 73.1 mm^3 (Figure 5.20A).

Then, I investigated whether suspending the treatment allowed the restart of tumor growth. After 12 days of treatment suspension I measured the tumor volumes. The mean volume size of the untreated control group reached a tumor volume of about 969.6 ± 204.8 mm^3, whereas the volumes of the lipoplatin treated group were about 107.4 ± 30.3 mm^3 (Figure 5.20A, dotted line), with a tumor growth inhibition of about 89% (Figure 5.20B).

There was no histological detectable cytotoxicity involving the animals' heart, spleen, liver, and kidney, whereas treatment with the same concentration of cisplatin was lethally toxic for mice (data not shown).

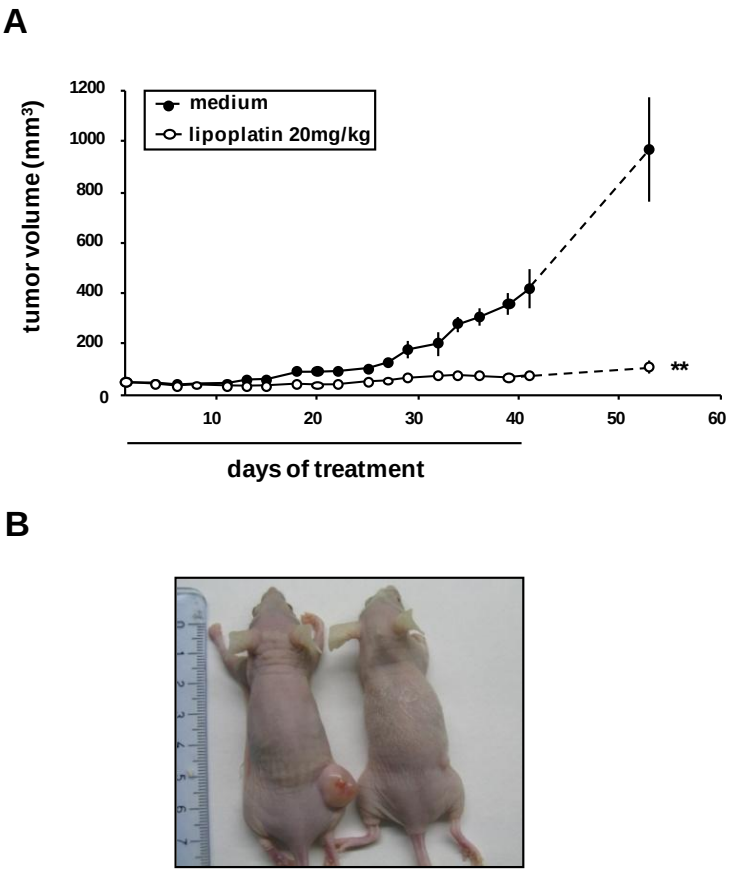

Figure 5.20 *In vivo* anticancer activity of lipoplatin (xenograft). **(A)** Tumor volume was measured in female athymic nude mice after intraperitoneal (i.p.) injection of either drug-free medium or containing 20 mg/kg lipoplatin, three times a week using a caliper. Points represent the mean ± SEM of seven animals per group. Dotted lines represent treatment suspension. **P < 0.01 lipoplatin *vs* control. **(B)** Image showing untreated mouse (right) and lipoplatin treated mouse (left).

6. DISCUSSION

Cisplatin is highly effective in the treatment of testicular and ovarian cancers and it is also widely employed for treating bladder, cervical, head and neck, oesophageal, and small cell lung cancer. Despite its success, cisplatin has several disadvantages, which comprise severe side effects that reduce the dose that can be applied to patients (Giaccone, 2000). Moreover, the use of cisplatin in cancer chemotherapy is limited by acquired or intrinsic resistance (Fuertes et al., 2003). Patients usually have a good initial response to cisplatin-based chemotherapy but later relapse, because the development of cisplatin resistance markedly reduces its clinical effectiveness. The molecular mechanisms that underlie cisplatin resistance are poorly understood because cisplatin has many different routes of cell entry and multiple cellular targets (Shen et al., 2012). Considering these drawbacks, one of the key research areas in oncology has been to engineer new platinum drug formulations to reduce the severe toxicities and to enhance the therapeutic effectiveness against cisplatin-resistant tumors (Boulikas et al., 2007). Such efforts have led to the reformulation of platinum drugs using liposomes. Liposomes possess several attractive biological activities, including biocompatibility, high drug loading, and improved pharmacokinetics, that are well suited for platinum drug delivery (Liu et al., 2013). However, few liposomal formulations have demonstrated a significant advantage in therapeutic terms. At the moment, lipoplatin (Biopharmaceutical Company Regulon, Athens, Greece) represents the most promising cisplatin liposomal formulation (Zalba and Garrido, 2013).

The advantage of lipoplatin over cisplatin is the reduced toxicity that results from the ability of lipoplatin to target primary tumors and metastases. The enhanced permeability and retention effect (EPR) allows the extravasation of lipoplatin nanoparticles preferentially in the tumor area through the leaky vasculature of newly formed tumor vessels. Indeed, as demonstrated in human studies, lipoplatin showed an enhanced concentration in tumors and metastases, at levels up to 200-fold higher compared to the adjacent normal tissue (Stathopoulos and Boulikas, 2012).

Moreover, lipoplatin nanoparticles displayed enhanced circulation in body fluids and evaded immune surveillance by their coating with PEG. The long circulation of lipoplatin is a property necessary for its preferential extravasation through the leaky vasculature of tumors. The half-life of total platinum in human plasma was determined to be 60-117 hours for lipoplatin, compared to ~6 hours for cisplatin (Stathopoulos et al., 2005). Interestingly, in clinical trials lipoplatin was administered as intravenous infusion without the need for pre- or post-hydration of the patient. This is in contrast to cisplatin chemotherapy that requires admittance of the patient the night before infusion for hydration, as well as extended stay in the hospital after infusion for post hydration, to reduce the

nephrotoxicity of the drug, with improvement in the quality of life and clear pharmacoeconomic benefits (Boulikas, 2009).

There are preclinical data of lipoplatin in cancer cell cultures and in animals as well as clinical data which involve Phase I studies, pharmacokinetics and Phase II and Phase III studies. Clinical studies were performed in patients with pancreatic cancer, non-small-cell lung cancer (NSCLC), head and neck, breast, gastric, and bladder cancer.

The most effective chemotherapeutic agent for the treatment of cervical and ovarian cancer is cisplatin. However, severe renal, neurologic, and gastrointestinal side effects and acquired chemoresistance are the major reasons of cisplatin treatment failure in cancer of the cervix and of the ovary (Leath and Straughn, 2013; Siegel et al., 2012).

In this study I evaluated the activity of lipoplatin in cervical and ovarian cancer models. For this purpose I used the cervical cancer-derived tumor cell line ME-180 and its cisplatin-resistant clone R-ME-180, and a panel of ovarian cancer cell lines with different histotypes and with various degrees of cisplatin sensitivity.

The IC_{50} of cisplatin in R-ME-180 cervical cancer cells was almost 9-fold higher than in ME-180 cells.

OVCAR3 (Godwin et al., 1992), OVCAR5 (Chock et al., 2010), and SKOV3 ovarian cancer cell lines were reported to be cisplatin-resistant (Mistry et al., 1992). The panel also included the cisplatin-sensitive cell line A2780 and its parental cisplatin-resistant cell line A2780cis, which presented a 7-fold higher IC_{50} for cisplatin.

In all cell lines, lipoplatin significantly reduced cell proliferation with comparable IC_{50}. Lipoplatin also potently inhibited the proliferation of the cisplatin-resistant R-ME-180 cell line with an IC_{50} comparable to that of the parent cisplatin-sensitive ME-180 and of HeLa cell lines. Interestingly, lipoplatin displayed an antiprolifeartive activity in cell lines of different ovarian cancer histology origins: ovarian carcinoma (A2780 and A27080cis), clear cell carcinoma (TOV21G), endometriod carcinoma (MDAH), and malignant cells derived from the ascites (OVCAR3, OVCAR5, and SKOV3).

These results demonstrated that lipoplatin affected cell proliferation exhibiting a similar cytotoxic effect in cell lines with a wide range in sensitivity to cisplatin, including cisplatin-resistant cell lines. Lipoplatin bypassed cisplatin resistance mechanisms likely because it has a different mechanism of cell influx. Cisplatin enters the cell by passive diffusion or active uptake, while it has been demonstrated that lipoplatin directly fuses with the cell membrane, thanks to the fusogenic dipalmitoyl phosphatidyl glycerol (DPPG) lipids that compose its shell, delivering cisplatin across the membrane barrier (Boulikas, 2007).

Subsequent studies in ovarian cancer cells were performed using the cisplatin-resistant cell line OVCAR5, and SKOV3 cells capable to generate compact tumor spheres (Ma et al., 2010).

Many anticancer drugs affect the cell cycle progression and then induce cell death by apoptosis (Pietenpol and Stewart, 2002). G2 arrest seems to be essential to trigger cisplatin-induced cell death (Cepeda et al., 2007). Accordingly, lipoplatin treatment determined an arrest of the cell cycle in the G2/M phase in SKOV3 cells, and an increase in S and G2/M phase in OVCAR5 cells.

Cisplatin is believed to kill cancer cells by inducing apoptosis (Brozovic et al., 2010), as demonstrated in HeLa cervical cancer cell line (Liu et al., 2008). Upon entrance to the cytoplasm, also lipoplatin leads to the induction of tumor cell apoptosis (Arienti et al., 2008). In agreement with Arieti et al., I demonstrated that lipoplatin induced its potent cytotoxic effect, on both cervical (ME-180, R-ME-180) and ovarian cancer cells (OVCAR5, SKOV3), by activating apoptosis, inducing mitochondrial membrane depolarization, cytochrome-c release, and caspases 9 and 3 activation, indicating that its activity was exerted through the mitochondrial intrinsic apoptotic pathway. Consistently, the pro-survival protein Bcl-2 was reduced, and the pro-apoptotic Bax protein increased (Youle and Strasser, 2008).

The intrinsic apoptotic pathway is activated by cytotoxic drugs that perturb the redox balance within a cell (Tonissen and Di Trapani, 2009). Many studies have indicated that platinum compounds might also target the Thioredoxin (Trx) system, which is related to different cellular processes including antioxidant defense, redox and cell growth regulation, as well as selenium metabolism (Cai et al., 2012; Liu et al., 2012; Mahmood et al., 2013). One of the main functions of the Trx system is to counteract oxidative stress by scavenging reactive oxygen species (ROS) and by regulating other enzymes that help to reduce oxidative stress. The Trx reductase (TrxR) enzyme shows elevated levels in several human cancer cell lines and appears increased in tumors as compared with normal tissue (Berggren et al., 1996). The cisplatin-resistant variants of HeLa cells, established by continuous exposure to cisplatin exhibited an increased expression and activity of TrxR, as well as Trx, compared with the parental cells (Sasada et al., 1999). Thus, TrxR-targeting may contribute to prevent or reverse resistance mechanisms (Urig and Becker, 2006). Moreover, inhibiting the function of Trx system can lead to an imbalance in the redox state that can ultimately cause apoptosis (Tonissen and Di Trapani, 2009). Consistently, we found that R-ME-180 cells expressed 3-fold more TrxR than ME-180 cells. Lipoplatin remarkably reduced TrxR enzymatic activity with enhanced ROS accumulation, possibly overcoming the resistance mediated by TrxR over-expression. Cisplatin decreased TrxR levels in R-ME-180 cells to a lesser extent than lipoplatin, and to levels comparable to those of untreated cisplatin-sensitive cells, suggesting that cisplatin resistance depends on a reduced capability to increase ROS levels because of the higher TrxR enzymatic activity in R-ME-180 cells. Also in ovarian cancer cell lines, OVCAR5 and SKOV3, lipoplatin induced a dose-dependent induction of ROS

and inhibition of TrxR enzymatic activity, possibly overcoming a cisplatin-resistance mediated by TrxR over-expression.

Proteins over-expressed on the surface of tumor cells can be selectively targeted in cancer therapy. Epidermal growth factor receptor (EGFR) is among the most often targeted proteins. There are two different ways to pharmacologically target EGFR: anti-EGFR monoclonal antibodies (cetuximab, panitumumab) and specific inhibitors of the EGFR tyrosine kinase domain (gefitinib, erlotinib and lapatinib). Currently, EGFR-target therapy for the treatment of cervical and ovarian cancer is not defined for clinical use (Soonthornthum et al., 2011), even though the presence of EGFR has been associated with accelerated tumor progression, poor prognosis and therapeutic resistance (Siwak et al., 2009; Iida et al., 2011; Shen et al., 2008) .

EGFR activation is related with cell proliferation, resistance to cell apoptosis and cancer progression. HB-EGF, a ligand of EGFR produced by stromal fibroblasts in uterine cervical cancer, contributes to ME-180 cell proliferation (Murata et al., 2011). In addition, treatment with cisplatin led to EGFR degradation in sensitive head and neck cancer cell lines, and this degradation strongly correlates with cytotoxicity (Ahsan et al., 2010).

I demonstrated that the R-ME-180 cells expressed higher amounts of EGFR than ME-180 cells and lipoplatin, but not cisplatin, down-modulated EGFR expression in cisplatin-resistant cells. As a consequence, lipoplatin, by reducing EGFR, could exert not only direct cytotoxic effects on cervical cancer cells, but also affect the proliferation induced by HB-EGF secreting stromal cells of the tumor microenvironment. Lipoplatin, and also cisplatin, decreased EGFR expression in cisplatin-sensitive cells: this implies that an appropriate treatment schedule should be considered when cisplatin and gefitinib, or other similar drugs, are used together since cisplatin treatment might hinder targeted therapy against molecules susceptible to down-regulation.

EGFR is directly involved in ovarian cancer cell invasion, and angiogenesis (Jeong et al., 2013). OVCAR5 and SKOV3 showed comparable EGFR expression and invasive properties. SKOV3 cell line was reported as a strong EGFR-expressing (Gottschalk et al., 2012) and as a highly invasive cell line (Dolo, 2009). Lipoplatin potently decreased EGFR expression in OVCAR5 and SKOV3 cells. Moreover, I found that lipoplatin significantly reduced the invasiveness of both cell lines. Therefore, the reduction of EGFR expression by lipoplatin could enhance chemotherapy effect by decreasing tumor progression, invasion, and metastasis.

EGF has also been reported as a potent stimulator of cervical cancer cell invasiveness, and EGFR signaling is involved in the regulatory mechanisms of epithelial-mesenchymal transition (EMT) of cervical cancer cells. Acquisition of EMT by primary carcinoma cells is associated with disrupted epithelial integrity, local invasion, and ultimately metastasis. Cervical cancer usually spreads to the

adjacent organs through the angiolymphatic system. Although uncommon at initial diagnosis, metastatic disease will develop in a high percentage of patients, usually within the first two years of completing treatment and in the majority of cases metastatic cervical cancer is not curable (Scatchard et al., 2012).

Interestingly, R-ME-180 cells exhibited enhanced invasive properties compared to ME-180 cells. My study showed that lipoplatin inhibited cell migration and invasion of cisplatin-resistant cells, opening the possibility that this drug formulation could be effective also to reduce/inhibit cancer cell local invasion and metastases.

Chemotherapy regimens or treatment plans may use a single drug or a combination of drugs. A drug combination is synergistic, additive or antagonistic if the effect is greater than, equal to, or less than the summed effects of the partner drugs (Chou, 2006). The term synergy is derived from the Greek syn-ergos, "working together". Synergistic drug combinations have been explored to achieve one or more favorable outcomes: enhanced efficacy; decreased dosage at equal or increased level of efficacy; reduced or delayed development of drug resistance; and simultaneous enhancement of therapeutic actions and reduction of unwanted actions (efficacy synergism plus toxicity antagonism) (Jia et al., 2009).

The standard approach for the treatment of ovarian cancer is the combination of a platinum compound, such as cisplatin or carboplatin, with a taxane, such as paclitaxel (Taxol®) or docetaxel (Taxotere®) (Jelovac and Armstrong, 2011). One of the alternatives for recurrent is doxorubicin, an anthracycline antiobiotic (Ushijima, 2009). I combined lipoplatin with doxorubicin and three different taxanes: abraxane, docetaxel and paclitaxel. Paclitaxel and docetaxel share a similar mechanism of action: the promotion of microtubule assembly and inhibition of microtubule disassembly. Abraxane is the albumin-bound formulation of paclitaxel. The simultaneous combination of lipoplatin with paclitaxel or docetaxel showed a moderate synergy or even an additive effect, whereas the combination of lipoplatin with abraxane or doxorubicin demonstrated a synergistic effect. Interestingly, both cell lines showed a comparable sensitivity to abraxane, but not to paclitaxel, that resulted less active in SKOV3 cells (IC_{50} 5-fold higher than OVCAR5 cells), which were reported to be paclitaxel-resistant (Chen et al., 2005; Wang et al., 2013). These results indicated that an appropriate drug combination should be adopted to obtain an enhanced therapeutic effect and among the tested taxanes the best to use in combination with lipoplatin could be abraxane.

One of the current emerging concepts concerning tumorigenesis is that tumors are composed of heterogeneous populations of cells with different biological properties and tumorigenic potentials. Cancer stem cells or tumor-initiating cells (CSC/TIC) are a subpopulation able to form new tumors and metastases by their capacity to self-renew and originate all of the heterogeneous lineages of cells that comprise a tumor (Lopez et al., 2012). CSC/TICs are thought to play a crucial role

in tumor development, chemoresistance, and relapse after initial treatment in cervical cancer (Feng et al., 2009) and ovarian cancer (Skubitz et al., 2013).
The ability to form spheroids (Djordjevic et al., 2012; Feng et al., 2009) and several cell surface markers, including CD133 and aldehyde dehydrogenase (ALDH), define CSC/TIC populations in cervical (Liu and Zheng, 2013) and ovarian tumors (Silva et al., 2011). Importantly, in ovarian cancer these markers, not only identify CSC/TICs, but are also associated with poor clinical outcome of patients, being therefore promising targets for treatment (Silva et al., 2011). Preclinical studies demonstrate that knockdown of ALDH can restore chemosensitivity in ovarian cancer cell lines (Burgos-Ojeda et al., 2012; Wintzell et al., 2012).
R-ME-180 cells were able to generate spheroids and expressed ALDH positive cells, displaying a putative stem-like signature. Lipoplatin inhibited spheroid formation and reduced the percentage of ALDH+ cells. OVCAR5 and SKOV3 cell lines showed a significant percentage of ALDH and CD133 positive cells that decreased in a dose-dependent manner in the presence of lipoplatin.
These results suggested that the treatment with lipoplatin could decrease CSC/TIC population and as a consequence reduce tumor relapse due to this chemo-resistant subpopulation. Furthermore, lipoplatin could avoid CSC/TICs induction by cisplatin-based chemotherapy (Latifi et al., 2011; Wintzell et al., 2012).
Epithelial ovarian cancer has an unusual mechanism of dissemination that rarely requires blood or lymph vessels (Naora and Montell, 2005). Malignant cells are shed from the primary tumor into the peritoneal cavity where they are disseminated throughout the abdominal cavity by peritoneal fluid or ascites. These malignant cells often aggregate and form spheroid-like structures (Allen et al., 1987) and are proposed to attach to and invade the peritoneum and potentially seed metastatic tumor growth (Burleson et al., 2006). Additionally, it has become apparent that aggregates of malignant cells, contained within malignant ascites, represent a significant impediment to efficacious treatment of late stage ovarian cancer (Shield et al., 2009).
SKOV3 cells spontaneously produced compact spheroids when cultured under non-adherent conditions. Lipoplatin was able to inhibit spheroid formation and induce apoptosis. Moreover, using a new spheroid migration assay as a model for tumor cell dissemination from a solid micrometastasis or a spheroid, I found that lipoplatin decreased cell migration. Taken together these data indicated that the formation of spheroids and their ability to contribute to metastasis formation by tumor cell migration/dissemination could be strongly reduced by lipoplatin treatment.
Spheroids are extensively used in preclinical studies to investigate the effect of various therapies. In the clinical setting, the efficacy of any treatment is proven by reduced tumor growth and, eventually, reduced tumor mass. Analogously, spheroid volume can be used as a measure of efficacy in preclinical therapy

studies (Rodday et al., 2011). The treatment with lipoplatin of SKOV3 spheroids showed a dose-dependent inhibition of the spheroid growth. Accordingly to the inhibitory effect of lipoplatin, I detected a cell viability decline in treated spheroids. To obtain a volume growth inhibition of spheroid with larger size I had to increase lipoplatin concentrations.

Finally, lipoplatin strongly decreased tumor xenograft of cisplatin-resistant cervical R-ME-180 and ovarian cancer OVCAR5 cells without apparent toxicities. Interestingly, ovarian cancer tumor xenografts, after treatment suspension, did not start to grow showing an irreversible effect of lipoplatin. Cisplatin, used at the same concentration, caused severe toxicities in nude mice (Chahinian et al., 1984). The lower toxicity of lipoplatin compared to cisplatin may be due to alterations in its pharmacokinetics, preferential localization to tumors containing compromised vasculature and differences in cellular uptake (Devarajan et al., 2004).

A better radiosensitizing activity of lipoplatin compared to cisplatin has been shown in preclinical studies (Charest et al., 2010). Because cisplatin is the standard care for the treatment of cervical cancer in combination with radiation therapy (RT), replacement of cisplatin by lipoplatin against cervical cancer would add the advantage of lower toxicities to patients as shown in randomized Phase II and Phase III studies against NSCLC (Stathopoulos et al., 2011; Mylonakis et al., 2010).

In conclusion, lipoplatin was able to exhert a cytotoxic effect on conventional monolayer cultures, on three-dimensional spheroids, and also *in vivo*. Hence, these promising results suggest that lipoplatin could be used for the treatment of cervical and ovarian cancer patients, single or in combination therapy, as an alternative or a substitute of cisplatin to reduce cisplatin's systemic toxicity while improving the targeting of the drug to the tumor.

7. REFERENCES

A Farghaly, S. (2013). Anti- Metastatic Gene Therapy in Patients with Advanced Epithelial Ovarian Cancer (EOC). J. Cell Sci. Ther. *04*.

Adams, J.M., and Cory, S. (1998). The Bcl-2 Protein Family: Arbiters of Cell Survival. Science *281*, 1322–1326.

Aebi, S., Kurdi-Haidar, B., Gordon, R., Cenni, B., Zheng, H., Fink, D., Christen, R.D., Boland, C.R., Koi, M., Fishel, R., et al. (1996). Loss of DNA mismatch repair in acquired resistance to cisplatin. Cancer Res. *56*, 3087–3090.

Ahmad, S. (2010). Platinum-DNA interactions and subsequent cellular processes controlling sensitivity to anticancer platinum complexes. Chem. Biodivers. *7*, 543–566.

Ahsan, A., Hiniker, S.M., Ramanand, S.G., Nyati, S., Hegde, A., Helman, A., Menawat, R., Bhojani, M.S., Lawrence, T.S., and Nyati, M.K. (2010). Role of epidermal growth factor receptor degradation in cisplatin-induced cytotoxicity in head and neck cancer. Cancer Res. *70*, 2862–2869.

Akaboshi, M., Kawai, K., Maki, H., Akuta, K., Ujeno, Y., and Miyahara, T. (1992). The number of platinum atoms binding to DNA, RNA and protein molecules of HeLa cells treated with cisplatin at its mean lethal concentration. Jpn. J. Cancer Res. Gann *83*, 522–526.

Akbarzadeh, A., Rezaei-Sadabady, R., Davaran, S., Joo, S.W., Zarghami, N., Hanifehpour, Y., Samiei, M., Kouhi, M., and Nejati-Koshki, K. (2013). Liposome: classification, preparation, and applications. Nanoscale Res. Lett. *8*, 102.

Albertella, M.R., Lau, A., and O'Connor, M.J. (2005). The overexpression of specialized DNA polymerases in cancer. DNA Repair *4*, 583–593.

Alderden, Rebecca A., Hall, Matthew D., Hambley, and Trevor, W. (2006).The Discovery and Development of Cisplatin. J. Chem. Educ. *83*, 728–734.

Allen, H.J., Porter, C., Gamarra, M., Piver, S., and Johnson, E.A.Z. (1987). Isolation and Morphologic Characterization of Human Ovarian Carcinoma Cell Clusters Present in Effusions. Pathobiology *55*, 194–208.

Allen, T.M., and Chonn, A. (1987). Large unilamellar liposomes with low uptake into the reticuloendothelial system. FEBS Lett. *223*, 42–46.

Allen, T.M., and Cleland, L.G. (1980). Serum-induced leakage of liposome contents. Biochim. Biophys. Acta *597*, 418–426.

Allen, T.M., and Cullis, P.R. (2013). Liposomal drug delivery systems: from concept to clinical applications. Adv. Drug Deliv. Rev. *65*, 36–48.

Anevlavis, S., Pataka, A., Kouliatsis, G., et al. (2008). A phase II trial of Lipoplatin-gemcitabine in patients with advanced NSCLC: preliminary results. Eur. Respir. J. *32*,762s.

Arienti, C., Tesei, A., Ravaioli, A., Ratta, M., Carloni, S., Mangianti, S., Ulivi, P., Nicoletti, S., Amadori, D., and Zoli, W. (2008). Activity of lipoplatin in tumor and in normal cells in vitro. Anticancer. Drugs *19*, 983–990.

Bandak, S., Goren, D., Horowitz, A., Tzemach, D., and Gabizon, A. (1999). Pharmacological studies of cisplatin encapsulated in long-circulating liposomes in mouse tumor models. Anticancer. Drugs *10*, 911–920.

Bandekar, A., Karve, S., Chang, M.-Y., Mu, Q., Rotolo, J., and Sofou, S. (2012). Antitumor efficacy following the intracellular and interstitial release of liposomal doxorubicin. Biomaterials *33*, 4345–4352.

Bell, D.A. (2005). Origins and molecular pathology of ovarian cancer. Mod. Pathol. *18*, S19–S32.

Berggren, M., Gallegos, A., Gasdaska, J.R., Gasdaska, P.Y., Warneke, J., and Powis, G. (1996). Thioredoxin and thioredoxin reductase gene expression in human tumors and cell lines, and the effects of serum stimulation and hypoxia. Anticancer Res. *16*, 3459–3466.

Bianchi, R., Brines, M., Lauria, G., Savino, C., Gilardini, A., Nicolini, G., Rodriguez-Menendez, V., Oggioni, N., Canta, A., Penza, P., et al. (2006). Protective effect of erythropoietin and its carbamylated derivative in experimental Cisplatin peripheral neurotoxicity. Clin. Cancer Res. Off. J. Am. Assoc. Cancer Res. *12*, 2607–2612.

Bibi, S., Lattmann, E., Mohammed, A.R., and Perrie, Y. (2012). Trigger release liposome systems: local and remote controlled delivery? J. Microencapsul. *29*, 262–276.

Bijnsdorp, I.V., Giovannetti, E., and Peters, G.J. (2011). Analysis of Drug Interactions. In Cancer Cell Culture, I.A. Cree, ed. (Totowa, NJ: Humana Press), pp. 421–434.

Boulikas T. (1998). Status of gene therapy in 1997: molecular mechanisms, disease targets, and clinical applications. Gene Ther. Mol. Biol. *1*,1-172.

Boulikas, T. (2004). Low toxicity and anticancer activity of a novel liposomal cisplatin (Lipoplatin) in mouse xenografts. Oncol. Rep. *12*, 3–12.

Boulikas, T. (2007). Molecular mechanisms of cisplatin and its liposomally encapsulated form, Lipoplatin™. Lipoplatin™ as a chemotherapy and antiangiogenesis drug. J. Cancer Ther. *5*, 351-376.

Boulikas, T. (2009). Clinical overview on Lipoplatin: a successful liposomal formulation of cisplatin. Expert Opin. Investig. Drugs *18*, 1197–1218.

Boulikas T, Pantos A, Bellis E,and Christofis, P. (2007). Designing platinum compounds in cancer: structures and mechanisms. Cancer Ther. *5*, 537–583.

Boulikas, T., Stathopoulos, G.P., Volakakis, N., and Vougiouka, M. (2005). Systemic Lipoplatin infusion results in preferential tumor uptake in human studies. Anticancer Res. *25*, 3031–3039.

Bove, L., Picardo, M., Maresca, V., Jandolo, B., and Pace, A. (2001). A pilot study on the relation between cisplatin neuropathy and vitamin E. J. Exp. Clin. Cancer Res. CR *20*, 277–280.

Bradford, L., and Goodman, A. (2013). Cervical cancer screening and prevention in low-resource settings. Clin. Obstet. Gynecol. *56*, 76–87.

Bravo-Cordero, J.J., Hodgson, L., and Condeelis, J. (2012). Directed cell invasion and migration during metastasis. Curr. Opin. Cell Biol. *24*, 277–283.

Brozovic, A., Ambriović-Ristov, A., and Osmak, M. (2010). The relationship between cisplatin-induced reactive oxygen species, glutathione, and BCL-2 and resistance to cisplatin. Crit. Rev. Toxicol. *40*, 347–359.

Bruhn, S.L., Pil, P.M., Essigmann, J.M., Housman, D.E., and Lippard, S.J. (1992). Isolation and characterization of human cDNA clones encoding a high mobility group box protein that recognizes structural distortions to DNA caused by binding of the anticancer agent cisplatin. Proc. Natl. Acad. Sci. U. S. A. *89*, 2307–2311.

Burgos-Ojeda, D., Rueda, B.R., and Buckanovich, R.J. (2012). Ovarian cancer stem cell markers: Prognostic and therapeutic implications. Cancer Lett. *322*, 1–7.

Burleson, K.M., Boente, M.P., Pambuccian, S.E., and Skubitz, A.P. (2006). Disaggregation and invasion of ovarian carcinoma ascites spheroids. J. Transl. Med. *4*, 6.

Cabanes, A., Briggs, K.E., Gokhale, P.C., Treat, J.A., and Rahman, A. (1998). Comparative in vivo studies with paclitaxel and liposome-encapsulated paclitaxel. Int. J. Oncol. *12*, 1035–1040.

Cai, W., Zhang, B., Duan, D., Wu, J., and Fang, J. (2012). Curcumin targeting the thioredoxin system elevates oxidative stress in HeLa cells. Toxicol. Appl. Pharmacol. *262*, 341–348.

Campos, C.B.L., Paim, B.A., Cosso, R.G., Castilho, R.F., Rottenberg, H., and Vercesi, A.E. (2006). Method for monitoring of mitochondrial cytochrome c release during cell death: Immunodetection of cytochrome c by flow cytometry after selective permeabilization of the plasma membrane. Cytom. Part J. Int. Soc. Anal. Cytol. *69*, 515–523.

Cannistra, S.A. (2004). Cancer of the ovary. N. Engl. J. Med. *351*, 2519–2529.

Cepeda, V., Fuertes, M.A., Castilla, J., Alonso, C., Quevedo, C., and Pérez, J.M. (2007). Biochemical mechanisms of cisplatin cytotoxicity. Anticancer Agents Med. Chem. *7*, 3–18.

Chahinian, A.P., Norton, L., Holland, J.F., Szrajer, L., and Hart, R.D. (1984). Experimental and clinical activity of mitomycin C and cis-diamminedichloroplatinum in malignant mesothelioma. Cancer Res. *44*, 1688–1692.

Chang, H.-I., and Yeh, M.-K. (2012). Clinical development of liposome-based drugs: formulation, characterization, and therapeutic efficacy. Int. J. Nanomedicine *7*, 49–60.

Charest, G., Paquette, B., Fortin, D., Mathieu, D., and Sanche, L. (2010). Concomitant treatment of F98 glioma cells with new liposomal platinum compounds and ionizing radiation. J. Neurooncol. *97*, 187–193.

Chen, S., Iversen, E.S., Friebel, T., Finkelstein, D., Weber, B.L., Eisen, A., Peterson, L.E., Schildkraut, J.M., Isaacs, C., Peshkin, B.N., et al. (2006). Characterization of BRCA1 and BRCA2 mutations in a large United States sample. J. Clin. Oncol. Off. J. Am. Soc. Clin. Oncol. *24*, 863–871.

Chen, T., Pengetnze, Y., and Taylor, C.C. (2005). Src inhibition enhances paclitaxel cytotoxicity in ovarian cancer cells by caspase-9-independent activation of caspase-3. Mol. Cancer Ther. *4*, 217–224.

Chock, K.L., Allison, J.M.S., Shimizu, Y., and ElShamy, W.M. (2010). BRCA1-IRIS Overexpression Promotes Cisplatin Resistance in Ovarian Cancer Cells. Cancer Res. *70*, 8782–8791.

Chou, T.-C. (2010). Drug combination studies and their synergy quantification using the Chou-Talalay method. Cancer Res. *70*, 440–446.

Chou, T.-C. (2006). Theoretical basis, experimental design, and computerized simulation of synergism and antagonism in drug combination studies. Pharmacol. Rev. *58*, 621–681.

Chou, T.C., and Talalay, P. (1984). Quantitative analysis of dose-effect relationships: the combined effects of multiple drugs or enzyme inhibitors. Adv. Enzyme Regul. *22*, 27–55.

Ciarimboli, G., Ludwig, T., Lang, D., Pavenstädt, H., Koepsell, H., Piechota, H.-J., Haier, J., Jaehde, U., Zisowsky, J., and Schlatter, E. (2005). Cisplatin nephrotoxicity is critically mediated via the human organic cation transporter 2. Am. J. Pathol. *167*, 1477–1484.

Ciarimboli, G., Deuster, D., Knief, A., Sperling, M., Holtkamp, M., Edemir, B., Pavenstädt, H., Lanvers-Kaminsky, C., am Zehnhoff-Dinnesen, A., Schinkel, A.H., et al. (2010). Organic cation transporter 2 mediates cisplatin-induced oto- and nephrotoxicity and is a target for protective interventions. Am. J. Pathol. *176*, 1169–1180.

Cullis, P.R., and Hope, M.J. (1980). The bilayer stabilizing role of sphingomyelin in the presence of cholesterol: a 31P NMR study. Biochim. Biophys. Acta *597*, 533–542.

Cutts, F.T., Franceschi, S., Goldie, S., Castellsague, X., de Sanjose, S., Garnett, G., Edmunds, W.J., Claeys, P., Goldenthal, K.L., Harper, D.M., et al. (2007). Human papillomavirus and HPV vaccines: a review. Bull. World Health Organ. *85*, 719–726.

Dabholkar, M., Vionnet, J., Bostick-Bruton, F., Yu, J.J., and Reed, E. (1994). Messenger RNA levels of XPAC and ERCC1 in ovarian cancer tissue correlate with response to platinum-based chemotherapy. J. Clin. Invest. *94*, 703–708.

Dan, H.C., Sun, M., Kaneko, S., Feldman, R.I., Nicosia, S.V., Wang, H.-G., Tsang, B.K., and Cheng, J.Q. (2004). Akt phosphorylation and stabilization of X-linked inhibitor of apoptosis protein (XIAP). J. Biol. Chem. *279*, 5405–5412.

Datta, S.R., Brunet, A., and Greenberg, M.E. (1999). Cellular survival: a play in three Akts. Genes Dev. *13*, 2905–2927.

Daubeuf, S., Leroy, P., Paolicchi, A., Pompella, A., Wellman, M., Galteau, M.M., and Visvikis, A. (2002). Enhanced resistance of HeLa cells to cisplatin by overexpression of gamma-glutamyltransferase. Biochem. Pharmacol. *64*, 207–216.

Deacon, J.M., Evans, C.D., Yule, R., Desai, M., Binns, W., Taylor, C., and Peto, J. (2000). Sexual behaviour and smoking as determinants of cervical HPV infection and of CIN3 among those infected: a case-control study nested within the Manchester cohort. Br. J. Cancer *83*, 1565–1572.

DeConti, R.C., Toftness, B.R., Lange, R.C., and Creasey, W.A. (1973). Clinical and pharmacological studies with cis-diamminedichloroplatinum (II). Cancer Res. *33*, 1310–1315.

Devarajan, P., Tarabishi, R., Mishra, J., Ma, Q., Kourvetaris, A., Vougiouka, M., and Boulikas, T. (2004). Low renal toxicity of lipoplatin compared to cisplatin in animals. Anticancer Res. *24*, 2193–2200.

Dickey, D.T., Wu, Y.J., Muldoon, L.L., and Neuwelt, E.A. (2005). Protection against cisplatin-induced toxicities by N-acetylcysteine and sodium thiosulfate as assessed at the molecular, cellular, and in vivo levels. J. Pharmacol. Exp. Ther. *314*, 1052–1058.

Djordjevic, B., Stojanovic, S., Conic, I., Jankovic-Velickovic, L., Vukomanovic, P., Zivadinovic, R., and Vukadinovic, M. (2012). Current approach to epithelial ovarian cancer based on the concept of cancer stem cells. J. BUON Off. J. Balk. Union Oncol. *17*, 627–636.

Dolo (2009). Vasculogenic mimicry of human ovarian cancer cells: Role of CD147. Int. J. Oncol. *35*.

Egger, A.E., Hartinger, C.G., Ben Hamidane, H., Tsybin, Y.O., Keppler, B.K., and Dyson, P.J. (2008). High resolution mass spectrometry for studying the interactions of cisplatin with oligonucleotides. Inorg. Chem. *47*, 10626–10633.

Eisenkop, S.M., and Spirtos, N.M. (2001). The clinical significance of occult macroscopically positive retroperitoneal nodes in patients with epithelial ovarian cancer. Gynecol. Oncol. *82*, 143–149.

Ellens, H., Mayhew, E., and Rustum, Y.M. (1982). Reversible depression of the reticuloendothelial system by liposomes. Biochim. Biophys. Acta *714*, 479–485.

Farhat, F.S., Temraz, S., Kattan, J., Ibrahim, K., Bitar, N., Haddad, N., Jalloul, R., Hatoum, H.A., Nsouli, G., and Shamseddine, A.I. (2011). A phase II study of lipoplatin (liposomal cisplatin)/vinorelbine combination in HER-2/neu-negative metastatic breast cancer. Clin. Breast Cancer *11*, 384–389.

Feng, D., Peng, C., Li, C., Zhou, Y., Li, M., Ling, B., Wei, H., and Tian, Z. (2009). Identification and characterization of cancer stem-like cells from primary carcinoma of the cervix uteri. Oncol. Rep. *22*, 1129–1134.

Florea, A.M.,and Büsselberg, D. (2011). Cisplatin as an Anti-Tumor Drug: Cellular Mechanisms of Activity, Drug Resistance and Induced Side Effects. Cancers *3*, 1351-1371.

Froudarakis, M.E., Pataka, A., Pappas, P., Anevlavis, S., Argiana, E., Nikolaidou, M., Kouliatis, G., Pozova, S., Marselos, M., and Bouros, D. (2008). Phase 1 trial of lipoplatin and gemcitabine as a second-line chemotherapy in patients with nonsmall cell lung carcinoma. Cancer *113*, 2752–2760.

Froudarakis, M.E., Greillier, L., Monjanel-Mouterde, S., Koutsopoulos, A., Devictor-Pierre, B., Guilhaumou, R., Karpathiou, G., Botaitis, S., and Astoul, P. (2011). Intrapleural administration of lipoplatin in an animal model. Lung Cancer Amst. Neth. *72*, 78–83.

Fuertes, M.A., Castilla, J., Alonso, C., and Pérez, J.M. (2002). Novel concepts in the development of platinum antitumor drugs. Curr. Med. Chem. Anti-Cancer Agents *2*, 539–551.

Fuertes, M.A., Alonso, C., and Pérez, J.M. (2003). Biochemical modulation of Cisplatin mechanisms of action: enhancement of antitumor activity and circumvention of drug resistance. Chem. Rev. *103*, 645–662.

Gabizon, A.A. (2002). Liposomal drug carrier systems in cancer chemotherapy: current status and future prospects. J. Drug Target. *10*, 535–538.

Gabizon, A., Catane, R., Uziely, B., Kaufman, B., Safra, T., Cohen, R., Martin, F., Huang, A., and Barenholz, Y. (1994). Prolonged circulation time and enhanced accumulation in malignant exudates of doxorubicin encapsulated in polyethylene-glycol coated liposomes. Cancer Res. *54*, 987–992.

Gately, D.P., and Howell, S.B. (1993). Cellular accumulation of the anticancer agent cisplatin: a review. Br. J. Cancer *67*, 1171–1176.

Giaccone, G. (2000). Clinical perspectives on platinum resistance. Drugs *59 Suppl 4*, 9–17; discussion 37–38.

Gleeson, M.J., Browning, G., Burton, M.J., Clarke, R.C., Hibbert, J., Jones, N., Lund, V.J., Luxon, L.M., and Watkinson, J. (2008). Scott-Brown's Otorhinolaryngology: Head and Neck Surgery 7Ed: 3 volume set (CRC Press).

Godwin, A.K., Meister, A., O'Dwyer, P.J., Huang, C.S., Hamilton, T.C., and Anderson, M.E. (1992). High resistance to cisplatin in human ovarian cancer cell lines is associated with marked increase of glutathione synthesis. Proc. Natl. Acad. Sci. U. S. A. *89*, 3070–3074.

Gómez-Ruiz, S., Maksimović-Ivanić, D., Mijatović, S., and Kaluđerović, G.N. (2012). On the discovery, biological effects, and use of Cisplatin and metallocenes in anticancer chemotherapy. Bioinorg. Chem. Appl. *2012*, 140284.

Gonzalez, V.M., Fuertes, M.A., Alonso, C., and Perez, J.M. (2001). Is cisplatin-induced cell death always produced by apoptosis? Mol. Pharmacol. *59*, 657–663.

Gottschalk, N., Lang, S., Kimmig, R., Singh, M., and Brandau, S. (2012). Monocytes and the 38kDa-antigen of mycobacterium tuberculosis modulate natural killer cell activity and their cytolysis directed against ovarian cancer cell lines. BMC Cancer *12*, 1–11.

Gregoriadis, G. (1973). Drug entrapment in liposomes. FEBS Lett. *36*, 292–296.

Gregoriadis, G., Wills, E.J., Swain, C.P., and Tavill, A.S. (1974). Drug-carrier potential of liposomes in cancer chemotherapy. Lancet *1*, 1313–1316.

Gui, T., and Shen, K. (2012). The epidermal growth factor receptor as a therapeutic target in epithelial ovarian cancer. Cancer Epidemiol. *36*, 490–496.

Guichard, S.M., and Danks, M.K. (1999). Topoisomerase enzymes as drug targets. Curr. Opin. Oncol. *11*, 482–489.

Guo, X., and Szoka, F.C., Jr (2001). Steric stabilization of fusogenic liposomes by a low-pH sensitive PEG--diortho ester--lipid conjugate. Bioconjug. Chem. *12*, 291–300.

Hankinson, S.E., Hunter, D.J., Colditz, G.A., Willett, W.C., Stampfer, M.J., Rosner, B., Hennekens, C.H., and Speizer, F.E. (1993). Tubal ligation, hysterectomy, and risk of ovarian cancer. A prospective study. JAMA J. Am. Med. Assoc. *270*, 2813–2818.

Haran, G., Cohen, R., Bar, L.K., and Barenholz, Y. (1993). Transmembrane ammonium sulfate gradients in liposomes produce efficient and stable entrapment of amphipathic weak bases. Biochim. Biophys. Acta *1151*, 201–215.

Harrington, K.J., Lewanski, C.R., Northcote, A.D., Whittaker, J., Wellbank, H., Vile, R.G., Peters, A.M., and Stewart, J.S. (2001). Phase I-II study of pegylated liposomal cisplatin (SPI-077) in patients with inoperable head and neck cancer. Ann. Oncol. Off. J. Eur. Soc. Med. Oncol. ESMO *12*, 493–496.

Havener, J.M., Nick McElhinny, S.A., Bassett, E., Gauger, M., Ramsden, D.A., and Chaney, S.G. (2003). Translesion synthesis past platinum DNA adducts by human DNA polymerase mu. Biochemistry (Mosc.) *42*, 1777–1788.

Henkels, K.M., and Turchi, J.J. (1997). Induction of apoptosis in cisplatin-sensitive and -resistant human ovarian cancer cell lines. Cancer Res. *57*, 4488–4492.

Hernández Losa, J., Parada Cobo, C., Guinea Viniegra, J., Sánchez-Arevalo Lobo, V.J., Ramón y Cajal, S., and Sánchez-Prieto, R. (2003). Role of the p38 MAPK pathway in cisplatin-based therapy. Oncogene *22*, 3998–4006.

Hockenbery, D.M., Oltvai, Z.N., Yin, X.M., Milliman, C.L., and Korsmeyer, S.J. (1993). Bcl-2 functions in an antioxidant pathway to prevent apoptosis. Cell *75*, 241–251.

Hoekstra, K., van Renswoude, J., Tomasini, R., and Scherphof, G. (1981). Interaction of phospholipid vesicles with rat hepatocytes: further characterization of vesicle-cell surface interaction; use of serum as a physiological modulator. Membr. Biochem. *4*, 129–147.

Von Hoff, D.D., Schilsky, R., Reichert, C.M., Reddick, R.L., Rozencweig, M., Young, R.C., and Muggia, F.M. (1979). Toxic effects of cis-dichlorodiammineplatinum(II) in man. Cancer Treat. Rep. *63*, 1527–1531.

Hoffmann, J.S., Pillaire, M.J., Garcia-Estefania, D., Lapalu, S., and Villani, G. (1996). In vitro bypass replication of the cisplatin-d(GpG) lesion by calf thymus DNA polymerase beta and human immunodeficiency virus type I reverse transcriptase is highly mutagenic. J. Biol. Chem. *271*, 15386–15392.

Holzer, A.K., Samimi, G., Katano, K., Naerdemann, W., Lin, X., Safaei, R., and Howell, S.B. (2004). The copper influx transporter human copper transport protein 1 regulates the uptake of cisplatin in human ovarian carcinoma cells. Mol. Pharmacol. *66*, 817–823.

Hossann, M., Syunyaeva, Z., Schmidt, R., Zengerle, A., Eibl, H., Issels, R.D., and Lindner, L.H. (2012). Proteins and cholesterol lipid vesicles are mediators of drug release from thermosensitive liposomes. J. Control. Release Off. J. Control. Release Soc. *162*, 400–406.

Hwang, K.J., Padki, M.M., Chow, D.D., Essien, H.E., Lai, J.Y., and Beaumier, P.L. (1987). Uptake of small liposomes by non-reticuloendothelial tissues. Biochim. Biophys. Acta *901*, 88–96.

Ikari, A., Nagatani, Y., Tsukimoto, M., Harada, H., Miwa, M., and Takagi, K. (2005). Sodium-dependent glucose transporter reduces peroxynitrite and cell injury caused by cisplatin in renal tubular epithelial cells. Biochim. Biophys. Acta *1717*, 109–117.

Iida, K., Nakayama, K., Rahman, M.T., Rahman, M., Ishikawa, M., Katagiri, A., Yeasmin, S., Otsuki, Y., Kobayashi, H., Nakayama, S., et al. (2011). EGFR gene amplification is related to adverse clinical outcomes in cervical squamous cell carcinoma, making the EGFR pathway a novel therapeutic target. Br. J. Cancer *105*, 420–427.

Immordino, M.L., Dosio, F., and Cattel, L. (2006). Stealth liposomes: review of the basic science, rationale, and clinical applications, existing and potential. Int. J. Nanomedicine *1*, 297–315.

Ishida, S., Lee, J., Thiele, D.J., and Herskowitz, I. (2002). Uptake of the anticancer drug cisplatin mediated by the copper transporter Ctr1 in yeast and mammals. Proc. Natl. Acad. Sci. U. S. A. *99*, 14298–14302.

Ishikawa, T., and Ali-Osman, F. (1993). Glutathione-associated cis-diamminedichloroplatinum(II) metabolism and ATP-dependent efflux from leukemia cells. Molecular characterization of glutathione-platinum complex and its biological significance. J. Biol. Chem. *268*, 20116–20125.

Isonishi, S., Saitou, M., Yasuda, M., and Tanaka, T. (2001). Mitochondria in platinum resistant cells. Hum. Cell *14*, 203–210.

Ivanov, A.I., Christodoulou, J., Parkinson, J.A., Barnham, K.J., Tucker, A., Woodrow, J., and Sadler, P.J. (1998). Cisplatin binding sites on human albumin. J. Biol. Chem. *273*, 14721–14730.

Ivascu, A., and Kubbies, M. (2006). Rapid generation of single-tumor spheroids for high-throughput cell function and toxicity analysis. J. Biomol. Screen. *11*, 922–932.

Jacobs, I., and Bast, R.C., Jr (1989). The CA 125 tumour-associated antigen: a review of the literature. Hum. Reprod. Oxf. Engl. *4*, 1–12.

Jain, R.K., and Stylianopoulos, T. (2010). Delivering nanomedicine to solid tumors. Nat. Rev. Clin. Oncol. *7*, 653–664.

Jehn, C.F., Boulikas, T., Kourvetaris, A., Kofla, G., Possinger, K., and Lüftner, D. (2008). First safety and response results of a randomized phase III study with liposomal platin in the treatment of advanced squamous cell carcinoma of the head and neck (SCCHN). Anticancer Res. *28*, 3961–3964.

Jelovac, D., and Armstrong, D.K. (2011). Recent progress in the diagnosis and treatment of ovarian cancer. CA. Cancer J. Clin. *61*, 183–203.

Jeong, K.J., Cho, K.H., Panupinthu, N., Kim, H., Kang, J., Park, C.G., Mills, G.B., and Lee, H.Y. (2013). EGFR mediates LPA-induced proteolytic enzyme expression and ovarian cancer invasion: Inhibition by resveratrol. Mol. Oncol. *7*, 121–129.

Jemal, A., Siegel, R., Ward, E., Hao, Y., Xu, J., Murray, T., and Thun, M.J. (2008). Cancer statistics, 2008. CA. Cancer J. Clin. *58*, 71–96.

Jia, J., Zhu, F., Ma, X., Cao, Z.W., Li, Y.X., and Chen, Y.Z. (2009). Mechanisms of drug combinations: interaction and network perspectives. Nat. Rev. Drug Discov. *8*, 111–128.

Johnson, S.W., Laub, P.B., Beesley, J.S., Ozols, R.F., and Hamilton, T.C. (1997). Increased platinum-DNA damage tolerance is associated with cisplatin resistance and cross-resistance to various chemotherapeutic agents in unrelated human ovarian cancer cell lines. Cancer Res. *57*, 850–856.

Johnston, M.J.W., Semple, S.C., Klimuk, S.K., Edwards, K., Eisenhardt, M.L., Leng, E.C., Karlsson, G., Yanko, D., and Cullis, P.R. (2006). Therapeutically optimized rates of drug release can be achieved by varying the drug-to-lipid ratio in liposomal vincristine formulations. Biochim. Biophys. Acta *1758*, 55–64.

Jones, S.L., Hickson, I.D., Harris, A.L., and Harnett, P.R. (1994). Repair of cisplatin-DNA adducts by protein extracts from human ovarian carcinoma. Int. J. Cancer J. Int. Cancer *59*, 388–393.

Jordan, P., and Carmo-Fonseca, M. (2000). Molecular mechanisms involved in cisplatin cytotoxicity. Cell. Mol. Life Sci. CMLS *57*, 1229–1235.

Juliano, R.L., and Stamp, D. (1975). The effect of particle size and charge on the clearance rates of liposomes and liposome encapsulated drugs. Biochem. Biophys. Res. Commun. *63*, 651–658.

Kahn, J.A. (2009). HPV vaccination for the prevention of cervical intraepithelial neoplasia. N. Engl. J. Med. *361*, 271–278.

Karpathiou, G., Argiana, E., Koutsopoulos, A., and Froudarakis, M.E. (2007). Response of a patient with pleural and peritoneal mesothelioma after second-line chemotherapy with lipoplatin and gemcitabine. Oncology *73*, 426–429.

Kartalou, M., and Essigmann, J.M. (2001). Mechanisms of resistance to cisplatin. Mutat. Res. *478*, 23–43.

Kasahara, K., Fujiwara, Y., Nishio, K., Ohmori, T., Sugimoto, Y., Komiya, K., Matsuda, T., and Saijo, N. (1991). Metallothionein content correlates with the sensitivity of human small cell lung cancer cell lines to cisplatin. Cancer Res. *51*, 3237–3242.

Katano, K., Kondo, A., Safaei, R., Holzer, A., Samimi, G., Mishima, M., Kuo, Y.-M., Rochdi, M., and Howell, S.B. (2002). Acquisition of resistance to cisplatin is accompanied by changes in the cellular pharmacology of copper. Cancer Res. *62*, 6559–6565.

Kim, S.-W., Suh, C., Lee, S.D., Kim, W.S., Kim, D.S., Kim, W.D., and Lee, J.S. (2003). Weekly low dose paclitaxel and cisplatin as first-line chemotherapy for advanced non-small cell lung cancer. Lung Cancer Amst. Neth. *41*, 221–226.

Klibanov, A.L., Maruyama, K., Torchilin, V.P., and Huang, L. (1990). Amphipathic polyethyleneglycols effectively prolong the circulation time of liposomes. FEBS Lett. *268*, 235–237.

Köberle, B., Masters, J.R., Hartley, J.A., and Wood, R.D. (1999). Defective repair of cisplatin-induced DNA damage caused by reduced XPA protein in testicular germ cell tumours. Curr. Biol. CB *9*, 273–276.

Komatsu, M., Sumizawa, T., Mutoh, M., Chen, Z.S., Terada, K., Furukawa, T., Yang, X.L., Gao, H., Miura, N., Sugiyama, T., et al. (2000). Copper-transporting P-type adenosine triphosphatase (ATP7B) is associated with cisplatin resistance. Cancer Res. *60*, 1312–1316.

Kool, M., de Haas, M., Scheffer, G.L., Scheper, R.J., van Eijk, M.J., Juijn, J.A., Baas, F., and Borst, P. (1997). Analysis of expression of cMOAT (MRP2), MRP3, MRP4, and MRP5, homologues of the multidrug resistance-associated protein gene (MRP1), in human cancer cell lines. Cancer Res. *57*, 3537–3547.

Kosmas, C., Angel, J., Athanasiou, A., et al. (20-24 Sept 2009). Interim Phase III analysis of Lipoplatin plus Gemcitabine versus Cisplatin plus Gemcitabine in advanced NSCLC. Abstract number: E15-1858. Submitted to ECCO 15 - 34th ESMO Multidisciplinary Congress, Berlin.

Kostova, I. (2006). Platinum complexes as anticancer agents. Recent Patents Anticancer Drug Discov. *1*, 1–22.

Koukourakis, M.I., Giatromanolaki, A., Pitiakoudis, M., Kouklakis, G., Tsoutsou, P., Abatzoglou, I., Panteliadou, M., Sismanidou, K., Sivridis, E., and Boulikas, T. (2010). Concurrent liposomal cisplatin (Lipoplatin), 5-fluorouracil and radiotherapy for the treatment of locally advanced gastric cancer: a phase I/II study. Int. J. Radiat. Oncol. Biol. Phys. *78*, 150–155.

Lai, G.M., Ozols, R.F., Smyth, J.F., Young, R.C., and Hamilton, T.C. (1988). Enhanced DNA repair and resistance to cisplatin in human ovarian cancer. Biochem. Pharmacol. *37*, 4597–4600.

Lai, G.M., Ozols, R.F., Young, R.C., and Hamilton, T.C. (1989). Effect of glutathione on DNA repair in cisplatin-resistant human ovarian cancer cell lines. J. Natl. Cancer Inst. *81*, 535–539.

Latifi, A., Abubaker, K., Castrechini, N., Ward, A.C., Liongue, C., Dobill, F., Kumar, J., Thompson, E.W., Quinn, M.A., Findlay, J.K., et al. (2011). Cisplatin treatment of primary and metastatic epithelial ovarian carcinomas generates residual cells with mesenchymal stem cell-like profile. J. Cell. Biochem. *112*, 2850–2864.

Lau, A.H. (1999). Apoptosis induced by cisplatin nephrotoxic injury. Kidney Int. *56*, 1295–1298.

Leath, C.A., 3rd, and Straughn, J.M., Jr (2013). Chemotherapy for advanced and recurrent cervical carcinoma: results from cooperative group trials. Gynecol. Oncol. *129*, 251–257.

Lengyel, E. (2010). Ovarian Cancer Development and Metastasis. Am. J. Pathol. *177*, 1053–1064.

Liang, X.-J., Mukherjee, S., Shen, D.-W., Maxfield, F.R., and Gottesman, M.M. (2006). Endocytic recycling compartments altered in cisplatin-resistant cancer cells. Cancer Res. *66*, 2346–2353.

Liang, C.-C., Park, A.Y., and Guan, J.-L. (2007). In vitro scratch assay: a convenient and inexpensive method for analysis of cell migration in vitro. Nat. Protoc. *2*, 329–333.

Liang, X.-J., Finkel, T., Shen, D.-W., Yin, J.-J., Aszalos, A., and Gottesman, M.M. (2008). SIRT1 contributes in part to cisplatin resistance in cancer cells by altering mitochondrial metabolism. Mol. Cancer Res. MCR *6*, 1499–1506.

Liu, D., He, C., Wang, A.Z., and Lin, W. (2013). Application of liposomal technologies for delivery of platinum analogs in oncology. Int. J. Nanomedicine *8*, 3309–3319.

Liu, M., Howes, A., Lesperance, J., Stallcup, W.B., Hauser, C.A., Kadoya, K., Oshima, R.G., and Abraham, R.T. (2005). Antitumor activity of rapamycin in a transgenic mouse model of ErbB2-dependent human breast cancer. Cancer Res. *65*, 5325–5336.

Liu, Q., Guntuku, S., Cui, X.S., Matsuoka, S., Cortez, D., Tamai, K., Luo, G., Carattini-Rivera, S., DeMayo, F., Bradley, A., et al. (2000). Chk1 is an essential kinase that is regulated by Atr and required for the G(2)/M DNA damage checkpoint. Genes Dev. *14*, 1448–1459.

Liu, S., and Zheng, P. (2013). High aldehyde dehydrogenase activity identifies cancer stem cells in human cervical cancer. Oncotarget *4*, 2462–2475.

Liu, Y., Xing, H., Han, X., Shi, X., Liang, F., Cheng, G., Lu, Y., and Ma, D. (2008). Apoptosis of HeLa cells induced by cisplatin and its mechanism. J. Huazhong Univ. Sci. Technolog. Med. Sci. *28*, 197–199.

Liu, Y., Li, Y., Yu, S., and Zhao, G. (2012). Recent advances in the development of thioredoxin reductase inhibitors as anticancer agents. Curr. Drug Targets *13*, 1432–1444.

López, J., Ruíz, G., Organista-Nava, J., Gariglio, P., and García-Carrancá, A. (2012). Human papillomavirus infections and cancer stem cells of tumors from the uterine cervix. Open Virol. J. *6*, 232–240.

Ma, L., Lai, D., Liu, T., Cheng, W., and Guo, L. (2010). Cancer stem-like cells can be isolated with drug selection in human ovarian cancer cell line SKOV3. Acta Biochim. Biophys. Sin. *42*, 593–602.

Macciò, A., and Madeddu, C. (2013). Cisplatin : an old drug with a newfound efficacy - from mechanisms of action to cytotoxicity. Expert Opin. Pharmacother. *14*, 1839–1857.

Madden, T.D., Harrigan, P.R., Tai, L.C., Bally, M.B., Mayer, L.D., Redelmeier, T.E., Loughrey, H.C., Tilcock, C.P., Reinish, L.W., and Cullis, P.R. (1990). The accumulation of drugs within large unilamellar vesicles exhibiting a proton gradient: a survey. Chem. Phys. Lipids *53*, 37–46.

Maeda, H., and Matsumura, Y. (2011). EPR effect based drug design and clinical outlook for enhanced cancer chemotherapy. Adv. Drug Deliv. Rev. *63*, 129–130.

Mahmood, D.F.D., Abderrazak, A., El Hadri, K., Simmet, T., and Rouis, M. (2013). The Thioredoxin System as a Therapeutic Target in Human Health and Disease. Antioxid. Redox Signal. *19*, 1266–1303.

Malhotra, V., and Perry, M.C. (2003). Classical chemotherapy: mechanisms, toxicities and the therapeutic window. Cancer Biol. Ther. *2*, S2–4.

Mann, S.C., Andrews, P.A., and Howell, S.B. (1991). Modulation of cis-diamminedichloroplatinum(II) accumulation and sensitivity by forskolin and 3-isobutyl-1-methylxanthine in sensitive and resistant human ovarian carcinoma cells. Int. J. Cancer J. Int. Cancer *48*, 866–872.

Mansouri, A., Ridgway, L.D., Korapati, A.L., Zhang, Q., Tian, L., Wang, Y., Siddik, Z.H., Mills, G.B., and Claret, F.X. (2003). Sustained activation of JNK/p38 MAPK pathways in response to cisplatin leads to Fas ligand induction and cell death in ovarian carcinoma cells. J. Biol. Chem. *278*, 19245–19256.

Manzoor, A.A., Lindner, L.H., Landon, C.D., Park, J.-Y., Simnick, A.J., Dreher, M.R., Das, S., Hanna, G., Park, W., Chilkoti, A., et al. (2012). Overcoming limitations in nanoparticle drug delivery: triggered, intravascular release to improve drug penetration into tumors. Cancer Res. *72*, 5566–5575.

Marr, A.K., Kurzman, I.D., and Vail, D.M. (2004). Preclinical evaluation of a liposome-encapsulated formulation of cisplatin in clinically normal dogs. Am. J. Vet. Res. *65*, 1474–1478.

Martin, F., and Boulikas ,T. (1998). The challenge of liposomes in gene therapy. Gene Ther. Mol. Biol. *1*, 173-214

Matsuoka, S., Rotman, G., Ogawa, A., Shiloh, Y., Tamai, K., and Elledge, S.J. (2000). Ataxia telangiectasia-mutated phosphorylates Chk2 in vivo and in vitro. Proc. Natl. Acad. Sci. U. S. A. *97*, 10389–10394.

Mattheolabakis, G., Rigas, B., and Constantinides, P.P. (2012). Nanodelivery strategies in cancer chemotherapy: biological rationale and pharmaceutical perspectives. Nanomed. *7*, 1577–1590.

Maurer, N., Wong, K.F., Hope, M.J., and Cullis, P.R. (1998). Anomalous solubility behavior of the antibiotic ciprofloxacin encapsulated in liposomes: a 1H-NMR study. Biochim. Biophys. Acta *1374*, 9–20.

Mehta, G., Hsiao, A.Y., Ingram, M., Luker, G.D., and Takayama, S. (2012). Opportunities and challenges for use of tumor spheroids as models to test drug delivery and efficacy. J. Controlled Release *164*, 192–204.

Meijer, C., de Vries, E.G., Marmiroli, P., Tredici, G., Frattola, L., and Cavaletti, G. (1999). Cisplatin-induced DNA-platination in experimental dorsal root ganglia neuronopathy. Neurotoxicology *20*, 883–887.

Mistry, P., Kelland, L.R., Loh, S.Y., Abel, G., Murrer, B.A., and Harrap, K.R. (1992). Comparison of cellular accumulation and cytotoxicity of cisplatin with that of tetraplatin and amminedibutyratodichloro(cyclohexylamine)platinum(IV) (JM221) in human ovarian carcinoma cell lines. Cancer Res. *52*, 6188–6193.

Murata, T., Mizushima, H., Chinen, I., Moribe, H., Yagi, S., Hoffman, R.M., Kimura, T., Yoshino, K., Ueda, Y., Enomoto, T., et al. (2011). HB-EGF and PDGF mediate reciprocal interactions of carcinoma cells with cancer-associated fibroblasts to support progression of uterine cervical cancers. Cancer Res. *71*, 6633–6642.

Murphy, D., McGown, A.T., Crowther, D., Mander, A., and Fox, B.W. (1991). Metallothionein levels in ovarian tumours before and after chemotherapy. Br. J. Cancer *63*, 711–714.

Mylonakis, N., Athanasiou, A., Ziras, N., Angel, J., Rapti, A., Lampaki, S., Politis, N., Karanikas, C., and Kosmas, C. (2010). Phase II study of liposomal cisplatin (Lipoplatin) plus gemcitabine versus cisplatin plus gemcitabine as first line treatment in inoperable (stage IIIB/IV) non-small cell lung cancer. Lung Cancer Amst. Neth. *68*, 240–247.

N, A., Mi, E., Sc, M., Sw, J., and Tc, H. (1998). The biology of ovarian cancer. Semin. Oncol. *25*, 281–304.

Nakayama, K., Kanzaki, A., Terada, K., Mutoh, M., Ogawa, K., Sugiyama, T., Takenoshita, S., Itoh, K., Yaegashi, N., Miyazaki, K., et al. (2004). Prognostic value of the Cu-transporting ATPase in ovarian carcinoma patients receiving cisplatin-based chemotherapy. Clin. Cancer Res. Off. J. Am. Assoc. Cancer Res. *10*, 2804–2811.

Naora, H., and Montell, D.J. (2005). Ovarian Cancer Metastasis: Integrating insights from disparate model organisms. Nat. Rev. Cancer *5*, 355–366.

Newman, M.S., Colbern, G.T., Working, P.K., Engbers, C., and Amantea, M.A. (1999). Comparative pharmacokinetics, tissue distribution, and therapeutic effectiveness of cisplatin encapsulated in long-circulating, pegylated liposomes (SPI-077) in tumor-bearing mice. Cancer Chemother. Pharmacol. *43*, 1–7.

De Oliveira, M.C., Fattal, E., Couvreur, P., Lesieur, P., Bourgaux, C., Ollivon, M., and Dubernet, C. (1998). pH-sensitive liposomes as a carrier for

oligonucleotides: a physico-chemical study of the interaction between DOPE and a 15-mer oligonucleotide in quasi-anhydrous samples. Biochim. Biophys. Acta *1372*, 301–310.

Olson, F., Hunt, C.A., Szoka, F.C., Vail, W.J., and Papahadjopoulos, D. (1979). Preparation of liposomes of defined size distribution by extrusion through polycarbonate membranes. Biochim. Biophys. Acta *557*, 9–23.

Page, R. (2001). Principles of chemotherapy. In: Pazdur, R, Hoskins, WJ, Coia, LR, Wagman, LD, editors. Cancer management: a multidisciplinary approach, 5th ed. Melville, NY: PRR, Inc.; 21-37.

Pasquetto, M.V., Vecchia, L., Covini, D., Digilio, R., and Scotti, C. (2011). Targeted drug delivery using immunoconjugates: principles and applications. J. Immunother. Hagerstown Md 1997 *34*, 611–628.

Pattanaik, A., Bachowski, G., Laib, J., Lemkuil, D., Shaw, C.F., 3rd, Petering, D.H., Hitchcock, A., and Saryan, L. (1992). Properties of the reaction of cis-dichlorodiammineplatinum(II) with metallothionein. J. Biol. Chem. *267*, 16121–16128.

Peleg-Shulman, T., and Gibson, D. (2001). Cisplatin-protein adducts are efficiently removed by glutathione but not by 5'-guanosine monophosphate. J. Am. Chem. Soc. *123*, 3171–3172.

Pendergrass, W., Wolf, N., and Poot, M. (2004). Efficacy of MitoTracker Green and CMXrosamine to measure changes in mitochondrial membrane potentials in living cells and tissues. Cytom. Part J. Int. Soc. Anal. Cytol. *61*, 162–169.

Peyrone ,M. (1844). 'Ueber die Einwirkung des Ammoniaks auf Platinchlorür'[On the Influence of Ammonia on Platinum Chloride]. Ann. Chem. Pharm. 51, 1.

Pietenpol, J.A., and Stewart, Z.A. (2002). Cell cycle checkpoint signaling:: Cell cycle arrest versus apoptosis. Toxicology *181–182*, 475–481.

Pisano, C., Pratesi, G., Laccabue, D., Zunino, F., Lo Giudice, P., Bellucci, A., Pacifici, L., Camerini, B., Vesci, L., Castorina, M., et al. (2003). Paclitaxel and Cisplatin-induced neurotoxicity: a protective role of acetyl-L-carnitine. Clin. Cancer Res. Off. J. Am. Assoc. Cancer Res. *9*, 5756–5767.

Pizzorno, G., Handschumacher, R.E., and Cheng, Y.-C. (2000). Pyrimidine and Purine Antimetabolites.

Pommier, Y. (2006). Topoisomerase I inhibitors: camptothecins and beyond. Nat. Rev. Cancer *6*, 789–802.

Rabik, C.A., and Dolan, M.E. (2007). Molecular mechanisms of resistance and toxicity associated with platinating agents. Cancer Treat. Rev. *33*, 9–23.

Reed, E. (1999). Cisplatin. Cancer Chemother. Biol. Response Modif. *18*, 144–151.

Rodday, B., Hirschhaeuser, F., Walenta, S., and Mueller-Klieser, W. (2011). Semiautomatic Growth Analysis of Multicellular Tumor Spheroids. J. Biomol. Screen. 1087057111419501.

Rosenberg, B. (1977). Noble metal complexes in cancer chemotherapy. Adv. Exp. Med. Biol. *91*, 129–150.

Rosenberg, B., and VanCamp, L. (1970). The successful regression of large solid sarcoma 180 tumors by platinum compounds. Cancer Res. *30*, 1799–1802.

Rosenberg, B., Renshaw, E., Vancamp, L., Hartwick, J., and Drobnik, J. (1967). Platinum-induced filamentous growth in Escherichia coli. J. Bacteriol. *93*, 716–721.

Rosenberg, B., VanCamp, L., Trosko, J.E., and Mansour, V.H. (1969). Platinum compounds: a new class of potent antitumour agents. Nature *222*, 385–386.

Rosenberg, B., VanCamp, L., and Krigas, T. (1965). Inhibition of cell division in Escherichia Coli by electrolysis products from a platinum electrode. Nature *205*, 698–699.

Rybak, L.P., and Whitworth, C.A. (2005). Ototoxicity: therapeutic opportunities. Drug Discov. Today *10*, 1313–1321.

Safra, T., Muggia, F., Jeffers, S., Tsao-Wei, D.D., Groshen, S., Lyass, O., Henderson, R., Berry, G., and Gabizon, A. (2000). Pegylated liposomal doxorubicin (doxil): reduced clinical cardiotoxicity in patients reaching or exceeding cumulative doses of 500 mg/m2. Ann. Oncol. Off. J. Eur. Soc. Med. Oncol. ESMO *11*, 1029–1033.

Sakakura, C., Sweeney, E.A., Shirahama, T., Igarashi, Y., Hakomori, S., Tsujimoto, H., Imanishi, T., Ogaki, M., Ohyama, T., Yamazaki, J., et al. (1997). Overexpression of bax sensitizes breast cancer MCF-7 cells to cisplatin and etoposide. Surg. Today *27*, 676–679.

Samimi, G., Fink, D., Varki, N.M., Husain, A., Hoskins, W.J., Alberts, D.S., and Howell, S.B. (2000). Analysis of MLH1 and MSH2 expression in ovarian cancer before and after platinum drug-based chemotherapy. Clin. Cancer Res. Off. J. Am. Assoc. Cancer Res. *6*, 1415–1421.

Sanjosé, de S., Serrano, B., Castellsagué, X., Brotons, M., Muñoz, J., Bruni, L., and Bosch, F.X. (2012). A WHO/ICO HPV Information Centre Report. Human Papillomavirus (HPV) and Related Cancers in the Global Alliance for Vaccines and Immunization (GAVI) Countries. Vaccine, 30S, D1- D83.

Sapra, P., and Allen, T.M. (2002). Internalizing antibodies are necessary for improved therapeutic efficacy of antibody-targeted liposomal drugs. Cancer Res. *62*, 7190–7194.

Sasada, T., Nakamura, H., Ueda, S., Sato, N., Kitaoka, Y., Gon, Y., Takabayashi, A., Spyrou, G., Holmgren, A., and Yodoi, J. (1999). Possible involvement of thioredoxin reductase as well as thioredoxin in cellular sensitivity to cis-diamminedichloroplatinum (II). Free Radic. Biol. Med. *27*, 504–514.

Scatchard, K., Forrest, J.L., Flubacher, M., Cornes, P., and Williams, C. (2012). Chemotherapy for metastatic and recurrent cervical cancer. Cochrane Database Syst. Rev. *10*, CD006469.

Shank, J.J., Yang, K., Ghannam, J., Cabrera, L., Johnston, C.J., Reynolds, R.K., and Buckanovich, R.J. (2012). Metformin targets ovarian cancer stem cells in vitro and in vivo. Gynecol. Oncol. *127*, 390–397.

Shen, D.-W., Pouliot, L.M., Hall, M.D., and Gottesman, M.M. (2012). Cisplatin resistance: a cellular self-defense mechanism resulting from multiple epigenetic and genetic changes. Pharmacol. Rev. *64*, 706–721.

Shen, L., Shui, Y., Wang, X., Sheng, L., Yang, Z., Xue, D., and Wei, Q. (2008). EGFR and HER2 expression in primary cervical cancers and corresponding lymph node metastases: Implications for targeted radiotherapy. BMC Cancer *8*, 232.

Shield, K., Ackland, M.L., Ahmed, N., and Rice, G.E. (2009). Multicellular spheroids in ovarian cancer metastases: Biology and pathology. Gynecol. Oncol. *113*, 143–148.

Siddik, Z.H. (2003). Cisplatin: mode of cytotoxic action and molecular basis of resistance. Oncogene *22*, 7265–7279.

Siegel, R., Naishadham, D., and Jemal, A. (2012). Cancer statistics, 2012. CA. Cancer J. Clin. *62*, 10–29.

Silva, I.A., Bai, S., McLean, K., Yang, K., Griffith, K., Thomas, D., Ginestier, C., Johnston, C., Kueck, A., Reynolds, R.K., et al. (2011). Aldehyde dehydrogenase in combination with CD133 defines angiogenic ovarian cancer stem cells that portend poor patient survival. Cancer Res. *71*, 3991–4001.

Skubitz, A.P.N., Taras, E.P., Boylan, K.L.M., Waldron, N.N., Oh, S., Panoskaltsis-Mortari, A., and Vallera, D.A. (2013). Targeting CD133 in an in vivo ovarian cancer model reduces ovarian cancer progression. Gynecol. Oncol. *130*, 579–587.

Soonthornthum, T., Arias-Pulido, H., Joste, N., Lomo, L., Muller, C., Rutledge, T., and Verschraegen, C. (2011). Epidermal growth factor receptor as a biomarker for cervical cancer. Ann. Oncol. Off. J. Eur. Soc. Med. Oncol. ESMO *22*, 2166–2178.

Soriţău, O. (2010). Enhanced chemoresistance and tumor sphere formation as a laboratory model for peritoneal micrometastasis in epithelial ovarian cancer. Rom. J. Morphol. Embryol. *51*, 259–264.

Söti, C., Rácz, A., and Csermely, P. (2002). A Nucleotide-dependent molecular switch controls ATP binding at the C-terminal domain of Hsp90. N-terminal nucleotide binding unmasks a C-terminal binding pocket. J. Biol. Chem. *277*, 7066–7075.

Spessotto, P., Lacrima, K., Nicolosi, P.A., Pivetta, E., Scapolan, M., and Perris, R. (2009). Fluorescence-based assays for in vitro analysis of cell adhesion and migration. Methods Mol. Biol. Clifton NJ *522*, 221–250.

Stathopoulos, G.P., Antoniou, D., Dimitroulis, J., Stathopoulos, J., Marosis, K., and Michalopoulou, P. (2011). Comparison of liposomal cisplatin versus cisplatin in non-squamous cell non-small-cell lung cancer. Cancer Chemother. Pharmacol. *68*, 945–950.

Stathopoulos, G.P., and Boulikas, T. (2012). Lipoplatin formulation review article. J. Drug Deliv. *2012*, 581363.

Stathopoulos, G.P., Boulikas, T., Rigatos, S.K., et al. (2002). Liposomal cisplatin combined with gemcitabine in pretreated advanced cancer patients. Phase I-II study. Ann. Oncol. *13*,25.

Stathopoulos, G.P., Boulikas, T., Vougiouka, M., Deliconstantinos, G., Rigatos, S., Darli, E., Viliotou, V., and Stathopoulos, J.G. (2005). Pharmacokinetics and adverse reactions of a new liposomal cisplatin (Lipoplatin): phase I study. Oncol. Rep. *13*, 589–595.

Stathopoulos, G.P., Boulikas, T., Vougiouka, M., Rigatos, S.K., and Stathopoulos, J.G. (2006). Liposomal cisplatin combined with gemcitabine in pretreated advanced pancreatic cancer patients: a phase I-II study. Oncol. Rep. *15*, 1201–1204.

Stathopoulos, G.P., Rigatos, S., and Stathopoulos, J. (2010).Liposomal cisplatin dose escalation for determining the maximum tolerated dose and dose-limiting toxicity: a phase I study. Anticancer Research. *30*, 1317-1321,.

Stathopoulos, G.P., Rigatos, S., Stathopoulos, J., and Batzios, S. (2012). Liposom al cisplatin in cancer patients with renal failure. J. Drug Deliv. *2*, 106-109.

Stewart, D.J. (2007). Mechanisms of resistance to cisplatin and carboplatin. Crit. Rev. Oncol. Hematol. *63*, 12–31.

Sugihara, E., and Saya, H. (2013). Complexity of cancer stem cells. Int. J. Cancer J. Int. Cancer *132*, 1249–1259.

Sugimoto, C., Fujieda, S., Seki, M., Sunaga, H., Fan, G.K., Tsuzuki, H., Borner, C., Saito, H., and Matsukawa, S. (1999). Apoptosis-promoting gene (bax) transfer potentiates sensitivity of squamous cell carcinoma to cisplatin in vitro and in vivo. Int. J. Cancer J. Int. Cancer *82*, 860–867.

Talley, R.W., O'Bryan, R.M., Gutterman, J.U., Brownlee, R.W., and McCredie, K.B. (1973). Clinical evaluation of toxic effects of cis-diamminedichloroplatinum (NSC-119875)--phase I clinical study. Cancer Chemother. Rep. *57*, 465–471.

Tanaka, T., Kojima, I., Ohse, T., Inagi, R., Miyata, T., Ingelfinger, J.R., Fujita, T., and Nangaku, M. (2005). Hypoxia-inducible factor modulates tubular cell survival in cisplatin nephrotoxicity. Am. J. Physiol. Renal Physiol. *289*, F1123–1133.

Taylor, J.K., Zhang, Q.Q., Monia, B.P., Marcusson, E.G., and Dean, N.M. (1999). Inhibition of Bcl-xL expression sensitizes normal human keratinocytes and epithelial cells to apoptotic stimuli. Oncogene *18*, 4495–4504.

Toffoli, G., Bevilacqua, C., Franceschin, A., and Boiocchi, M. (1989). Effect of hyperthermia on intracellular drug accumulation and chemosensitivity in drug-sensitive and drug-resistant P388 leukaemia cell lines. Int. J. Hyperth. Off. J. Eur. Soc. Hyperthermic Oncol. North Am. Hyperth. Group *5*, 163–172.

Tonissen, K.F., and Di Trapani, G. (2009). Thioredoxin system inhibitors as mediators of apoptosis for cancer therapy. Mol. Nutr. Food Res. *53*, 87–103.

Torchilin, V.P. (2005). Recent advances with liposomes as pharmaceutical carriers. Nat. Rev. Drug Discov. *4*, 145–160.

Turchi, J.J., and Henkels, K. (1996). Human Ku autoantigen binds cisplatin-damaged DNA but fails to stimulate human DNA-activated protein kinase. J. Biol. Chem. *271*, 13861–13867.

Urig, S., and Becker, K. (2006). On the potential of thioredoxin reductase inhibitors for cancer therapy. Semin. Cancer Biol. *16*, 452–465.

Ushijima, K. (2009). Treatment for Recurrent Ovarian Cancer—At First Relapse. J. Oncol. *2010*.

Vaisman, A., Varchenko, M., Umar, A., Kunkel, T.A., Risinger, J.I., Barrett, J.C., Hamilton, T.C., and Chaney, S.G. (1998). The role of hMLH1, hMSH3, and hMSH6 defects in cisplatin and oxaliplatin resistance: correlation with replicative bypass of platinum-DNA adducts. Cancer Res. *58*, 3579–3585.

Veal, G.J., Griffin, M.J., Price, E., Parry, A., Dick, G.S., Little, M.A., Yule, S.M., Morland, B., Estlin, E.J., Hale, J.P., et al. (2001). A phase I study in paediatric patients to evaluate the safety and pharmacokinetics of SPI-77, a liposome encapsulated formulation of cisplatin. Br. J. Cancer *84*, 1029–1035.

Vinci, M., Gowan, S., Boxall, F., Patterson, L., Zimmermann, M., Court, W., Lomas, C., Mendiola, M., Hardisson, D., and Eccles, S.A. (2012). Advances in establishment and analysis of three-dimensional tumor spheroid-based functional assays for target validation and drug evaluation. BMC Biol. *10*, 29.

Wang, D., and Lippard, S.J. (2004). Cisplatin-induced post-translational modification of histones H3 and H4. J. Biol. Chem. *279*, 20622–20625.

Wang, D., and Lippard, S.J. (2005). Cellular processing of platinum anticancer drugs. Nat. Rev. Drug Discov. *4*, 307–320.

Wang, P., Chen, J., Mu, L.-H., Du, Q.-H., Niu, X.-H., and Zhang, M.-Y. (2013). Propofol inhibits invasion and enhances paclitaxel- induced apoptosis in ovarian cancer cells through the suppression of the transcription factor slug. Eur. Rev. Med. Pharmacol. Sci. *17*, 1722–1729.

Wang, X., Martindale, J.L., and Holbrook, N.J. (2000). Requirement for ERK activation in cisplatin-induced apoptosis. J. Biol. Chem. *275*, 39435–39443.

Warwick, G.P. (1963). The Mechanism of action of alkylating agents. Cancer Res. *23*, 1315–1333.

Weinstein, J.N., Magin, R.L., Yatvin, M.B., and Zaharko, D.S. (1979). Liposomes and local hyperthermia: selective delivery of methotrexate to heated tumors. Science *204*, 188–191.

Will, J., Wolters, D.A., and Sheldrick, W.S. (2008). Characterisation of cisplatin binding sites in human serum proteins using hyphenated multidimensional liquid chromatography and ESI tandem mass spectrometry. ChemMedChem *3*, 1696–1707.

Wiltshaw, E. (1979). Cisplatin in the Treatment of Cancer. The first metal anti-tumour drug. Platinum Metals Rev. 23, 90–98.

Wiltshaw, E., and Kroner, T. (1976). Phase II study of cis-dichlorodiammineplatinum(II) (NSC-119875) in advanced adenocarcinoma of the ovary. Cancer Treat. Rep. *60*, 55–60.

Wintzell, M., Löfstedt, L., Johansson, J., Pedersen, A.B., Fuxe, J., and Shoshan, M. (2012). Repeated cisplatin treatment can lead to a multiresistant tumor cell population with stem cell features and sensitivity to 3-bromopyruvate. Cancer Biol. Ther. *13*, 1454–1462.

Wolf, C.R., Hayward, I.P., Lawrie, S.S., Buckton, K., McIntyre, M.A., Adams, D.J., Lewis, A.D., Scott, A.R., and Smyth, J.F. (1987). Cellular heterogeneity and drug resistance in two ovarian adenocarcinoma cell lines derived from a single patient. Int. J. Cancer J. Int. Cancer *39*, 695–702.

Woo, J., Chiu, G.N.C., Karlsson, G., Wasan, E., Ickenstein, L., Edwards, K., and Bally, M.B. (2008). Use of a passive equilibration methodology to encapsulate cisplatin into preformed thermosensitive liposomes. Int. J. Pharm. *349*, 38–46.

Wp, M., and Rf, O. (1998). Chemotherapy of advanced ovarian cancer. Semin. Oncol. *25*, 340–348.

Yee, G.P.C., de Souza, P., and Khachigian, L.M. (2013). Current and potential treatments for cervical cancer. Curr. Cancer Drug Targets *13*, 205–220.

Youle, R.J., and Strasser, A. (2008). The BCL-2 protein family: opposing activities that mediate cell death. Nat. Rev. Mol. Cell Biol. *9*, 47–59.

Zalba, S., and Garrido, M.J. (2013). Liposomes, a promising strategy for clinical application of platinum derivatives. Expert Opin. Drug Deliv. *10*, 829–844.

Zamble, D.B., Mu, D., Reardon, J.T., Sancar, A., and Lippard, S.J. (1996). Repair of cisplatin--DNA adducts by the mammalian excision nuclease. Biochemistry (Mosc.) *35*, 10004–10013.

Zamboni, W.C., Gervais, A.C., Egorin, M.J., Schellens, J.H.M., Zuhowski, E.G., Pluim, D., Joseph, E., Hamburger, D.R., Working, P.K., Colbern, G., et al. (2004). Systemic and tumor disposition of platinum after administration of cisplatin or STEALTH liposomal-cisplatin formulations (SPI-077 and SPI-077 B103) in a preclinical tumor model of melanoma. Cancer Chemother. Pharmacol. *53*, 329–336.

Zhang, Y., Rohde, L.H., and Wu, H. (2009). Involvement of nucleotide excision and mismatch repair mechanisms in double strand break repair. Curr. Genomics *10*, 250–258.

Zwielly, A., Mordechai, S., Brkic, G., Bogomolny, E., Pelly, I.Z., Moreh, R., and Gopas, J. (2011). Grading of intrinsic and acquired cisplatin-resistant human melanoma cell lines: an infrared ATR study. Eur. Biophys. J. *40*, 795–804.

8. ACKNOWLEDGEMENTS

I would like to express my gratitude to my co-supervisors Prof. Alfonso Colombatti and Dott.ssa Donatella Aldinucci for giving me the opportunity to do this PhD in their lab at CRO Aviano National Cancer Institute. Thank you for giving me the freedom to develop this project, for the guidance, the support and for the critical discussions. It would not have been possible to write this doctoral thesis without your help. I would like to thank you also for encouraging my research and for allowing me to grow as a research scientist.

A great thanks also to all the members of the lab, those present at the moment and those that have witnessed only a portion of this incredible experience: you all have contributed somehow to my PhD and I can associate at least one unforgettable memory to each and every one of you. Nevertheless there are some members in particular that deserve a special thank. To Marta Celegato for helping me every time I needed, for the gossips, for your honesty and for being a really good friend: thank you. To Cinzia Borghese for your help, suggestions and support.

I wish to express my sincere appreciation to those who have contributed to this thesis and supported me in one way or the other during this experience. Most of all, I am deeply grateful to my parents for their support, encouragement, for believing in me and for being the best family. Special thanks also go to my sister Lara and to Davide for their love and for always being there for me.

Gynecologic Oncology 131 (2013) 744–752

Contents lists available at ScienceDirect

Gynecologic Oncology

journal homepage: www.elsevier.com/locate/ygyno

Preclinical evaluation of a new liposomal formulation of cisplatin, lipoplatin, to treat cisplatin-resistant cervical cancer

Naike Casagrande [a], Monica De Paoli [a], Marta Celegato [a], Cinzia Borghese [a], Maurizio Mongiat [a], Alfonso Colombatti [a,b,c], Donatella Aldinucci [a,*]

[a] Experimental Oncology 2, Centro di Riferimento Oncologico, IRCCS, National Cancer Institute, Aviano, PN, Italy
[b] Department of Medical and Biological Science Technology, University of Udine, Italy
[c] MATI (Microgravity Ageing Training Immobility) Excellence Center, University of Udine, Italy

HIGHLIGHTS

- Lipoplatin is active in cisplatin-resistant cervical cancer cells.
- Lipoplatin inhibits cell migration and invasion, spheroid formation and decreases the percentage of cancer stem cells (ALDH+ cells).
- Lipoplatin may represent a novel therapeutic strategy for cisplatin-resistant recurrent cervical cancer.

ARTICLE INFO

Article history:
Received 28 June 2013
Accepted 31 August 2013
Available online 10 September 2013

Keywords:
Cervical cancer
Cisplatin-resistance
liposomal cisplatin
Spheroids
Migration
Cancer stem cells

ABSTRACT

Objective. Cisplatin-based chemotherapy has been shown to improve survival in cervical cancer; however, treatment is associated with tumor resistance and significant toxicity. Lipoplatin is a new liposomal formulation of cisplatin, developed to reduce cisplatin toxicity, to improve drug accumulation at tumor sites and to overcome drug resistance.
The aim of this study is to analyze the antitumoral activity of lipoplatin against cisplatin-resistant cervical cancer cells and to investigate its mechanism of action.

Methods. The activity and mechanism of action of lipoplatin were studied in the ME-180 cervical cancer cell line and its cisplatin-resistant clone R-ME-180 and HeLa cells using cell proliferation assays, flow cytometry, ELISA assay, cell migration, spheroids and tumor xenograft.

Results. We demonstrated that lipoplatin exhibited a potent antitumoral activity on HeLa, ME-180 cells and its cisplatin-resistant clone R-ME-180. Lipoplatin inhibited cell proliferation in a dose-dependent manner and was more active than the reference drug cisplatin in R-ME-180 cells and induced apoptosis, as evaluated by Annexin-V staining and DNA fragmentation, caspases 9 and 3 activation, Bcl-2, and Bcl-xL down-regulation, but Bax up-regulation inhibited thioredoxin reductase (TrxR) enzymatic activity and increased reactive oxygen species (ROS) accumulation; reduced EGFR expression and inhibited both migration and invasion. R-ME-180, but not ME-180 cells, generated three-dimensional (3D)-multicellular spheroids expressing the cancer stem cell marker ALDH. The ability of R-ME-180 cells to form spheroids *in vitro* and tumors in nude mice was also remarkably decreased by lipoplatin.

Conclusions. Overall, our results suggest that lipoplatin has potential for the treatment of cisplatin-resistant cervical cancer.

Introduction

Cervical cancer is the third most common cancer worldwide with an annual incidence of 530,000 cases [1]. Based on Phase III results, the combination of cisplatin and paclitaxel remains the standard of care for treatment of recurrent cervical cancer, although clinical benefit is limited. In fact, although cisplatin is the most effective agent for metastatic cervical cancer, prolonged treatment induces multiple mechanisms of tumor resistance and is associated with significant toxicity [1]. Therefore, the development of new cisplatin formulations to overcome both resistance and toxicity remains a high priority [2] and is crucial for a better treatment and a more prolonged survival.

Presently, one of the main goals is to identify compounds with superior efficacy, reduced toxicity and a lack of cross-resistance as

* Corresponding author at: Experimental Oncology 2, Centro di Riferimento Oncologico, via F. Gallini 2, Aviano I-33081, Italy. Fax: +39 0434 659428.
E-mail address: daldinucci@cro.it (D. Aldinucci).

0090-8258/$ – see front matter
http://dx.doi.org/10.1016/j.ygyno.2013.08.041

compared with the parent compound cisplatin. In recent years different formulations of cisplatin encapsulated into liposomes were developed [3] demonstrating *in vitro* activity, but not very promising clinical results [4]. One remarkable exception is lipoplatin [5] that was developed to reduce the systemic toxicity of cisplatin, to escape immune surveillance, to improve drug targeting to the primary tumor and metastases, and to overcome cisplatin resistance at the cell membrane level. One of the mechanisms contributing to cisplatin resistance is the reduced intracellular accumulation or the increased efflux through the cell membrane [5]. Since liposomes directly fuse with the tumor cell membrane or are phagocytized inside the cells, lipoplatin could overcome drug resistance.

The lipids of lipoplatin are composed of soy phosphatidyl choline (SPC-3), cholesterol, dipalmitoyl phosphatidyl glycerol (DPPG), and methoxy-polyethylene glycoldistearoyl phosphatidylethanolamine (mPEG 2000-DSPE). These nanoparticles, displaying an enhanced half-life circulation time in body fluids and tissues, have the ability to target tumors and metastasis through the compromised endothelium of the tumor vasculature sprouted during neoangiogenesis, and there to reach concentration at levels up to 200-fold higher compared to the adjacent normal tissue [5]. Lipoplatin clinical trials have shown similar efficacy to those of cisplatin in pancreatic, head and neck cancer and in NSCLC, with the benefit of a reduced toxicity [6]. Similarly, in a Phase II trial the lipoplatin/vinorelbine combination demonstrated substantial reduced toxicities and enhanced or similar efficacy on HER-2/neu-Negative Metastatic Breast Cancer [7]. However, no data are available on cervical cancer. Indeed, despite survival improvement with the introduction of chemo-radiation, the prognosis for patients with cervical cancer remains poor. Therefore, lipoplatin could represent a new therapeutic option in this pathology. The aim of our study was to analyze the antitumor activity of lipoplatin against cisplatin-resistant cervical cancer cells and to investigate its mechanism of action.

Materials and methods

Drugs

Lipoplatin™, the liposomal formulation of cisplatin, was generously provided by Regulon (Regulon Inc., Mountain View, California); cisplatin was purchased from Mayne Pharma, Napoli, Italy.

Cell lines and culture conditions

HeLa (ATCC CCL-2) cells were purchased from the American Type Culture Collection (ATCC, Rockville, MD, USA). The highly invasive cervical cancer-derived ME-180 (HPV+) cell line was purchased by Dr. G. Toffoli (CRO, Aviano). Cisplatin-resistant R-ME-180 cells were developed in our laboratory by continuous exposure of ME-180 cells to cisplatin (1 μM). Cell lines were authenticated by BMR Genomics (Padova, Italy). Cells were cultured in DMEM medium (Sigma-Aldrich-Italy) with 10% heat-inactivated Fetal Bovine Serum (FBS; Sigma-Aldrich), 0.2 mg/ml penicillin/streptomycin (Sigma-Aldrich) and 0.1% (w/v) L-glutamine (Sigma-Aldrich) at 37 °C in a 5% CO_2 fully humidified atmosphere.

Cytotoxicity assay

4.0×10^3 cells were treated with increasing concentration of lipoplatin (2.5–100 μM) or cisplatin (2.5–100 μM) at 37 °C for 72 h. Triplicate cultures were established for each treatment. Cytotoxicity was measured by using MTT assay. IC_{50}, IC_{75} and IC_{90} values were calculated using the CalcuSyn software (Biosoft, Ferguson, MO, USA) [8].

Flow cytometry

1.0×10^5 tumor cells were incubated for 72 h on 6-well plates in complete medium in the presence of lipoplatin or cisplatin. Then Annexin-V binding (Becton-Dickinson [BD] Pharmingen, San Jose, CA), DNA fragmentation (BD), changes in mitochondrial membrane potential (Invitrogen, Milan, Italy) cytochrome-c release (BD), caspases 3 and 9 activation (Chemicon International, Milan, Italy), mitochondrial reactive oxygen species (ROS) (Invitrogen), B-cell lymphoma/leukemia-2 (Bcl-2) (DAKO Cytomation, Milan, Italy), B-cell lymphoma-extra large (Bcl-xL) (Cell Signalling, Danvers, MA, USA) and Bcl-2 associated x protein (Bax) (BD) analysis and the surface expression of EGFR were evaluated as previously described (anti-EGFR monoclonal antibody (mAb) 528 (Santa Cruz Biotechnology Inc., Santa Cruz, CA, USA)) [9]. Analyses were carried out using a FACSCalibur flow cytometer (BD).

Thioredoxin reductase (TrxR) enzyme activity assay

1.0×10^5 cells were treated with 20 and 30 μM lipoplatin or cisplatin for 72 h. TrxR activity was assessed using the Thioredoxin Reductase Assay Kit (Sigma-Aldrich), according to the manufacturer's instructions [9].

Cell migration and invasion assay

Cell migration was assessed using the scratch wound healing assay, as described elsewhere [10]. Briefly, cells were grown to confluence in tissue culture dishes, then 10 μM of lipoplatin, cisplatin or drug-free medium were added. After 72 h, cells were scraped up and cultured in DMEM with 0.5% FCS. Invasion was assessed by FATIMA assay after drug treatment (12 h with 30 μM lipoplatin) as previously described [11].

ALDH assay

Identification of cancer stem cells (CSCs) [11] was performed using the Aldeflour reagent based (Stem Cell Technologies, Vancouver, Canada) flow cytometry method according to the manufacturer's instructions. Briefly, cells (2×10^5/ml) were incubated for 40 min at 37 °C with Aldeflour reagent with and without the ALDH-inhibitor diethylaminobenzaldehyde (DEAB). Analyses were carried out using a FACSCalibur flow cytometer (BD).

3D-Multicellular spheroid formation assays

To obtain spheroids, 24-well plates were coated twice with 20 mg/ml of poly(2-hydroxyethyl methacrylate) (poly-HEMA; Sigma, Inc., St. Louis, MO, USA) [12] in 95% ethanol and washed once with PBS before cell seeding [13]. To evaluate lipoplatin activity on spheroid formation, R-ME-180 cells (5×10^4) were cultured for 72 h on poly-HEMA coated wells with increasing concentrations of lipoplatin (10, 25 or 50 μM). To evaluate apoptosis or ALDH activity, spheroids (72 h) were trypsinized in a single cell suspension. To obtain a second generation, formed spheroids (72 h) were dissociated and then replated on poly-HEMA coated wells.

Human cervical tumor xenograft experiments

Six-week-old female athymic nu/nu (nude) mice were purchased from Charles River (Lecco, Italy). 2.5×10^6 R-ME-180 cells suspended in 0.1 ml of Matrigel (1:3 in PBS) were inoculated in the right flank of each mouse. When tumors reached about 32 mm^3 in volume, mice were divided randomly into two groups of 5 mice each and treated every other day with intraperitoneal injection of 10 mg/kg lipoplatin or drug-free vehicle. Tumor size was measured over time

using a caliper. Tumor volumes were calculated according to the standard formula: $\pi LW^2 / 6$, where L indicates length and W indicates width. Mice were sacrificed after 28 days of treatment when control tumors had reached a volume of about 600 mm^3. The mouse organs were excised and fixed in formalin for tissue toxicity analyses.

To estimate the equal sample size for the mouse study groups, the experiment was designed to be able to detect a 0.60 difference with 0.90 power and an α error of 0.05.

Software and statistical analysis of data

Graphs were generated using Microsoft Office Excel (Microsoft Italia, Segrate, Italy) and SigmaPlot software (Systat Software Inc., San Jose, CA, USA). Values are presented as the mean with the standard error of not less than three measurements (unless otherwise stated) (mean ± SEM). Statistical analysis was performed using GraphPad Prism 6 Software (GraphPad, San Diego, CA, USA). The statistical significance of differences was determined by Student's *t*-test for comparison between the two groups. Analysis of variances (ANOVA) was used to evaluate the correlation of data among three or more groups; consecutive multiple comparison analysis was performed using Dunnett's or Tukey's test. Differences were considered statistically significant at $P < 0.05$.

Results

Lipoplatin inhibited cervical cancer cell proliferation and induced apoptosis

We compared the *in vitro* cytotoxic effects of lipoplatin (Fig. 1A) on HeLa, ME-180 cells and its cisplatin-resistant clone R-ME-180. Treatment with lipoplatin or cisplatin induced a dose-dependent inhibition of cell proliferation. HeLa (cisplatin, $IC_{50} = 8.6$ μM), ME-180 (cisplatin, $IC_{50} = 6.5$ μM) and R-ME-180 cells (cisplatin, $IC_{50} = 55.5$ μM) showed a comparable sensitivity to lipoplatin ($IC_{50} = 19.6$ μM, 24.8 μM, and 18.1 μM, respectively) (Fig. 1A). Lipoplatin induced apoptosis (Fig. 1B) in both cisplatin-sensitive (ME-180) and -resistant (R-ME-180) cells. On the contrary, cisplatin, used at the same concentrations, did not induce apoptosis in R-ME-180 cells. Consistently, cisplatin induced a remarkable DNA fragmentation only in ME-180 cells, whereas lipoplatin was active in both cell lines (Fig. 2A, left panel).

Lipoplatin affected mitochondrial functions, ROS formation and TrxR activity

Cisplatin damages tumors *via* induction of apoptosis that is mediated by various signals including the activation of mitochondrial pathways, and the formation of reactive oxygen species (ROS) [14]. Similarly, lipoplatin (30 μM) led to a decline in the mitochondrial membrane potential, increased the expression of Bax (pro-apoptotic), decreased

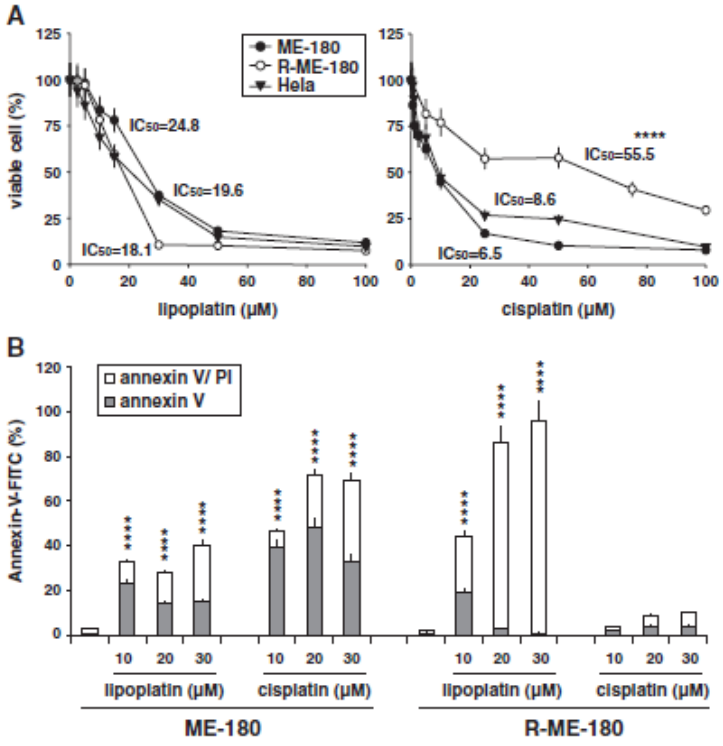

Fig. 1. Lipoplatin inhibits cell growth and induces apoptosis. (A) Cells were exposed to lipoplatin or cisplatin. After 72 h the viable cell number was evaluated by MTT staining. IC_{50} values (*i.e.* the concentration of drug that reduces cell growth by 50%) were calculated using the Calcusyn software. Results represent the mean ± SEM of three replicate wells from three independent experiments. (B) FACS analysis of cells after 72 h incubation at 37 °C with different concentrations of either lipoplatin or cisplatin and double stained with Annexin-V-FITC and PI. Values in the bar graph represent the mean ± SEM of three different experiments. ****$P < 0.0001$ drug *vs* medium.

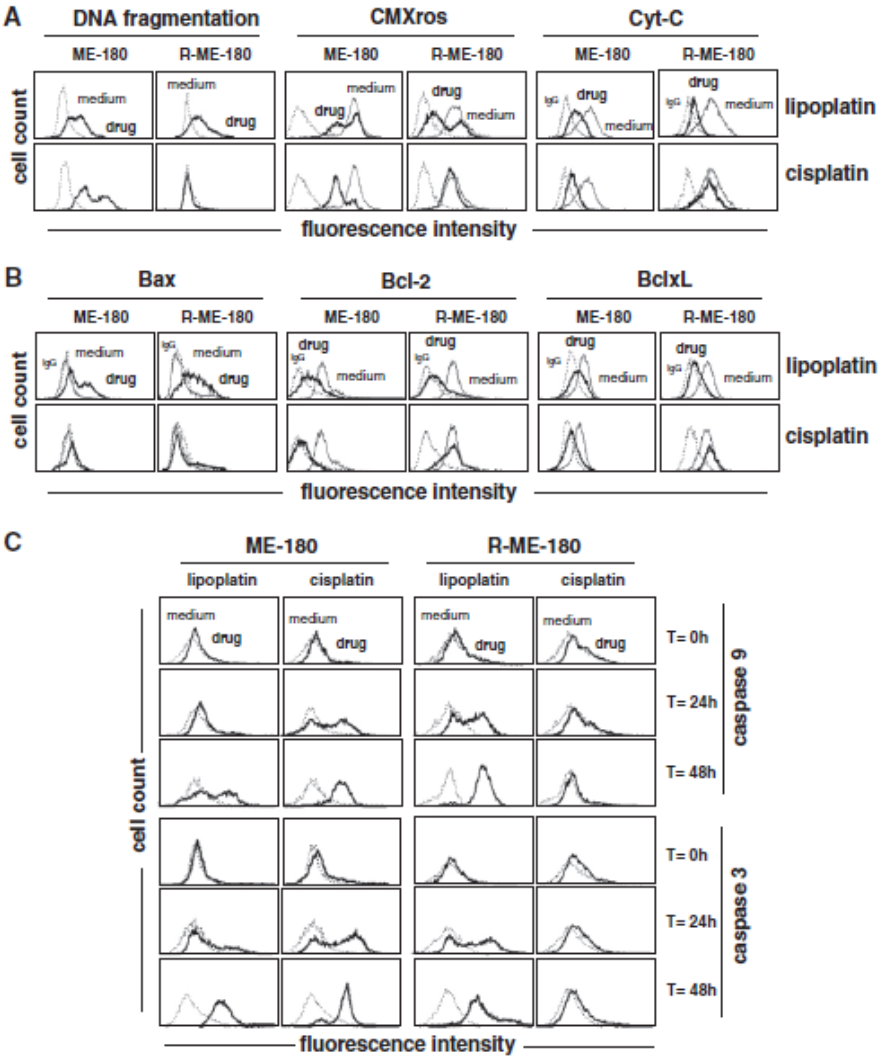

Fig. 2. Lipoplatin induces mitochondrion-mediated apoptosis and modulates Bax, Bcl-2 and Bcl-xL expression. (A) DNA fragmentation (Apo-Direct), mitochondrial membrane permeabilization (CMXRos), and cytochrome-c release were assessed by flow cytometry after treatment for 72 h with either lipoplatin or cisplatin (30 μM). (B) Analysis of Bax, Bcl-2 and Bcl-xL expression. Cells were incubated with either lipoplatin or cisplatin (30 μM). After 72 h, Bax, Bcl-2, and Bcl-xL expression was assessed by flow cytometry. (C) Analysis of caspase activation after incubating cells with either lipoplatin or cisplatin (30 μM) for 24 and 48 h. Cells were harvested, washed and resuspended in complete medium supplemented with FLICA for 1 h at 37 °C, then washed again and analyzed by flow cytometry. Dotted lines indicate background fluorescence of cells. X- and Y-axes indicate the logarithms of the relative fluorescence intensity and relative cell number, respectively. FACS histograms are representative of one of three different experiments.

the anti-apoptotic molecules Bcl-xL and Bcl-2 and cytochrome-c release from the mitochondria in both cell lines (Figs. 2A, B). Cisplatin, used at the same concentration, affected mitochondrial functions only in ME-180 cells (Fig. 2A). Consequently, lipoplatin (30 μM) led to activation of caspases 3 and 9 in both cell lines (Fig. 2C).

Lipoplatin induced ROS production in both cell lines while cisplatin was active only in ME-180 cells (Figs. 3A, B). TrxR is a selenoenzyme essential to maintain the balance of the cellular redox status and to protect the cells against oxidative damage due to ROS accumulation [15]. R-ME-180 cells expressed higher activity of TrxR than ME-180 cells (about 3 fold) (Fig. 3C). Both lipoplatin and cisplatin reduced TrxR activity in a dose-dependent manner (20, 30 μM) in both cell lines, but only lipoplatin (30 μM) was capable to reduce TrxR activity in R-ME-180 cells to levels lower than those of sensitive ME-180 cells.

Lipoplatin inhibited cancer cell migration, invasion and down-modulated EGFR expression

The effect of lipoplatin on cancer cell migration and invasion was measured using the scratch wound healing assay and the FATIMA assay, respectively. To exclude that a lower migration rate could be attributable to a decreased cell proliferation, cells were cultured in the presence of less drug (10 μM) and at low serum concentration. The migration rate (the percentage of the surface area covered by tumor

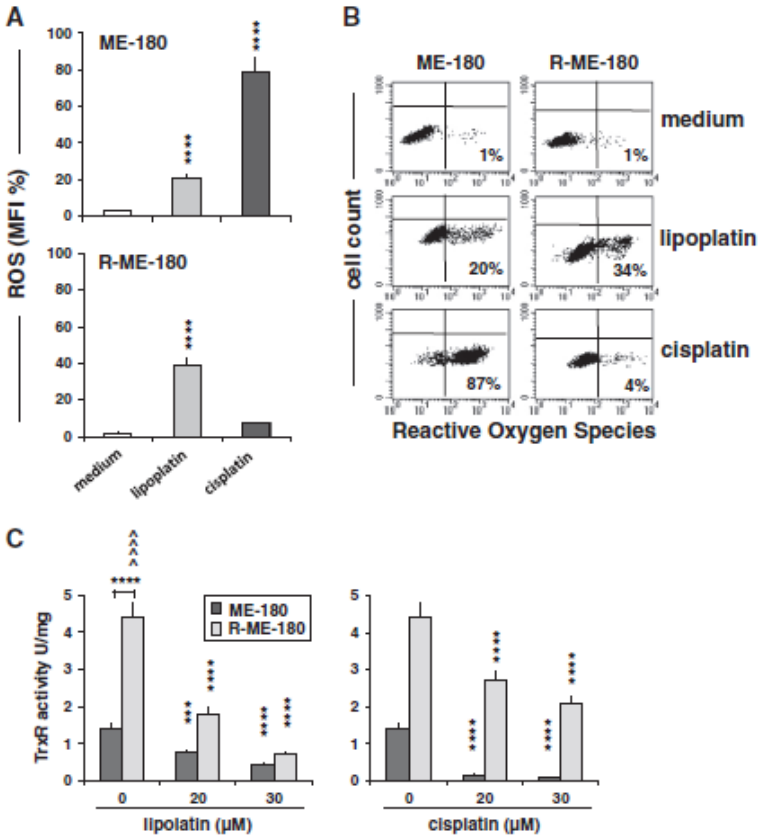

Fig. 3. Lipoplatin induces ROS accumulation and inhibition of TrxR activity. Cells treated with either lipoplatin or cisplatin (30 μM) for 72 h. (A) ROS production was analyzed with MitoSox reagent, the bar graphs represent the percentage of ROS (MFI = mean fluorescence intensity) as the mean ± SEM of three different experiments. (B) Representative FACS dot plots of one of three independent experiments showing ROS formation. (C) TrxR enzymatic activity evaluated with the Thioredoxin Reductase Assay Kit. Values in the bar graph represent the mean ± SEM of three different experiments. ***$P < 0.001$, ****$P < 0.0001$ drug *vs* medium, ^^^^$P < 0.0001$ R-ME-180 vs ME-180.

cells 24 and 48 h after the scratch) was reduced by lipoplatin in both cell lines whereas by cisplatin only in ME-180 cells (Figs. 4A, B). Then, we evaluated invasion of tumor cells treated for 12 h with 30 μM lipoplatin through a type I collagen-coated Boyden chamber. R-ME-180 cells exhibited enhanced invasive properties compared to ME-180 cells (Fig. 4C). At 24 h lipoplatin decreased cell invasion of about 35% and 50% in ME-180 and R-ME-180 cells, respectively (Fig. 4C).

EGFR is over-expressed in approximately 85% of invasive cervical tumors, it is associated with higher stages and poor prognosis [16], and its inhibition significantly decreases tumor cell metastases [16]. We detected higher EGFR levels in R-ME-180 cells (mean fluorescent intensity (MFI) = 387.26 ± 42) than in ME-180 cells (MFI = 201.68 ± 30). Lipoplatin (30 μM) decreased EGFR surface expression in both cell lines, while cisplatin (30 μM) remarkably down-modulated EGFR in ME-180 cells and only minimally affected R-ME-180 cells (Fig. 4D). A representative experiment is shown in Fig. 4E.

Spheroid-forming efficiency and ALDH are increased in R-ME-180 cells: lipoplatin inhibited spheroid formation and reduced ALDH + cells

Spheroids represent a three-dimensional *in vitro* system that more closely resembles the *in vivo* tumor microenvironment. A greater ability to form spheroids [17] and the expression of ALDH enzymes [18] usually indicate an increase in the cancer stem cell (CSC) population. R-ME-180, but not ME-180 cells, spontaneously formed spheroids when cultured on poly-HEMA coated wells. Consistently, we found that the percentage of cells expressing ALDH was 0.2% ± 0.01 in ME-180 and 0.51% ± 0.04 in R-ME-180 cells grown in monolayer. Then, we evaluated ALDH activity in R-ME-180 spheroids and found that it significantly increased in the first (I gen) (4.45-fold) and especially in the second generation (II gen) (6.82-fold) spheroids (Fig. 5A). A representative FACS dot plot showing ALDH expression is shown in Fig. 5B. Finally, we investigated whether lipoplatin could prevent spheroid formation. Lipoplatin (10–25–50 μM) but not cisplatin inhibited spheroid formation in poly-HEMA coated wells. R-ME-180 cells formed several large and dense spheroids, whereas lipoplatin, but not cisplatin, treated cells formed small spheroids, with dead cells interspersed among cell aggregates (Fig. 5C). At the highest lipoplatin concentration (50 μM) we detected only dead cells (Fig. 5C). Consistently, lipoplatin induced apoptosis in a dose dependent manner (Fig. 5D) and decreased the percentage of ALDH + cells (Figs. 5E, F).

Lipoplatin inhibited the growth of cervical cancer xenografts

Cisplatin-resistant R-ME-180 cells (2.5×10^6) were injected into the right flank of 6-week-old female athymic nude mice. After 4 days (tumor size of about 32 mm^3) mice were treated intraperitoneally with lipoplatin. Treatment for 28 days resulted in a significant ($P < 0.01$)

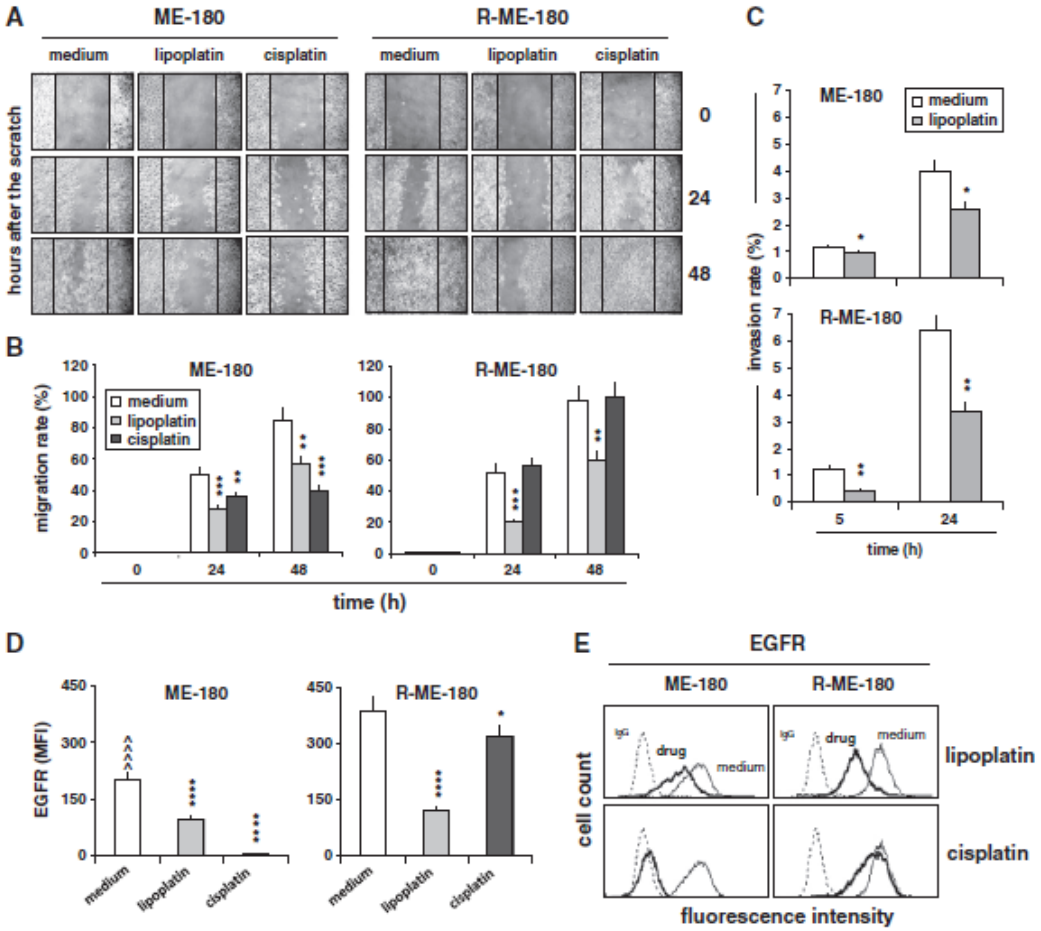

Fig. 4. Lipoplatin inhibits cell migration and decreases EGFR expression. Cells were treated with lipoplatin or cisplatin at 10 μM for 72 h. Then cell confluent monolayers were scraped up three times and cultured in low serum medium for additional 48 h: (A) representative scratch test analysis of cell migration (phase contrast microphotographs, original magnification 10×); (B) migration rate represented as the distance between the edges of the wound (defined by the lines), indicating the surface area occupied by the migrating cells after 24 and 48 h. Values in the bar graph represent the mean ± SEM of three different experiments. (C) Migration of cervical cancer cells through a collagen type I-coated Boyden chamber (invasion) after treatment for 12 h with 30 μM lipoplatin. $^{*}P < 0.05$, $^{**}P < 0.01$, $^{***}P < 0.001$ drug *vs* medium. (D) Cells were treated for 72 h with either lipoplatin or cisplatin (30 μM). Then EGFR surface expression was analyzed by flow cytometry using the anti-EGFR mAb 528. Values in the bar graph represent the mean ± SEM of three different experiments $^{*}P < 0.05$, $^{****}P < 0.0001$ drug *vs* medium. $^{\wedge\wedge\wedge\wedge}P < 0.0001$ R-ME-180 *vs* ME-180. (E) Representative FACS histograms of one of three independent experiments showing EGFR expression after drug treatment.

tumor growth inhibition. The tumors of the untreated control group grew to a mean tumor size of about 615.4 ± 50 mm^3, while in lipoplatin treated mice tumors reached a mean size of about 192 ± 15 mm^3 (Fig. 6). There was no histological detectable cytotoxicity involving the animals' heart, spleen, liver and kidney, whereas treatment with the same concentration of cisplatin was lethally toxic for mice (data not shown).

Discussion

Cisplatin has been very effective for the treatment of gynecological cancers, such as ovarian and cervical cancers, but the development of resistance in initially responsive tumors and its severe toxicity represent the most important problems in cisplatin-based chemotherapy [1].

Here lipoplatin potently inhibited the proliferation of the cisplatin-resistant R-ME-180 cells with an IC_{50} comparable to that of the parent cisplatin-sensitive cells (ME-180) and of HeLa cells, and strongly decreased xenograft tumor growth of the cisplatin-resistant R-ME-180 cells without apparent toxicity.

Lipoplatin induced its potent cytotoxic effect by activating apoptosis, inducing mitochondrial membrane depolarization, cytochrome-c release, and caspases 3 and 9 activation, indicating that its activity was exerted through the mitochondrial intrinsic apoptotic pathway. Accordingly, the pro-survival protein Bcl-2 and Bcl-xL were reduced and the pro-apoptotic Bax protein [19,20] increased.

TrxR is a ubiquitous enzyme over-expressed in many cancer cells, identified as a potential target of anticancer drugs. TrxR exhibits protective effects against various cellular stresses, including growth inhibition and cell death induced by ROS and chemotherapeutic agents [15,21,22]. Resistance to cisplatin increases Trx and TrxR levels in HeLa cervical cancer cells [23] as shown here for the R-ME-180 cells. The cisplatin-

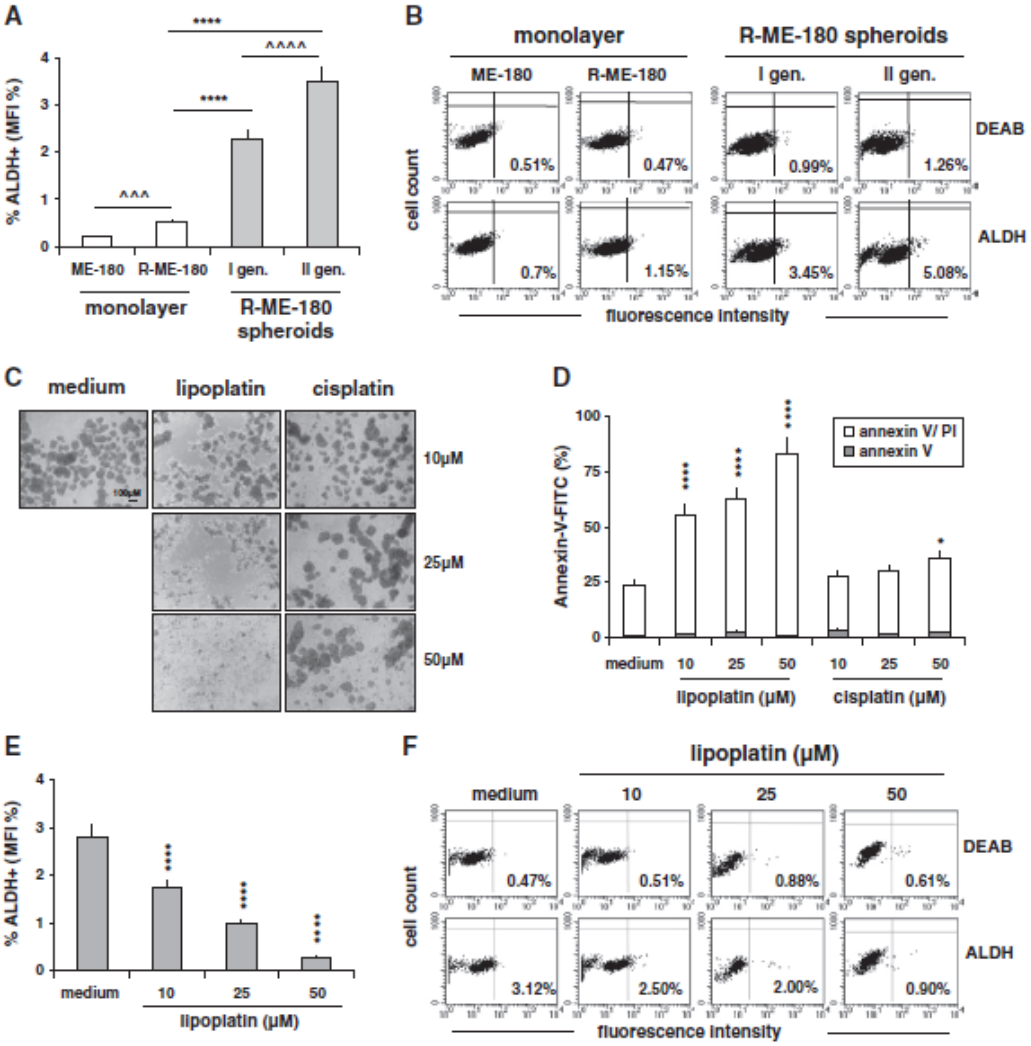

Fig. 5. Spheroid-forming efficiency and ALDH are increased in R-ME-180 cells: lipoplatin inhibits spheroid formation and reduces ALDH+ cells. (A) ALDH expression was evaluated by flow cytometry in ME-180 and R-ME-180 monolayers and in first (I gen) and second generation (II gen) spheroids. Values in the bar graph, reported as the percentage of ALDH positive cells, represent the mean ± SEM of three different experiments. ^^^$P < 0.001$ ME-180 *vs* R-ME-180 monolayer; ****$P < 0.0001$ R-ME-180 monolayer *vs* I and II gen spheroids, ^^^^$P < 0.0001$ I gen. *vs* II gen. spheroids. (B) Representative FACS dot plots of one of three independent experiments showing ALDH expression. (C) R-ME-180 cells, cultured on plates covered with poly-HEMA (2-hydroxyethyl methacrylate), were treated with (10, 25, 50 μM) lipoplatin or cisplatin. After 72 h spheroids were photographed (phase contrast microphotographs, original magnification 4×) and then disrupted to evaluate apoptosis (D) or ALDH expression (E–F). (D) The graph indicates the mean ± SEM values of the percentages of apoptotic cells evaluated by Annexin-V/PI staining from three independent experiments, each performed in duplicate. (E) The graph represents ALDH quantification, as MFI percentage, after spheroid treatment with lipoplatin. Data are expressed as mean ± SEM of three separate experiments. (F) Representative FACS dot plots of one of three independent experiments showing ALDH expression (% of positive cells).

resistant variants of HeLa cells, established by continuous exposure to cisplatin exhibited an increased expression and activity of TrxR as well as Trx compared with the parental cells [23]. Consistently, we found that R-ME-180 cells express more TrxR than ME-180 cells. Lipoplatin remarkably reduced TrxR enzymatic activity with up-regulation of ROS, possibly overcoming the resistance mediated by TrxR over-expression. On the contrary, cisplatin decreased TrxR levels to a lesser extent than lipoplatin, and to levels comparable to those of untreated cisplatin-sensitive cells, suggesting that cisplatin resistance could be due to the reduced capability to increase ROS levels because of the higher TrxR enzymatic activity in R-ME-180 cells.

The increased expression of EGFR is associated with bad prognosis in cervical cancer [24,25].

HB-EGF, a ligand of EGFR produced by stromal fibroblasts in uterine cervical cancer, contributes to ME-180 cell proliferation [26]. Moreover, treatment with cisplatin led to EGFR degradation in sensitive head and neck cancer cell lines, and this degradation strongly correlates with cytotoxicity [27]. We demonstrated that the R-ME-180 cells

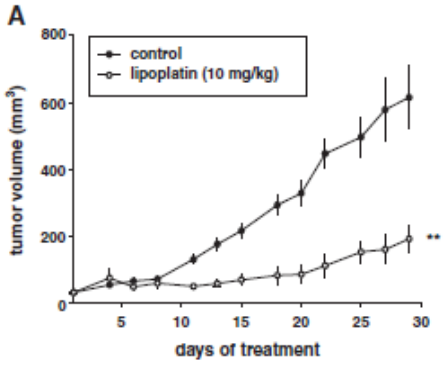

Fig. 6. *In vivo* anticancer activity of lipoplatin (xenograft). Tumor volume was measured in female athymic nude mice after intraperitoneal (i.p.) injection of either drug-free medium or containing 10 mg/kg lipoplatin, three times a week using a caliper. Points represent the mean ± SEM of five animals per group. **$P < 0.01$ lipoplatin *vs.* control.

expressed higher amounts of EGFR than ME-180 cells and lipoplatin, but not cisplatin, down-modulated EGFR expression in cisplatin-resistant cells. Our results suggest that lipoplatin, by reducing EGFR,could exert not only direct cytotoxic effects on cervical cancer cells, but also affect the proliferation induced by HB-EGF secreting stromal cells of the tumor microenvironment. Lipoplatin and also cisplatin decreased EGFR expression in cisplatin sensitive cells. This implies that an appropriate treatment schedule should be considered when cisplatin and gefitinib or other similar drugs are used together since cisplatin treatment might hinder targeted therapy against molecules susceptible to downregulation.

Cervical cancer usually spreads to the adjacent organs through the angiolymphatic system [28]. Although uncommon at initial diagnosis, metastatic disease will develop in a high percentage, usually within the first two years of completing treatment and in the majority of cases metastatic cervical cancer is not curable [28]. Therefore, suppressing not only cell proliferation, but also tumor metastasis is desirable to obtain clinically useful results in advanced cervical cancer. High levels of EGFR also promote cancer cell invasion and metastases [28]. Our study showed that lipoplatin inhibited cell migration and invasion of cisplatin-resistant cells, opening the possibility that this drug formulation could be effective also to reduce/inhibit cancer cell local invasion and metastases. The finding that only R-ME-180 cells formed spheroids and displayed a putative stem-like signature provided an experimental system to assay if lipoplatin could be effective on this three-dimensional *in vitro* model that more closely resembles the tumor microenvironment. Lipoplatin inhibited spheroid formation and reduced the percentage of CSCs (ALDH+ cells) suggesting that it could be used to treat *in vivo* tumors. Accordingly, lipoplatin inhibited tumor xenografts of R-ME-180 cells with minimal systemic toxicity, while cisplatin at the same concentration caused a severe toxicity in nude mice [29]. These results are promising in the light of using this drug, single or in combination therapy, as a novel therapeutic strategy for cisplatin-resistant recurrent cervical cancer.

Because cisplatin is the standard care for the treatment of cervical cancer in combination with radiation therapy (RT), replacement of cisplatin by lipoplatin against cervical cancer would add the advantage of lower toxicities to patients as shown in randomized Phase II and Phase III studies against NSCLC [30–32]. A better radiosensitizing activity of lipoplatin compared to cisplatin has also been shown in preclinical studies [33]. Adding the advantage of reducing the metastasis potential from lipoplatin treatment suggested from our current work we recommend that lipoplatin in combination with RT should be compared to cisplatin + RT in a randomized clinical study against cervical cancer.

Conflict of interest

The authors declare that they have no conflict of interest.

Acknowledgments

This research was supported by Ministero della Salute, Ricerca Finalizzata FSN, I.R.C.C.S., Rome, Italy.

References

[1] Leath III CA, Straughn Jr JM. Chemotherapy for advanced and recurrent cervical carcinoma: results from cooperative group trials. Gynecol Oncol 2013;129(1):251–7.
[2] Sancho-Martinez SM, Prieto-Garcia L, Prieto M, Lopez-Novoa JM, Lopez-Hernandez FJ. Subcellular targets of cisplatin cytotoxicity: an integrated view. Pharmacol Ther 2012;136(1):35–55.
[3] Huo T, Barth RF, Yang W, Nakkula RJ, Koynova R, Tenchov B, et al. Preparation, biodistribution and neurotoxicity of liposomal cisplatin following convection enhanced delivery in normal and F98 glioma bearing rats. PLoS One 2012;7(11):e48752.
[4] Zalba S, Garrido MJ. Liposomes, a promising strategy for clinical application of platinum derivatives. Expert Opin Drug Deliv 2013;10(6):829–44.
[5] Stathopoulos GP, Boulikas T. Lipoplatin formulation review article. J Drug Deliv 2012;2012:581363.
[6] Boulikas T. Clinical overview on lipoplatin: a successful liposomal formulation of cisplatin. Expert Opin Investig Drugs 2009;18:1197–218.
[7] Farhat FS, Temraz S, Kattan J, Ibrahim K, Bitar N, Haddad N, et al. A phase II study of lipoplatin (liposomal cisplatin)/vinorelbine combination in HER-2/neu-negative metastatic breast cancer. Clin Breast Cancer 2011;11:384–9.
[8] Chou TC, Talalay P. Quantitative analysis of dose–effect relationships: the combined effects of multiple drugs or enzyme inhibitors. Adv Enzyme Regul 1984;22:27–55.
[9] Cattaruzza L, Fregona D, Mongiat M, Ronconi L, Fassina A, Colombatti A, et al. Antitumor activity of gold(III)-dithiocarbamato derivatives on prostate cancer cells and xenografts. Int J Cancer 2011;128(1):206–15.
[10] Liang CC, Park AY, Guan JL. In vitro scratch assay: a convenient and inexpensive method for analysis of cell migration in vitro. Nat Protoc 2007;2:329–33.
[11] Spessotto P, Lacrima K, Nicolosi PA, Pivetta E, Scapolan M, Perris R. Fluorescence-based assays for in vitro analysis of cell adhesion and migration. Methods Mol Biol 2009;522:221–50.
[12] Ivascu A, Kubbies M. Rapid generation of single-tumor spheroids for high-throughput cell function and toxicity analysis. J Biomol Screen 2006;11:922–32.
[13] Phung YT, Barbone D, Broaddus VC, Ho M. Rapid generation of in vitro multicellular spheroids for the study of monoclonal antibody therapy. J Cancer 2011;2:507–14.
[14] Brozovic A, Ambriovic-Ristov A, Osmak M. The relationship between cisplatin-induced reactive oxygen species, glutathione, and BCL-2 and resistance to cisplatin. Crit Rev Toxicol 2010;40:347–59.
[15] Mahmood DF, Abderrazak A, Khadija EH, Simmet T, Rouis M. The thioredoxin system as a therapeutic target in human health and disease. Antioxid Redox Signal 2013 ahead of print. http://dx.doi.org/10.1089/ars.2012.4757 (in press).
[16] Soonthornthum T, Arias-Pulido H, Joste N, Lomo L, Muller C, Rutledge T, et al. Epidermal growth factor receptor as a biomarker for cervical cancer. Ann Oncol 2011;22:2166–78.
[17] Sugihara E, Saya H. Complexity of cancer stem cells. Int J Cancer 2013;132(6):1249–59.
[18] Lopez J, Ruiz G, Organista-Nava J, Gariglio P, Garcia-Carranca A. Human papillomavirus infections and cancer stem cells of tumors from the uterine cervix. Open Virol J 2012;6:232–40.
[19] Wu CC, Bratton SB. Regulation of the intrinsic apoptosis pathway by reactive oxygen species. Antioxid Redox Signal 2013;19(6):546–58.
[20] Youle RJ, Strasser A. The BCL-2 protein family: opposing activities that mediate cell death. Nat Rev Mol Cell Biol 2008;9:47–59.
[21] Cai W, Zhang B, Duan D, Wu J, Fang J. Curcumin targeting the thioredoxin system elevates oxidative stress in HeLa cells. Toxicol Appl Pharmacol 2012;262:341–8.
[22] Liu Y, Li Y, Yu S, Zhao G. Recent advances in the development of thioredoxin reductase inhibitors as anticancer agents. Curr Drug Targets 2012;13:1432–44.
[23] Sasada T, Nakamura H, Ueda S, Sato N, Kitaoka Y, Gon Y, et al. Possible involvement of thioredoxin reductase as well as thioredoxin in cellular sensitivity to cis-diamminedichloroplatinum (II). Free Radic Biol Med 1999;27:504–14.
[24] Narayanan R, Kim HN, Narayanan NK, Nargi D, Narayanan B. Epidermal growth factor-stimulated human cervical cancer cell growth is associated with EGFR and cyclin D1 activation, independent of COX-2 expression levels. Int J Oncol 2012;40:13–20.
[25] Iida K, Nakayama K, Rahman MT, Rahman M, Ishikawa M, Katagiri A, et al. EGFR gene amplification is related to adverse clinical outcomes in cervical squamous cell carcinoma, making the EGFR pathway a novel therapeutic target. Br J Cancer 2011;105:420–7.
[26] Murata T, Mizushima H, Chinen I, Moribe H, Yagi S, Hoffman RM, et al. HB-EGF and PDGF mediate reciprocal interactions of carcinoma cells with cancer-associated fibroblasts to support progression of uterine cervical cancers. Cancer Res 2011;71:6633–42.
[27] Ahsan A, Hiniker S, Ramanand S, Nyati S, Hegde A, Helman A, et al. Role of EGFR degradation in cisplatin-induced cytotoxicity in head and neck cancer. Cancer Res 2010;70(7):2862–9.
[28] Scatchard K, Forrest JL, Flubacher M, Cornes P, Williams C. Chemotherapy for metastatic and recurrent cervical cancer. Cochrane Database Syst Rev 2012;10:CD006469.

[29] Chahinian AP, Norton L, Holland JF, Szrajer L, Hart RD. Experimental and clinical activity of mitomycin C and cis-diamminedichloroplatinum in malignant mesothelioma. Cancer Res 1984;44:1688–92.
[30] Stathopoulos GP, Antoniou D, Dimitroulis J, Stathopoulos J, Marosis K, Michalopoulou P. Comparison of liposomal cisplatin versus cisplatin in non-squamous cell non-small-cell lung cancer. Cancer Chemother Pharmacol 2011;68(4):945–50.
[31] Mylonakis N, Athanasiou A, Ziras N, Angel J, Rapti A, Lampaki S, et al. Phase II study of liposomal cisplatin (Lipoplatin) plus gemcitabine versus cisplatin plus gemcitabine as first line treatment in inoperable (stage IIIB/IV) non-small cell lung cancer. Lung Cancer 2010;68(2):240–7.
[32] Stathopoulos GP, Antoniou D, Dimitroulis J, Michalopoulou P, Bastas A, Marosis K, et al. Liposomal cisplatin combined with paclitaxel versus cisplatin and paclitaxel in non-small-cell lung cancer: a randomized phase III multicenter trial. Ann Oncol 2010;21(11):2227–32.
[33] Charest G, Paquette B, Fortin D, Mathieu D, Sanche L. Concomitant treatment of F98 glioma cells with new liposomal platinum compounds and ionizing radiation. J Neurooncol 2010;97(2):187–93.